Report of Survey

Norfolk Island Nearshore and Coastal Habitat Mapping

DATE
22, December, 2022

CREATED BY
Ocean Infinity Pty Ltd

REVISION
Issue A

OCEAN INFINITY®

Ocean Infinity Group Limited
17 Grosvenor St, Mayfair, London W1K 4PZ
oceaninfinity.com

Contents

List of Figures

List of Tables

1. Executive Summary

Ocean Infinity (Australia) Pty Ltd (formerly iXblue Pty Ltd), in partnership with Deakin University's Marine Mapping Group, University of Wollongong, Tellus4D Geoimaging, University of Newcastle, University of New South Wales, University of Tasmania and Geoscience Australia, conducted an aerial survey and a hydrographic survey as part of the Norfolk Island Nearshore and Coastal Habitat Mapping project under the grant ID 4-FISKTDM. Prior to this project, Norfolk Marine Park dataset was limited to a terrestrial lidar survey from CSIRO (Gallant, 2020) and a nearshore seafloor classification from satellite bathymetry (EOMAP).

The marine survey was conducted by Ocean Infinity after the HIPP Nautical Charting Project SI1020 Banks Strait. This assures the reliability of the survey system used. Geoscience Australia and scientific experts from Deakin University's Marine Mapping Group actively participated for data acquisition, data processing and the redaction of this report.

From 21 to 24 July 2021 onboard M/V Offshore Solution, the team covered 108.6km^2 of the Norfolk Shelf with a multibeam echosounder Kongsberg EM2040 Mark II, a total of 44 locations of Baited Remote Underwater Videos in the NE and the S of the island and couple of sub-surface profiles with the Sub-Bottom Profiler Echoes 3500 T1. The coastal survey was conducted by Tellus4D Geoimaging in November 2021. The drone Mavic 2 was deployed from shore, to obtain high resolution photogrammetry at seven coastal sites of Norfolk Island: Captain Cook Lookout, Anson Bay, Puppy's Point, Headstone Point, Slaughter Bay and Bumbora Beach, and Cemetery and Emily Bay, for a total of 14km2.

Geomorphic interpretation of the photogrammetry was completed at the University of Wollongong. Variation in the coastal morphology of the island is dependent on the location and coastal exposure of the site. The North facing section of Norfolk Island, represented by Captain Cook Lookout, exhibits offshore stacks (such as Elephant and Bird Rock), dramatic cliffs and onshore and offshore platforms with pockets of rocky beaches.

The West side of the island, represented by Anson Bay, Puppy's Point and Headstone Point, is exposed to Westerlies and Eastward waves. The three sites show predominant morphology made of basaltic shore platforms and rocky beach. The cliffs are shaped by cyclic retreat process with alternance of caves, boulder beaches and undercut sections. Some mass movements are observed on the top section of the cliffs.

The South side, represented by Slaughter Bay, Emily Bay and Cemetery Bay, and Ball Bay, shows two geological formations: a sedimentary rock (calcarenite) and a volcanic rock (basalt). The South side of the Island offers sandy beaches, as well as rocky beaches and cliffs. The calcarenite platform at Slaughter Bay and Cemetery Bay act as natural waves breakers and create calmer environments and coral reef growth within Slaughter Bay. On shore, several localised mass movements are observed, the largest being in the Kingston Region, where the weathered basalt prone to failure.

From the multibeam bathymetric dataset, a series of bathymetric derived products are obtained to explores the morphology of the surveyed Norfolk Island seafloor. The characterisation and definition of the seabed are the results of analysis combination of the depth map, slope map, vector ruggedness measure (VRM)Bathymetric Position Index (BPI) (fine and broad), seabed reflectance and ground truthing with BRUV images. The submarine geomorphology of Norfolk bathymetry and shelf shows a large area of plane gradually descending to depth with a low slope made up of unconsolidated sandy sediments. Some of these sediments have formed into sand ridges up to 4 m in relative relief and up to ~1.5 km long. In some locations, hummocks or mounds in close proximity can be seen, caused by outcrops rock, sometimes veneered by deep water corals. These regions show subtle variations in slope and ruggedness, separating these features from the plane. Finally, in the southwest, the morphology shows a region of ridge-like features coupled with pockets of depression.

The analysis of the seafloor reflectance allows to define sub-categories of the unconsolidated and consolidated seafloor. For example, the northern region shows rocky seabed characterised by linear cracks filled by sediment,

whilst the southern region displays round shape patches interpreted as indurated seabed colonised by corals. The most extended rocky platform is the regional ridge with well delimited contours observed Est of Norfolk Island. The unconsolidated seafloors have variable acoustic responses suggesting a wide range of grain-size sediment, from coarse sand to very fine deposits. Local hydrodynamic conditions (waves, tide, deep currents) affect differently the deposits pattern in each region. The spatial repartition of the unconsolidated sediment and their nature (gravel, sand, silty sand, clayey sand, silt and sandy clay) suggested by the seabed nature map remain a hypothetic interpretation and deserve further ground truthing followed by grain-size analysis.

The Baited Remote Underwater Videos (BRUVs) data collected in this project around Norfolk Island provides a glimpse of the fish communities present and also can serve as a baseline dataset for future surveys to determine if there are changes in these communities through time. Across the 42 BRUVS successfully deployed, over 3,000 individual fish were observed, covering 76 taxa within 35 families. Both habitat type and depth had a significant effect on the species observed via BRUVS. The highest diversity occurred in intermediate depth (20–30 m) on infralittoral reef habitats, likely due to the prevalence of reef-associated species such as wrasse and damselfish species and the high number of reef deployments within this depth range. Abundance was also highest on reef habitats, but not affected by depth. Large sharks and rays and yellowtail kingfish contributed to the high biomass seen in deep (40+ m) deployments.

The sub-surface geology imaged by sub-bottom profiler along few profiles in the North area provide limited results. The hard surface of the seafloor (as observed in the bathymetry), is a natural barrier to the acoustic waves. Therefore, the profiles interpretation is limited to sand pockets where penetration is soft sediment is allowed.

This survey work and associated results provide an initial state of some of the coastal sites of the island and its marine shelf condition (morphology, nature, fish communities…). The information will help to manage the park and guide further studies, such as additional bathymetric survey within sensitive areas, investigation on the coastline, protection of fish and other marine species programs and ground truthing campaign to challenge hypothesis on the seabed nature and habitats.

2. Introduction

2.1 Australian Marine Park context

Norfolk Marine Park begins 1400 kilometres offshore, east of Evans Head in New South Wales. It covers 188,444 square kilometres, surrounding Norfolk island. The marine park is known for its diverse temperate and tropical marine life. A series of prominent pinnacles and seamounts that protrude the Norfolk Ridge act as biodiversity hotspots, attracting an abundance of fish species to the dense coral and sponge habitats. These unique seafloor features are also thought to act as stepping stones for faunal dispersal between New Caledonia and New Zealand.

The Norfolk Marine Park is managed by the Marine and Island Parks branch of Parks Australia, which manage, found and promote scientific research to improve understanding of and ability to effectively manage these parks. In 2020, Parks Australia founded the Norfolk Island Nearshore and Coastal Habitat Mapping project through the "Our Marine Parks" grant program, taking the opportunity to use vessel and survey system already in place for the SI1020 Hydrographic Survey planned in Tasmania.

During the month of July 2021, a collaborative group of scientists embarked onboard the M/V Offshore Solution vessel for a Habitat Mapping survey of Norfolk Island. The main objective of the mapping project was to map the seabed using high-resolution multibeam sonar (MBES) and sub-bottom profiling (SBP). Additionally, the team deployed Baited Remote Underwater Cameras (BRUVs) on the seabed to conduct a fish species survey around the island. In November 2021, a coastal mapping by drone was performed at seven bays and points of Norfolk Island.

This final document contains technical information about the survey systems used to collect data, the associated quality control and processing workflows and the interpretative sections based on the results including:

- Coastal geomorphology by drone photogrammetry over seven coastal sites of Norfolk Island;
- Morpho-bathymetry of the Norfolk Shelf, based on the 1m grid bathymetry and derived products such as depth map, slope aspect map, ruggedness map, Bathymetric Position Index (BPI) (fine and broad) maps.
- Seabed nature cartography based on the seabed reflectance measured with the multibeam echosounder;
- Diversity and abundance of the fish communities in two localised nearshore locations of the island, based on the analysis of BRUVs.

2.2 Survey Area Location,

2.2.1 Offshore survey areas

The survey areas defined offshore Norfolk Island are only a small part of the Norfolk Marine Park. The four areas, enclosed Norfolk Island with A, B, C and D respectively on North, East, South and West side of the island (Figure 2-1). The survey areas altogether represent 124.13km^2, less than 1% of the total surface of the Norfolk Marine Park (188444km^2).

These areas are located in the Special Purpose Zone that encloses a wider range of activities. This reflects the ongoing stewardship of these waters by the Norfolk Islanders, and the importance of this area for both conservation and providing a sustainable supply of local, fresh seafood (Discover Norfolk Marine Park - Norfolk Island Stories).

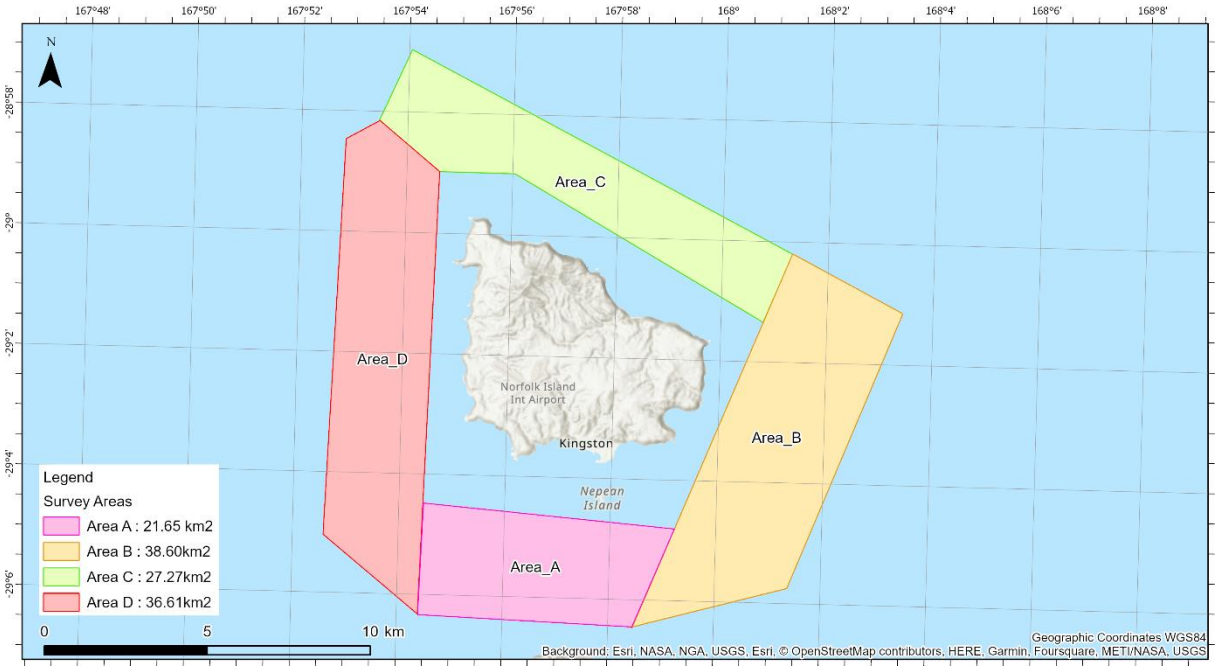

Figure 2-1: Norfolk Island and survey block location

2.2.2 Photogrammetry coastal survey areas

Drone photogrammetry survey was conducted around the coastline of Norfolk island. A total of 7 sites were surveyed (Figure 2-2):

- 1 site on the North coast : Captain Cook Lookout;
- 3 sites on the South coast: Ball Bay, Cemetery Bay and Slaughter Bay;
- 3 sites on the West coast: Headstone Point, Puppy's Point and Anson Bay.

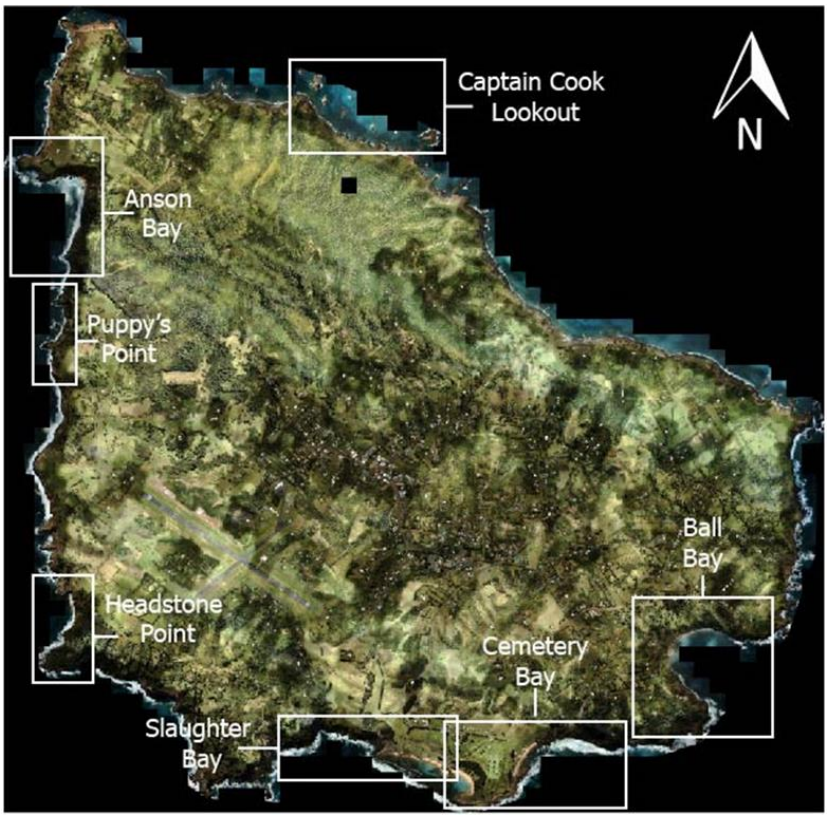

Figure 2-2: Drone photogrammetry survey sites

3. Survey Methodology

3.1 Geodetic Parameters

3.1.1 Datum and Projection

Data was referenced to the World Geodetic System 1984 (WGS84), using the Universal Transverse Mercator (UTM), Zone 58 South projection (Table 1).

Table 1: Geodetic Parameters

Geodetic Parameter	Geodetic Value
Datum	World Geodetic System (WGS84)
Ellipsoid	Geodetic Reference System 1980 (GRS80)
Semi-major Axis (a)	6 378 137.000m
Semi-minor axis (b)	6 356 752.314m
Eccentricity Squared (e2)	0.006694380
Flattening (1/f)	298.257223563
Projection	Universal Transverse Mercator (UTM)
Projection Type	Transverse Mercator
UTM Zone	58S
Central Meridian	165°
Scale Factor	0.9996
False Easting	500,000m
False Northing	10,000,000m
Latitude of Origin	0°
Unit of Measure	International Meter

The position system onboard is referenced to the International Terrestrial Reference Frame 2014 (ITRF2014). WGS 84 is aligned to ITRF to within one centimeter in each 3D component, therefore, no geodetic transformations are required.

3.1.2 Vertical Reference

Bathymetric data is referenced to Lowest Astronomic Tide (LAT), using the Kingston tide station (data supplied by BOM).

Table 2: Kingston Tide Station, Norfolk Island

Kingston Tide Station	
Gloss Number	124
Station Name	Norfolk Is.
Latitude	-29.05833500 N
Longitude	167.95356600 E
Instrumentation	Float
Data Acquisition Rate	15 min samples
Benchmark (Vertical Datum Reference)	
Tide Gauge Benchmark	BM 1: the top of a concrete block protruding about 0.3m above ground level and marked ZNI. It is surrounded by a rectangular concrete collar which shows latitude, longitude & height in feet above MSL.
Benchmark Relationships	Tide Gauge Zero (TGZ) = 5.432m below BM 1 (1965 onwards)
Auxiliary Benchmarks	BMR 8290 3092 NMV/C/443: small piece of blue metal gravel embedded in and protruding slightly above the concrete top of the sea wall. NMV/C/444 & NMV/C/445: centres of triangles carved in flat concrete on the top of the sea wall of the jetty, with their numbers next to them. TRIG 'M': drill hole in a damaged concrete block.

3.2 Vessel and personnel

The project was conducted from the M/V Offshore Solution (OS), outlined in Figure 3-1 and Table 3. The OS is aClass 1A, 54m DP2 Diesel Electric mono-hull vessel owned and operated by Guardian Offshore Pty Ltd and is Australian Flagged.

Figure 3-1: M/V Offshore Solution

Table 3: M/V Offshore Solution vessel details

Item	
Vessel Name	MV OFFSHORE SOLUTION
Flag of Registration Flag State)	Australia
Registration (IMO Number) / Call Sign	9784465 / VMGW
Survey Class	DNVGL (Unrestricted)
Length Overall	53.85m
Beam	11.30m
Draft	2.8m (MBES Stowed)
	3.0m (MBES Deployed)
Deadweight Tonnage / Gross Tonnage	585T / 902T
Year Built	2016
Construction	Steel Hull
Engine / Propulsion	Diesel Electric Propulsion System consisting of: 2 x Aft Azipod (650kW each) 1 x Bow Swing Down Azipod (650 kW) 1 x Bow Tunnel Thruster (400 kW)
2 x Aft Azipod (650kW each)	Propulsion Generators = 6 x D13 Volvo Penta (420kW each) Harbour and Emergency Generators = 2 x D9 Volvo Penta (260 kW each)

Table 4 details the personnel involved in the project, their company/university, and role.

Table 4: Personnel involved in the project

Personnel	Company / University	Role
Elizabeth Johnstone	iXblue/ Ocean Infinity Pty Ltd	Project manager (up to April 2022)
Agathe Hussherr	iXblue/ Ocean Infinity Pty Ltd	Project manager (from April 2022)
	iXblue/ Ocean Infinity Pty Ltd	Surveyor
Daniel Ierodiaconou	Deakin University	Associate Professor in Marine Science
Mary Young	Deakin University	Ph.D. Research Fellow in Marine Landscape Ecology
Peter Porskamp	Deakin University	
Rafael Carvalho	Deakin University	
Scott Gray	Deakin University	
Alysha Johnson	Univ. of Wollongong	Geologist
Michael Doane	Flinders University	

3.3 Survey System

The survey system used for Norfolk Island survey is identical to the survey system approved and used for the HIPP Nautical Charting Project SI1020 Banks Strait.

Figure 3-2 and Figure 3-3 detail the integration of the Hydrographic Survey System (HSS) onboard M/V Offshore Solution. All systems have been integrated according to manufacturer's specifications and industry best practice. Positioning systems (GNSS and motion sensor unit) are similar on each side however, the multibeam echosounder was installed on starboard side and the sub-bottom profiler was installed on portside.

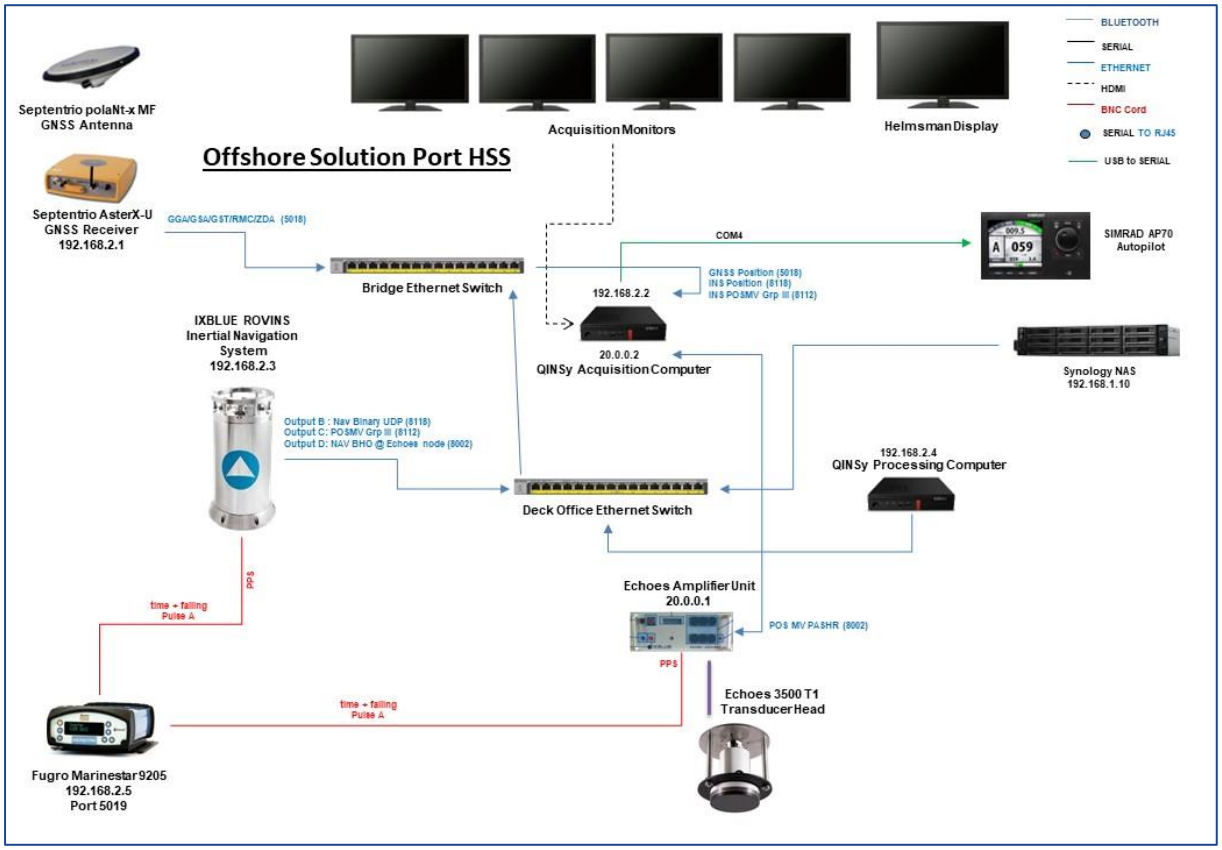

Figure 3-2: Survey systems installed on M/V Offshore Solution on Portside

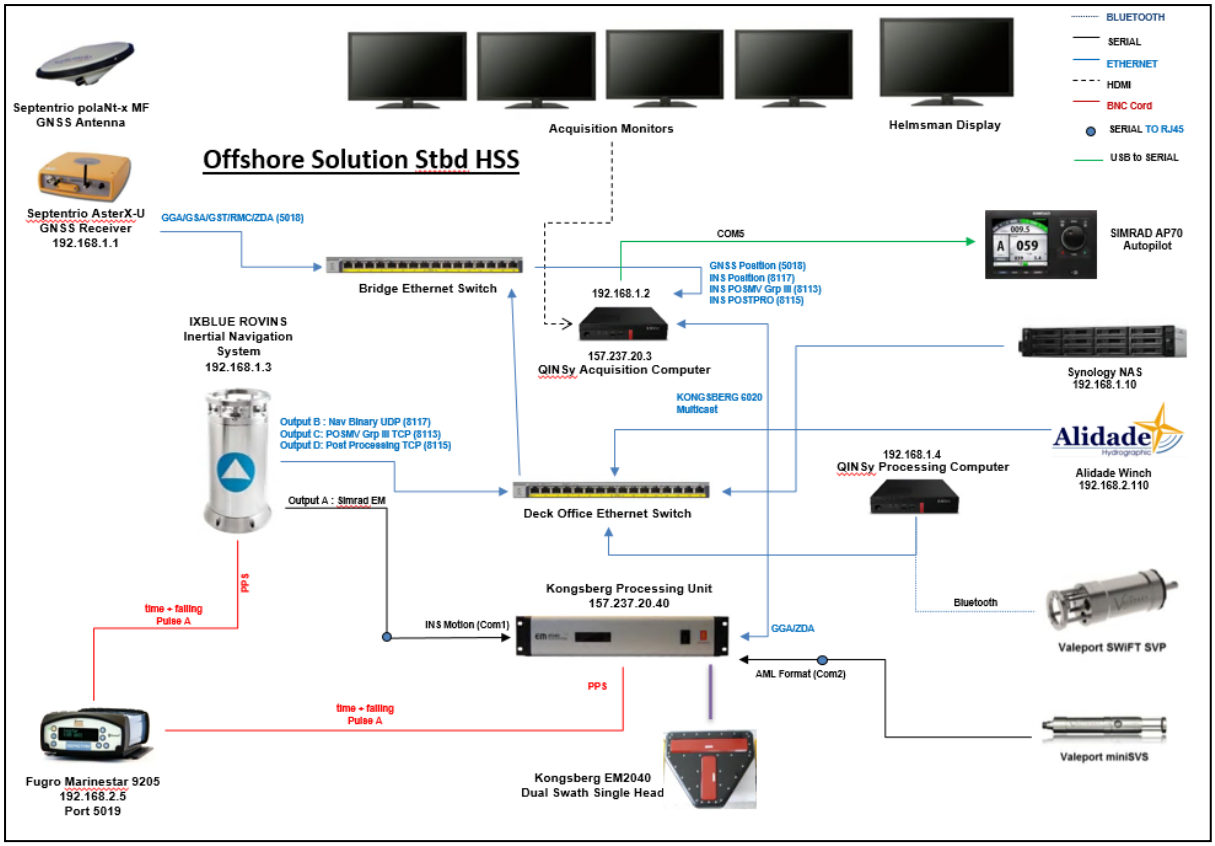

Figure 3-3: Survey systems installed on M/V Offshore Solution Starboard side

3.4 Dimensional Control

A Dimensional Control Survey was undertaken at Austal Shipyard, on 10 February 2021 and the report provided to the AHO on 14 February 2021 prior the start of the HIPP Nautical Charting Project SI1020 Banks Strait. The objective of the Dimensional Control Survey was to determine the relative position of the sensors with respect to the following Common Reference Point (CRP) and Vessel Reference Frame (VRF):

- The CRP is the (0,0,0) coordinate for offsets and is defined as the ROVINS INS P-Point.
- The VRF for all offsets is defined as the heading alignment of the ROVINS INS as determined by the ROVINS locating pins, and the pitch/roll alignment of the ROVINS base plate.

Table 5 details the results of the Dimensional Control Survey with respect to QINSy sign convention for the Port side HSS. All sensor offsets are relative to the ROVINS sensitive point “P” (0,0,0).

Table 5: QINSy Sensor Offsets – Port (SBP)

Offset Point	X (+ve STBD) (m)	Y (+ve FWD) (m)	Z (+ve UP) (m)	3D RMS Uncertainty (m)
Origin	0.000	0.000	0.000	-
ROVINS P-Point	0.000	0.000	0.000	0.001
Echoes T1	0.120	-0.002	-3.798	0.010
Septentrio GNSS Antenna-ARP	4.304	19.346	17.130	0.002
Water Line Reference	7.990	0.472	0.372	0.002
Centre of Gravity (CoG)	4.309	12.160	-0.045	0.100*

* Uncertainty in CoG value is representative of likely change in trim with different states of loading. Heave computation error is likely to be detectable in bathymetric data if the error in CoG is greater than 0.5m.

Table 6 details the results of the Dimensional Control Survey with respect to QINSy sign convention for the Starboard side HSS. All sensor offsets are relative to the ROVINS sensitive point “P” (0,0,0).

Table 6: QINSy Sensor Offsets – Starboard (MBES)

Offset Point	X (+ve STBD) (m)	Y (+ve FWD) (m)	Z (+ve UP) (m)	3D RMS Uncertainty (m)
Origin	0.000	0.000	0.000	-
ROVINS P-Point	0.000	0.000	0.000	0.001
MBES Tx	-0.120	-0.021	-3.961	0.003
MBES Rx	0.185	-0.020	-3.949	0.003
Septentrio GNSS Antenna-ARP	-2.304	19.943	17.081	0.002
Water Line Reference	0.446	0.440	0.348	0.002
Centre of Gravity (CoG)	-3.199	12.136	-0.135	0.100

* Uncertainty in CoG value is representative of likely change in trim with different states of loading. Heave computation error is likely to be detectable in bathymetric data if the error in CoG is greater than 0.5m.

3.5 Multibeam Echosounder

3.5.1 Installation

The multibeam echosounder was installed in the starboard side moonpool of the vessel. The transducers located approximately 0.5m below the hull.

The EM2040 Mark II is a wide band high resolution MBES system which uses electronic pitch and roll compensation. This has the benefit of ensuring that there is uniform sounding density in the along-track direction. The system fitted to M/V Offshore Solution was configured to work in Single Head Dual Swath Ultra High-Density Mode providing the maximum sensor data density and feature detection capabilities.

Table 7: MBES acquisition settings

EM2040 Single Head Dual Swath - Kongsberg	
Frequency	300 kHz
Maximum Ping Rate	50 Hz (Limited by two-way travel time, less 10-30% depending on detection mode selected).
Sounding Per Ping	1024 in Dual Swath Ultra High-Density Mode
Beamwidth	0.5 (Tx) x 1.0 (Rx) degrees at 300 kHz
Beam Spacing	Ultra-High Density Equidistant
Coverage Sector	120 degrees (>30m depth) and 140 degrees (<30m depth)
Maximum Stated Depth	600m -200 kHz cold ocean water
Transmit Beam Steering	+/- 10 degrees steps along track
Range Resolution	18 mm @ 25 µs pulse length
Beam Forming Method	Time delay with dynamic focusing in near field

The multibeam echosounder transducer was installed in the starboard side moonpool and once installed, was located approximately 0.5m below the hull.

3.5.2 Patch Test and Reference Surface

A calibration patch test (MPT) was conducted on the 28 March 2021, over flat seabed crossed by a ridge, when the OS was already mobilised and used for the nautical charting HIPP project SI1020 in Banks Strait. On site Patch Tests were conducted on the 28 April 2021 and 3 July 2021with no changes to the original results found.

MPTs were conducted in sea-state 1-3 and consisted of a series of 8 lines as follows:

- Pitch: Coincident survey lines acquired at 7 knots in opposite directions, where the transducer nadir beams transit directly across the target.
- Roll: Coincident survey lines acquired at 7 knots in opposite directions, over a flat seabed.
- Yaw: Parallel survey lines offset at 70 metres acquired at 7 knots in the same direction, where the transducer outer beams transit directly across the target
- Latency: Survey line acquired at 4 knots with coincident survey line acquired in the same direction at 7 knots.

MPT results from the 28 March 2021 are shown in Figure 3-4, showing a 2D profile before and after calibration. Calibration values are provided in Table 8.

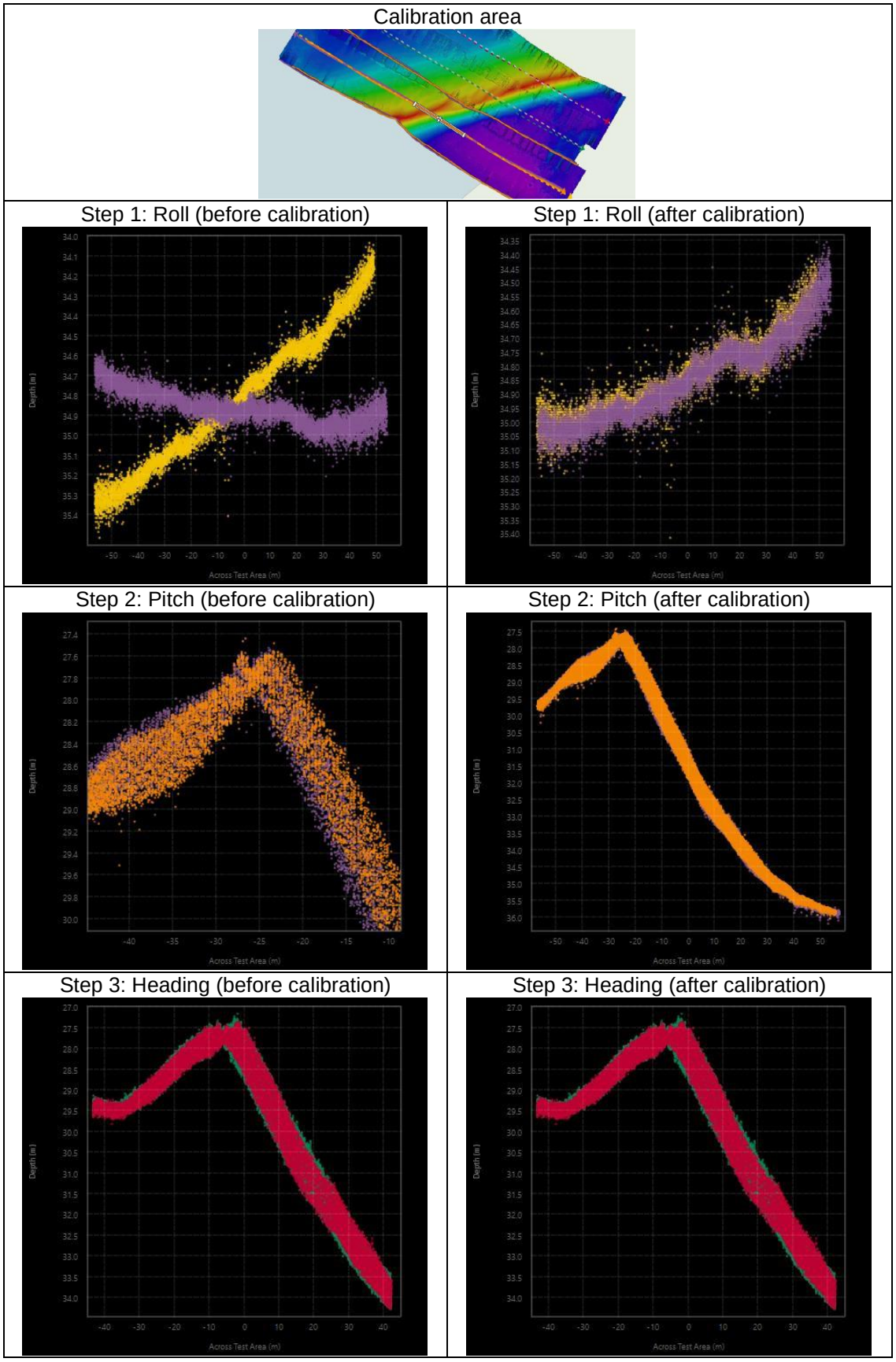

Figure 3-4: Patch Test Result from the 28 March 2021

Table 8: MBES Patch Test Result from the 28 March 2021

System	Roll (+ve STBD down) (°)	Pitch (+ve BOW up) (°)	Heading (+ve STBD) (°)	Latency (s)
MBES	0.386	-1.100	0.001	0.000

3.6 Sub-bottom profiler

The sub-bottom profiler (SBP) was installed in the portside moonpool and located approximately 0.5m below the hull once installed. This setup of the SBP and MBES on independent moonpools allowed the simultaneous acquisition of the bathymetry and the seismic profiles without interference.

Trial lines were run prior to start the acquisition to find the optimal settings for the SBP and are detailed in Table 17.

Table 9: SBP acquisition settings

	Echoes 3500 T1 - iXblue
Frequency	1700 -6000 Hz
Sampling Frequency	32000 Hz
Pulse Length	25 ms
Chirp level	100%
Ping Rate	2 Hz

The SBP line plan was defined on site based on the real time analysis of the sub-bottom profiles findings. Figure 3-5 shows the transects ran, consisting of:

- 7 lines (NW-SE) in Area C;
- 1 line (NNE-SSW) in Area B
- 2 lines (WWN-EES) in Area B.

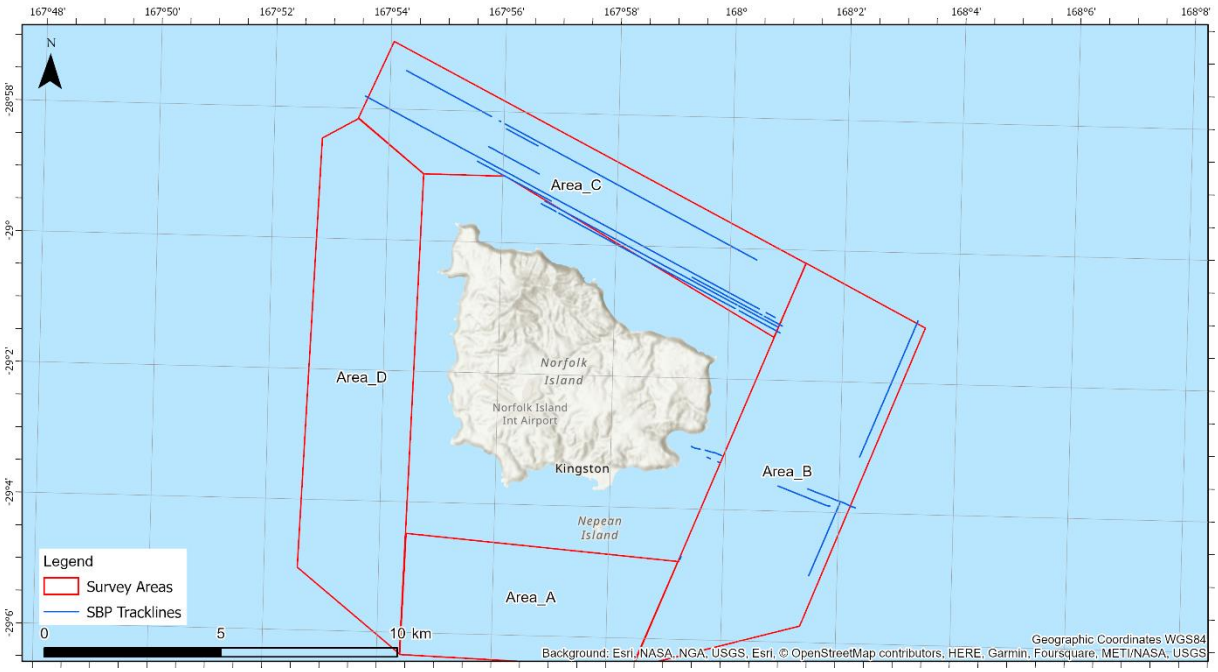

Figure 3-5: SBP Tracklines

3.7 Positioning Sensors

3.7.1 Installation

M/V Offshore Solution was fitted with two independent Septentrio AsteRx-U Marine GNSS Receivers, with PolaNt-x geodetic antennas augmented by Fugro MarineStar G4+ corrections (Table 8)..

The receivers were also used within the HSS as the aiding source for the ROVINS INS system. Due to the distance between GNSS receivers, the ROVINS and Kongsberg Processing Unit (PU) on the OS, a Trimble 9205 GNSS receiver was installed to provide PPS time synchronisation to the HSS.

Table 10: Septentrio AsteRx-U Marine GNSS specifications

Septentrio AsteRx-U Marine GNSS Receiver	
L1/L2/L3/L5 GPS Receiver	L1 C/A, L2C code, L1/L2/L2C full cycle carrier
L1/L2 GLONASS Receiver	L1/L2 full cycle carrier
B1, B2, B3 Beidou Receiver	Yes (not in use for SI1007)
E1/E5 Galileo Receiver	Yes
Channels	544
GNSS Antenna Type	Septentrio PolaNt-X MF
Correction Signals	MarineStar G4+
Horizontal accuracy GPS/GNSS	6cm (95%) (MarineStar G4+)
Vertical accuracy GPS/GNSS	8cm (95%) (MarineStar G4+)
Timing	1 PPS

3.7.2 Navigation check

Due to the M/V Offshore Solution being mobilised with two independent positioning systems (Port and Starboard Septentrio GNSS) a position check was undertaken between the two systems. As all elements (laybacks, GNSS antennae, GNSS receiver) are entirely independent, this permits a navigation validation by comparison of result data for a common point within the boat reference frame.

Both positioning systems were logged at a 1 second interval for 30 minutes through QINSy with a text file output being Date, Time, Easting, Northing, Height. Both systems were receiving G4+ corrections. No further post processing of the GNSS data has taken place. The output position was the common Water Line Reference mark as determined by the dimensional control survey. Logging both sensors as referred to this position provides not only a check on the GNSS systems but also a confirmation that the laybacks are correct.

Results from the Port GNSS were compared with the results from the Starboard GNSS to generate the difference between the two in Easting, Northing and Height. Table 9 details results of the comparison.

Table 11: Navigation Validation – Static Position Check Results

Sample Population: 1800	Δ Easting (m)	Δ Northing (m)	Δ Height (m)
Minimum	0.031	-0.032	-0.019
Maximum	0.067	0.016	0.034
Standard Deviation (1 σ)	0.007	0.009	0.008
95% Uncertainty (2 σ)	0.014	0.018	0.015
3D Radial Standard Deviation	0.0039		

The results validate the lever arm offsets applied in QINSy from the dimensional control. A 3D Radial Standard Deviation of 0.04m between the two independent positioning systems validates the GNSS units are providing accurate positions to within the specification of each device.

3.8 Motion Sensor

3.8.1 Installation

The MBES pole was fitted on with a mounting plate just below the deck level, to which an iXblue ROVINS Inertial Navigation System (INS) was fitted. The ROVINS employs Fibre Optic Gyroscope (FOG) and quartz accelerometer technology to output highly accurate pitch, roll, heave, heading and trajectory data. The inertial engine operates independently of any aiding GNSS and this permits real-time trajectory smoothing assisted by GNSS data.

Table 12: ROVINS Technical Specification

ROVINS – iXblue	
Heading Accuracy	0.05 deg secant latitude across full environmental range 0.024 deg typical in operating region
Roll and Pitch accuracy **RMS values** ***Secant latitude = 1/cosine latitude***	 0.01 deg (RMS) across full environmental range 0.001 deg (RMS) typical in operating region
Heave accuracy ***Smart Heave***	5cm or 5% of movement (real-time) 2.5cm or 2.5% of movement (100s delay)
Data output rate	0.1Hz to 200Hz

3.8.2 Heading Check

As the vessel was mobilised with two independent INS systems the heading check was run by comparing the output of the Port ROVINS and the output from the Starboard ROVINS. The offset between the two INS base plates has been calculated from the dimensional control survey and is compared to the difference between the two systems. Both systems were logged for 30 minutes at a 1 second interval in QINSy with the text file output being Data, Time, Heading.

Table 13: Vessel heading check results (subset of results and summary statistics)

UTC Date (dd/mm/yyyy)	UTC Time (hh:mm:ss)	Port ROVINS Heading (d.d)	Starboard ROVINS Heading (d.d)	Difference (d.d)
21/02/2021	20:02:53	206.192	205.966	0.226
21/02/2021	20:02:54	206.192	205.966	0.226
21/02/2021	20:02:55	206.192	205.966	0.226
21/02/2021	20:02:56	206.192	205.966	0.226
21/02/2021	20:02:57	206.192	205.966	0.226
21/02/2021	20:02:58	206.192	205.966	0.226
21/02/2021	20:02:59	206.197	205.972	0.225
21/02/2021	20:03:00	206.197	205.972	0.225
21/02/2021	20:03:01	206.197	205.972	0.225
21/02/2021	20:03:02	206.197	205.972	0.225
21/02/2021	20:03:03	206.197	205.972	0.225
21/02/2021	20:03:04	206.197	205.977	0.22
21/02/2021	20:03:05	206.203	205.977	0.226
21/02/2021	20:02:53	206.192	205.966	0.226
			Mean Difference (degrees) - From all data (1800 samples)	**0.219**
			Standard Deviation (1 sigma) - From all data (1800 samples)	**0.004**
			95% Uncertainty (2 sigma) - From all data (1800 samples)	**0.008**
			Difference (Degrees) Calculated from Dimensional Control Survey	**0.168**

The results confirm that both ROVINS have been installed correctly and the systems are aligned with each other to within 0.219°. The ROVINS heading agree with the results obtained by dimensional control to within 0.051°.

3.9 Sound Velocity

3.9.1 Valeport Mini SVS

OS was equipped with a Sound Velocity Surface for direct sound velocity reading at the MBES transducer. The data is input to the MBES software for beam forming correction.

Table 14: Valeport Mini SVS Specifications

Mini SVS - Valeport	
Sound Velocity	Range: 1375 – 1900 m/s Resolution: 0.001 m/s Accuracy: +/- 0.02 m/s

3.9.2 Valeport SWiFT SVT

OS was equipped with a Sound Velocity Profiler for water column sound velocity profiling.

Table 15: Valeport SWiFT Specifications

SVP SWiFT - Valeport	
Sound Velocity	Range: 1375 – 1900 m/s Resolution: 0.001 m/s Accuracy: +/- 0.02 m/s
Pressure	Range: 10 Bar or 20 Bar Resolution: 0.001% FS Accuracy: 0.05% FS
Resolution: 0.001% FS	Range: -5°C to +35°C Resolution: 0.001°C Accuracy: +/- 0.01°C
Accuracy: 0.05% FS	Conductivity: +/- 0.05 mS/cm Salinity: +/- 0.05 PSU Density: +/- 0.05 kg/m3

3.9.3 SVP sensors comparison

The three Valeport Swift SVP units used on this survey were tested against one another concurrently on 25 February 2021 by conducting a dip with all three units strapped to each other. The results are displayed in the below graph and indicate good correlation with each other with a maximum difference between the three units of 0.3 m/s.

The values of the two mini SVS have also been observed independently to the above SV dip and were reading within 0.07m/s of each other with values of 1540.40 (Port) and 1540.47 (Starboard).

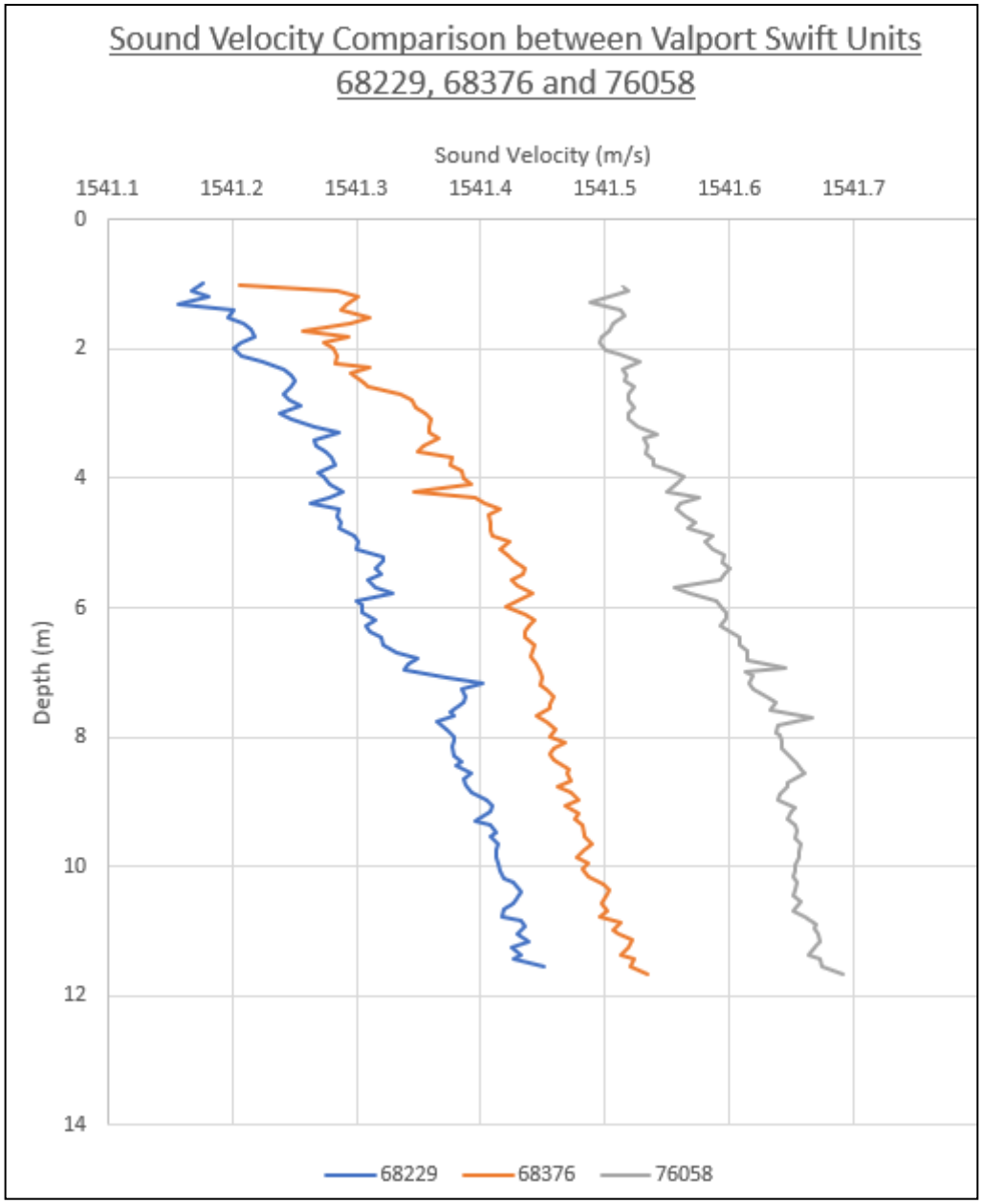

Figure 3-6: Comparison results of three Valeport Swift SV Probes

3.10 Baited Remote Underwater Videos

The seafloor maps, both multibeam data collected during survey and the LiDAR bathymetry data, were used to plan the sampling locations for the Baited Remote Underwater Video Stations (BRUVS). These maps were used to pinpoint areas of interest for potential fish habitat and then creating spatially balanced sampling points within those areas with a heavier weighting applied to reef habitat. Ten points were placed using the multibeam bathymetry data collected during this survey (9 in Area A, 1 in NW corner of Area B) while another 34 were placed based on the seafloor habitat derived from the LiDAR bathymetry (25 in the NE area of Norfolk Island, 3 off the south of Norfolk Island, and 6 NW of Philip Island). A total of 44 BRUVS were deployed for this survey.

3.10.1 Video Collection and Annotation

Stereo-BRUVs (SBRUVs) are an efficient tool for sampling fish assemblages across a range of depths and habitat (Whitmarsh et al. 2017, Langlois et al. 2020). This method is typically used to describe spatial and temporal patterns in fish communities (Cappo et al. 2011, Harvey et al. 2013a, Logan et al. 2017); fish activity patterns

(Bond et al. 2018); behaviour (Watson & Harvey 2007, Birt et al. 2012, Whitmarsh et al. 2018); assemblage structure in pelagic systems (Santana-Garcon et al. 2014, Clarke et al. 2019); responses to protected areas and anthropogenic pressures, fisheries-independent surveys to support targeted species stock assessments and in modelling species distributions (Wines et al. 2020).

Two high definition video cameras (GoPro Hero7 Black) were fitted on each SBRUV frame. The pairs of cameras were mounted 0.7 m apart and angled in at 8° to allow for stereo imaging. Filming in stereo adds the capability for making accurate measurements of individual fish, informing estimates of biomass (Harvey et al. 2003, Langlois et al. 2018). Each SBRUV frame was calibrated in a pool prior to fieldwork commencing. SBRUVs were baited with one kilogram of pacific sardines (*Sardinops sagax*) to attract fish into the field of view of ~~of~~ the cameras. They were then left to soak on the seafloor for a minimum of 60 minutes. Six SBRUVs were deployed simultaneously in rotation in clusters across the survey areas to minimise travel time and maximise survey efficiency.

Post-processing of SBRUVs footage was completed using the program EventMeasure (SeaGIS; https://www.seagis.com.au) by trained observers specialised in fish analyses. For each video, the *MaxN* (maximum number of individuals species in the frame at any given time) was recorded, providing a conservative estimate of relative abundance. *MaxN* is a widely recognised way of obtaining fish population data from SBRUVs and means that no individual is double counted (Cappo et al. 2004), thus not considered a measure of absolute abundance, but rather an estimate of relative abundance (i.e. relative to the abundances scored on other BRUVs). The total length of each individual fish counted in the *MaxN* for each species (where applicable) in each video was then measured to within 10 mm precision (with most measurements within 5 mm of precision) using standard metrics in EventMeasure (SeaGIS 2020). Weights of individuals of each species were estimated using length-weight relationships obtained from Fishbase (Froese & Pauly 2010). Where length-weight relationships were not available for a species, that of a close relative was used. Total biomass was calculated as the sum of individual weights of each species, for each site. Where all individuals were not able to be measured at the *MaxN*, the mean weight of that species was assigned based on the mean of the individuals for each species able to be measured for each season. Total species richness, family richness, total relative abundance and total relative biomass were subsequently calculated for each deployment.

Species were identified to the lowest taxonomic level possible. There were occasions where similar species were indistinguishable from the video footage that were classed to family or genus level where possible but still included in all analyses. This may lead to a conservative estimate of species count, especially if multiple likely species are potentially present contributing to complexes identified. Similarly, there were individuals or groups of species which were not able to be identified to species level.

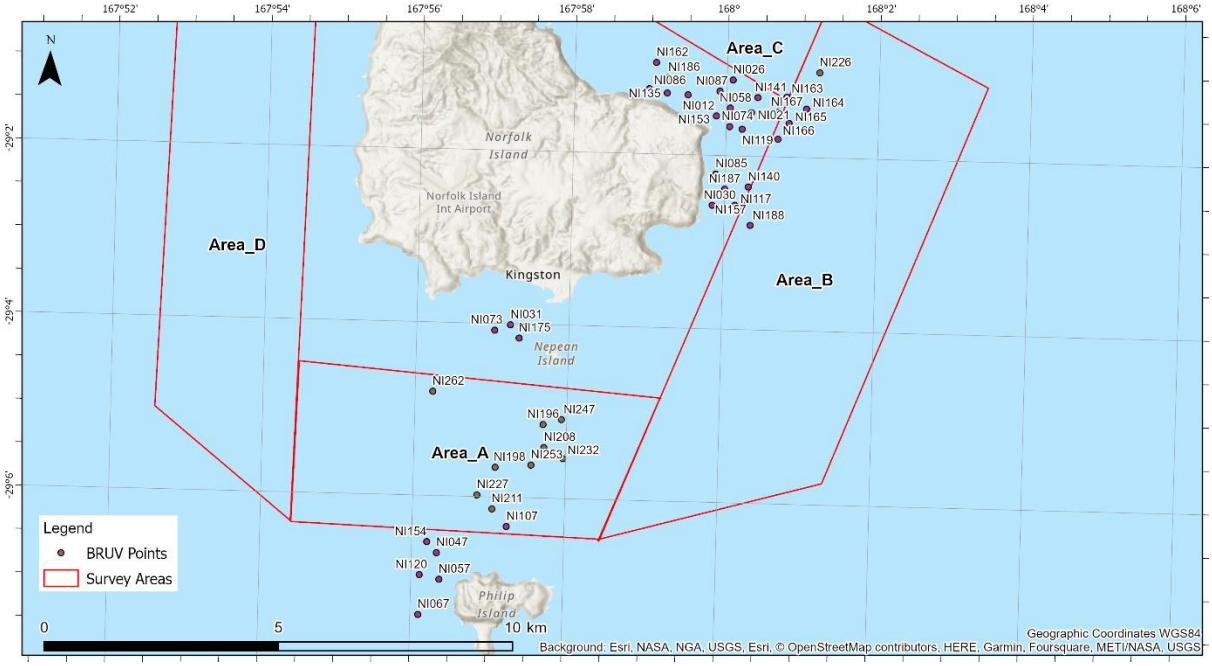

Figure 3-7: BRUVs location points

3.11 Aerial Coastal Mapping

Coastal mapping was performed by Tellus4D, using a Mavic 2 with built-in Hasselblad L1D-20c camera drone. The drone was deployed from shore, controlled by a certified and experienced operator. The position of the drone was provided by its internal GNSS, using GPS and GLONASS satellites constellation. Table 16 contains detailed specifications of the camera, the drone and its sensing system.

Table 16: Drone Photogrammetry Mavic 2 Pro Technical Specifications

Mavic 2 Pro	
Camera	
Sensor	1” CMOS. Effective Pixels: 20 million
Lens	FOV: about 77° 35 mm Format Equivalent: 28 mm Aperture: f/2.8–f/11 Shooting Range: 1 m to ∞
ISO Range	Video: 100-6400 Photo: 100-3200 (auto) 100-12800 (manual)
Shutter Speed	Electronic Shutter: 8–1/8000s
Still Image Size	5472×3648
Still Photography Modes	Single shot Burst shooting: 3/5 frame Auto Exposure Bracketing (AEB): 3/5 bracketed frames at 0.7 EV Bias Interval (JPEG: 2/3/5/7/10/15/20/30/60s RAW:5/7/10/15/20/30/60s)
Color Mode	Dlog-M (10bit), support HDR video (HLG 10bit)
Aircraft	
Takeoff Weight	Mavic 2 Pro: 907 g
Dimensions	Folded: 214×91×84 mm (length×width×height) Unfolded: 322×242×84 mm (length×width×height)
Diagonal Distance	354 mm
Max Ascent Speed	5 m/s (S-mode) 4 m/s (P-mode)
Max Descent Speed	3 m/s (S-mode) 3 m/s (P-mode)
Max Speed (near sea level, no wind)	72 kph (S-mode)
Maximum Takeoff Altitude	6000 m
Max Flight Time (no wind)	31 minutes (at a consistent 25 kph)

Max Hovering Time (no wind)	29 minutes
Max Flight Distance (no wind)	18 km (at a consistent 50 kph)
Max Wind Speed Resistance	29–38 kph
Max Tilt Angle	35° (S-mode, with remote controller) 25° (P-mode)
Max Angular Velocity	200°/s
Operating Temperature Range	-10°C to 40°C
Operating Frequency	2.400 - 2.483 GHz 5.725 - 5.850 GHz
GNSS	GPS+GLONASS
Hovering Accuracy Range	Vertical: ± 0.1 m (when vision positioning is active) ± 0.5 m (with GPS positioning) Horizontal: ± 0.3 m (when vision positioning is active) ± 1.5 m (with GPS positioning)
Sensing System	
Sensing System	Omnidirectional Obstacle Sensing[1]
Forward	Precision Measurement Range: 0.5 - 20 m Detectable Range: 20 - 40 m Effective Sensing Speed: ≤ 14m/s FOV: Horizontal: 40°, Vertical: 70°
Backward	Precision Measurement Range: 0.5 - 16 m Detectable Range: 16 - 32 m Effective Sensing Speed: ≤ 12m/s FOV: Horizontal: 60°, Vertical: 77°
Upward	Precision Measurement Range: 0.1 - 8 m
Downward	Precision Measurement Range: 0.5 - 11 m Detectable Range: 11 - 22 m
Sides	Precision Measurement Range: 0.5 - 10 m Effective Sensing Speed: ≤ 8m/s FOV: Horizontal: 80°, Vertical: 65°

For each site, the flight plan consisted in parallel lines with best orientation to cover the site in a minimum of lines. The navigation during survey was controlled by the autopilot of the navigation system under the operator's supervision, to ensure straight lines and a constant flying altitude (Figure 3-8). The Table 17 summarises the acquisition parameters of each survey sites.

Table 17:Drone acquisition settings for each survey site

Sites	Number of Images	Flying Altitude (m)	Ground Resolution (cm/pix)	Coverage Area (km²)	Line Direction
Captain Cook Lookout	664	187	3.77	6.01	SE-NW and W-E
Anson Bay	844	182	3.51	1.38	SE-NW
Puppy's Point	529	175	3.11	0.66	N-S
Headstone Bay	711	156	3.1	0.71	N-S
Slaughter Bay and Bumbora Beach	1439	104	2.08	1.86	WSW-ENE and WNW-ESE
Ball Bay	1582	197	4.03	1.12	SW-NE
Emily Bay and Cemetery Bay	1498	165	3.22	2.36	WNW-ESE and WSW-ENE

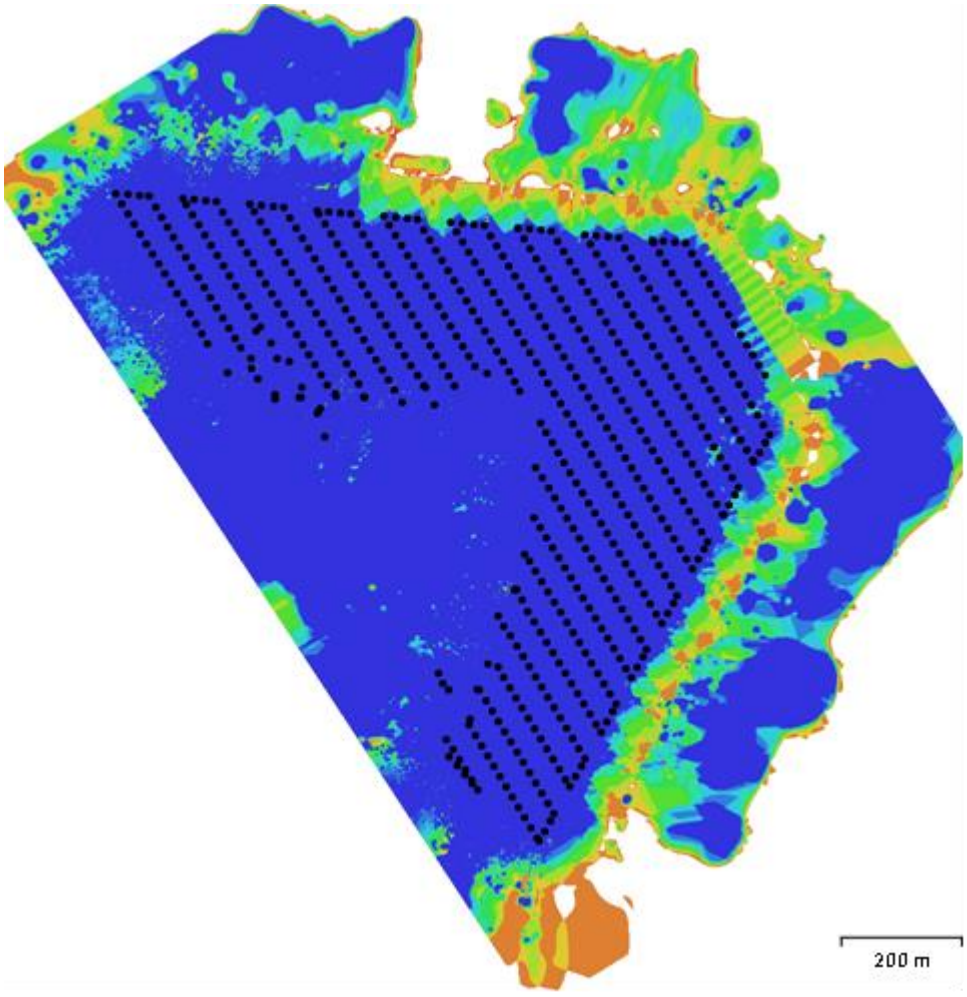

Figure 3-8: Example of flight plan at Anson Bay

4. Data Control Quality and Processing

4.1 Bathymetry

The survey system used for Norfolk Island survey is identical to the survey system approved for the prior Hydrographic Survey SI1020. The following sections are extracted from the reports provided for the Bank Strait survey project.

4.1.1 Data Processing

Raw multibeam data was acquired with Qinsy as .db and .qpd files. Data was processed using the combination of Qimera, Caris and NOAA QC Tools software (Figure 4-1).

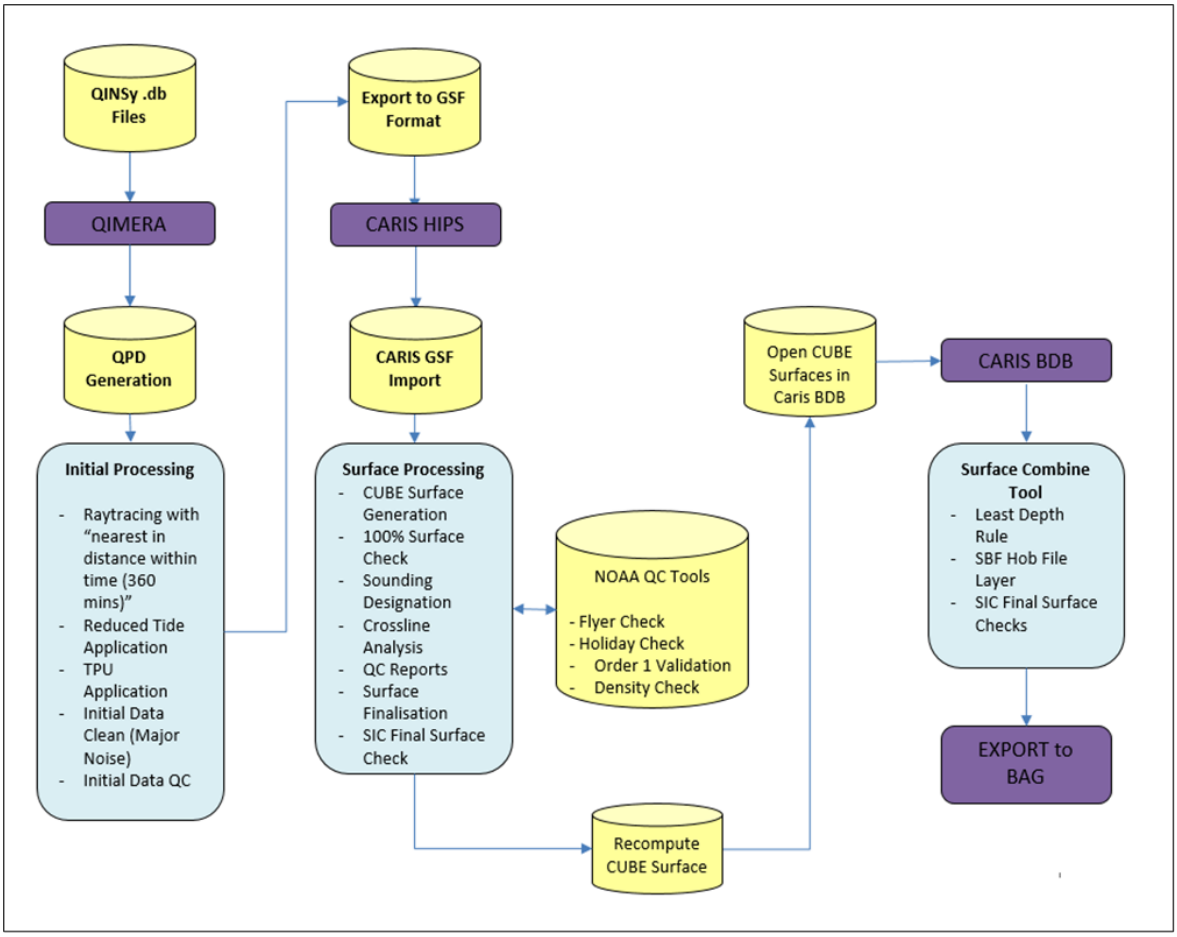

Figure 4-1: Qimera/ CARIS HIPS processing workflow

Initial processing and data qc was conducted in QIMERA where the following was applied:

- sound velocity strategy to "Nearest in distance, within Time"; 240minutes;
- Position, Motion and Heading sources are set to the INS as the primary source;
- SBET is prioritised for the motion where available
- Vertical reduction to local Chart Datum, using tide data at King Wharf;

A dynamic CUBE surface is then created from the georeferenced data using the NOAA_1m configuration settings (Figure 4-2). The surface is checked for any inconsistency or processing errors. Once validated, survey lines are then exported to GSF for ingestion to CARIS HIPS.

In CARIS, a CUBE CSAR surface is generated using the S44 Order-1a configuration (Figure 4-3). During the surface finalisation step, a minimum 95% uncertainty value of 0.437m was assigned, as defined by the crossline analysis (section 4.1.5).

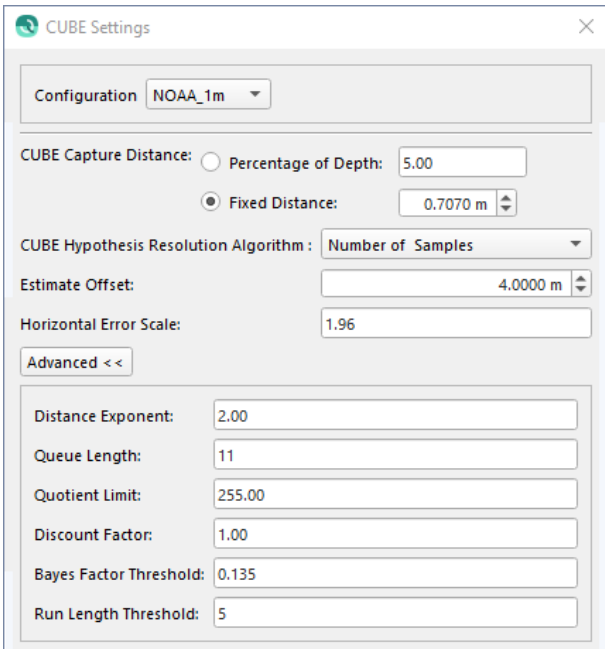

Figure 4-2: NOAA_1m configuration for Cube surface made in Qimera

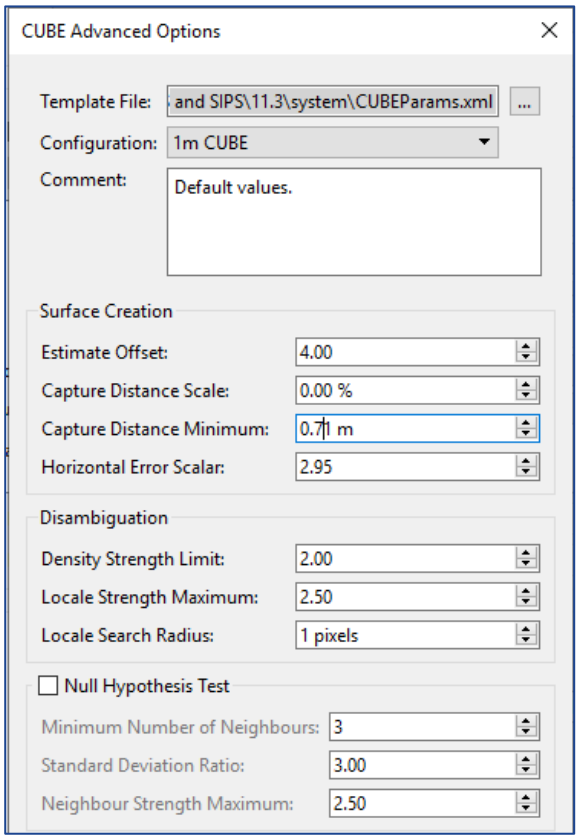

Figure 4-3: Cube surface configuration used in Caris

4.1.2 THU and TVU

Total Horizontal Uncertainty (THU) and Total Vertical Uncertainty (TVU) were initially calculated in Qimera, utilising the specified equipment and layback measurement inputs. Upon application of the reduced tide data, the individual line data containing calculated THU and TVU data was then exported to GSF, for ingestion into CARIS HIPS for further TPU assessment and final surface generation.

4.1.3 Accuracy Requirements

The following formula is used to calculate the accuracy requirements for IHO Order 1a:

Depth Accuracy Requirement (IHO Order 1a)

$$\boldsymbol{depth\ accuracy}\ (\boldsymbol{m}) = \pm(\boldsymbol{a}^2 + (\boldsymbol{bxd})^2)^{\frac{1}{2}}$$

$$\boldsymbol{a = constant\ depth\ uncertainty = 0.5m}$$

$$\boldsymbol{bxd = depth\ dependent\ uncertainty}$$

$$\boldsymbol{b = factor\ of\ depth\ uncertainty = 0.013m}$$

$$\boldsymbol{d = depth}$$

The depth accuracy requirements at the 95 percent confidence level for IHO Order 1a standard are provided in Table 18.

Table 18: IHO Order 1a standard depth accuracy requirements

Depth (m)	10	20	30	40	50	75	100	120
Accuracy (m)	0.517	0.564	0.634	0.721	0.820	1.096	1.393	1.638

The IHO Order 1a standard requires a horizontal accuracy of the position of soundings of:

Positional Accuracy Requirement (IHO Order 1a)

$$position\ accuracy\ (m) = 5m + 5\%\ of\ d$$

$$d = depth$$

The positional accuracy requirements at the 95 percent confidence level for IHO Order 1a standard are provided in Table 19.

Table 19: IHO Order 1a standard positional accuracy requirements

Depth (m)	10	20	30	40	50	75	100	120
Accuracy (m)	5.50	6.00	6.50	7.00	7.500	8.750	10.00	11.00

4.1.4 TPU

A series of assessed values for the various uncertainty sources have been entered into Qimera for each vessel configuration. This allows the computation of horizontal and vertical uncertainty associated with each individual sounding. As each vessel HSS was almost identical, TPU inputs were kept consistent. Qimera directly accounted for the change in MBES Sonar type for the INDIGO by direct reading from the database setup file.

The1σ static errors used to compute the total horizontal and vertical uncertainty are presented in Table 20. Once the individual lines are processed in Qimera, TVU and THU are output in terms of 2σ (95% CL). The exported GSF files used in CARIS are with respect to 2σ.

Table 20: Qimera vessel configuration TPU settings (1σ)

Uncertainty Source (System)	Value	Description
Echo Sounder (EM2040, EM2040P)	0.01º	SD Roll Offset
	0.01º	SD Pitch Offset
	0.01º	SD Heading Offset
	0.05m/s	SD Surface Sound Speed
Motion Sensor; R-P-H (ROVINS, HYDRINS)	0.01º	SD Roll & Pitch
	0.05m	SD Heave Fixed
	0.05%	SD Heave Variable
	0.002º	SD Roll Offset
	0.002º	SD Pitch Offset
Motion Sensor; Heading	0.05º	SD Heading
	0.05º	SD Heading Offset
Positioning System (ROVINS, HYDRINS)	0.1m	SD Horizontal
	0.1m	SD Vertical
Positioning System (Septentrio)	0.1m	SD Horizontal
	0.1m	SD Vertical
Object Track	0.1m	SD Horizontal
	0.1m	SD Vertical
Applied Surface Sound Speed	0.05m/s	SD Observation
Draft	0.05m	Observational Uncertainty
Squat SD	0.050m	Observational Uncertainty
Load SD	0.050m	Observational Uncertainty
Tide SD**	0.090m	Observational Uncertainty

4.1.5 Crossline checks

To account for any real-world effects that may have detracted from the performance of the system, such as poorly performing hardware or errors in the tidal computation an independent empirical check is required to validate the TPU calculations and provide an overall assessment as to whether IHO Order 1a standard has been achieved.

This independent assessment is achieved by comparing every sounding in the crosslines against the combined surface. As the check must be independent, the surface does not include crosslines.

The crossline comparison conducted against the combined surface are:

- **Overall IHO Order 1a Standard Check -** Each crossline is checked against the surface to assess the consistency of IHO Order 1a standard achieved across the survey area (1-512 in steps of 511).

  Crossline uncertainty is derived from the data extracted from CARIS' Line QC Tool and analysed further using the following steps:

1. Standard Deviation for each crossline is multiplied by 1.96 to provide 95% confidence interval (2 Standard Deviations).
2. The mean difference between the crossline and surface is added to the 2 Standard Deviations value to produce the vertical uncertainty for the crossline.

The overall 1m CUBE surface for each survey area was used with the selected attribute layer being the depth layer. The IHO Order 1a standard was used to determine the percentage of soundings compliant with the error limit for depth accuracy. Table 21 provides a statistical analysis between the crosslines and the depth surface and details the percentage of compliant crossline soundings in relation to IHO Order 1a.

Table 21: Result between crosslines and surface

Cross line	Beams	Count	Max (+)	Min (-)	Mean	St Dev	Order 1a % achieved	2SD	Mean+2 SD
0156	1 - 512	1,663,406	10.049	4.472	-0.088	0.135	99.97	0.265	0.353
0102	1 - 512	4,860,851	2.045	1.852	-0.015	0.109	99.96	0.214	0.229
0042	1 - 512	5,698,430	18.189	10.058	0.071	0.145	99.95	0.284	0.355
0044	1 - 512	4,868,396	16.389	5.310	0.028	0.128	99.97	0.251	0.279
0125	1 - 512	3,898,819	25.857	11.753	-0.114	0.438	99.50	0.858	0.972
				Total Average	**-0.0236**	**0.191**	**99.87**	**0.374**	**0.437**

All crosslines conducted throughout the course of the survey indicate that IHO Order 1a has been achieved.

4.1.6 Statement of Accuracy

The multibeam survey was conducted over a 4-day period. On the four areas initially planned, only 3 of them were completely surveyed. Due to the limited time and weather conditions, only a sample of the area D was covered.

Whilst the vertical accuracy data meets the IHO Order 1a requirements, the retained Order for the dataset has been assessed at the **IHO Order 1b standard,** due to feature detection over shoals not being achieved in all locations. This was a conscious decision by the project lead scientist to collect as much data as possible in the time allowed.

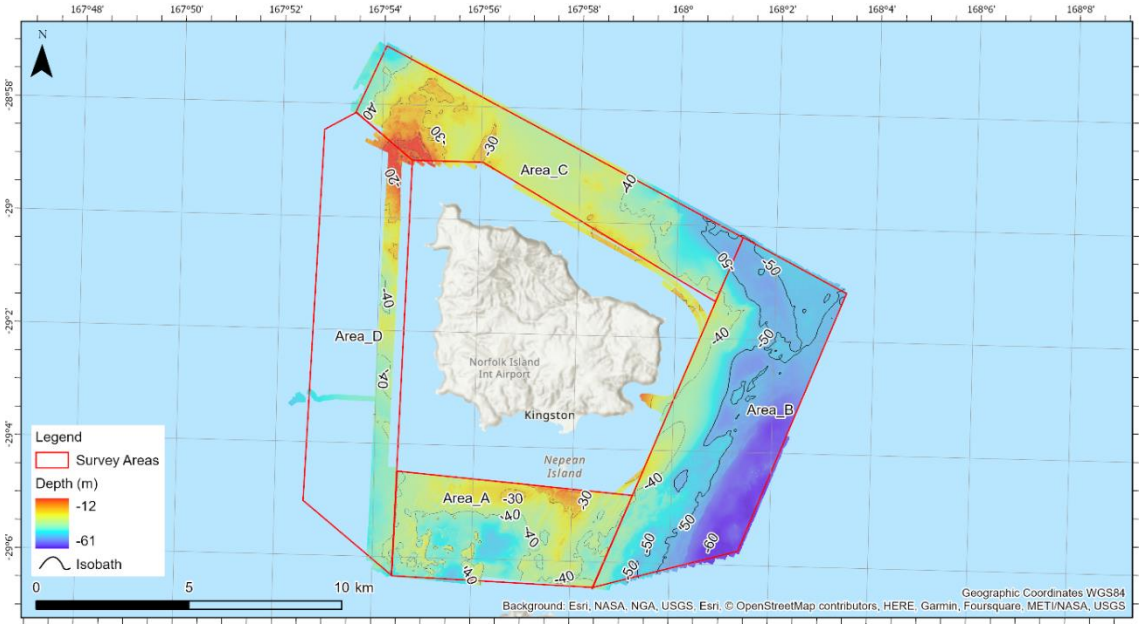

Figure 4-4: Processed bathymetry overview

4.2 Backscatter imagery

The workflow utilised for backscatter interpretation and mosaic construction in FMGT software is shown in Figure 4-5. These processing steps are recognised as best practice, detailed by the GEOHAB backscatter working group (http://geohab.org/bswg/) papers.

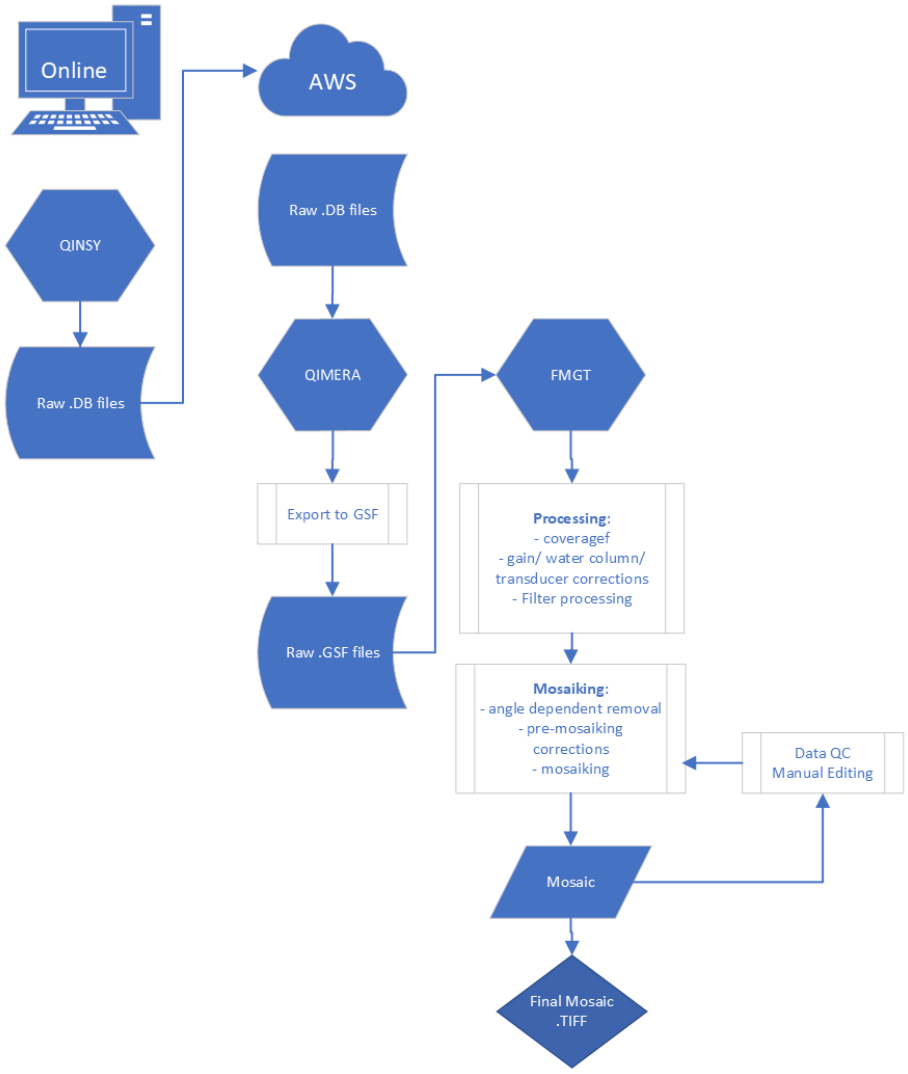

Figure 4-5: Backscatter processing workflow

The combined backscatter data from each survey line was systematically processed by correcting for physical factors that alter the amount of acoustic energy that reflects off the seafloor. Data is expressed in backscatter strength with a working unit of decibels (DB). Corrections applied to each ping before merging the results into a mosaic included:

- removal of transmission loss
- removal of sonar specific angular dependence model
- calculating angle of incidence
- calculating angular response within the working range
- removal of angular dependence and restoration of backscatter strength with reference to angle

Echo-sounder frequency and pulse length remained consistent throughout the survey. This contributed to a highly consistent backscatter mosaic, with minimal normalisation required between lines and areas.

The backscatter mosaics was generated at 1m resolution (Figure 4-6).

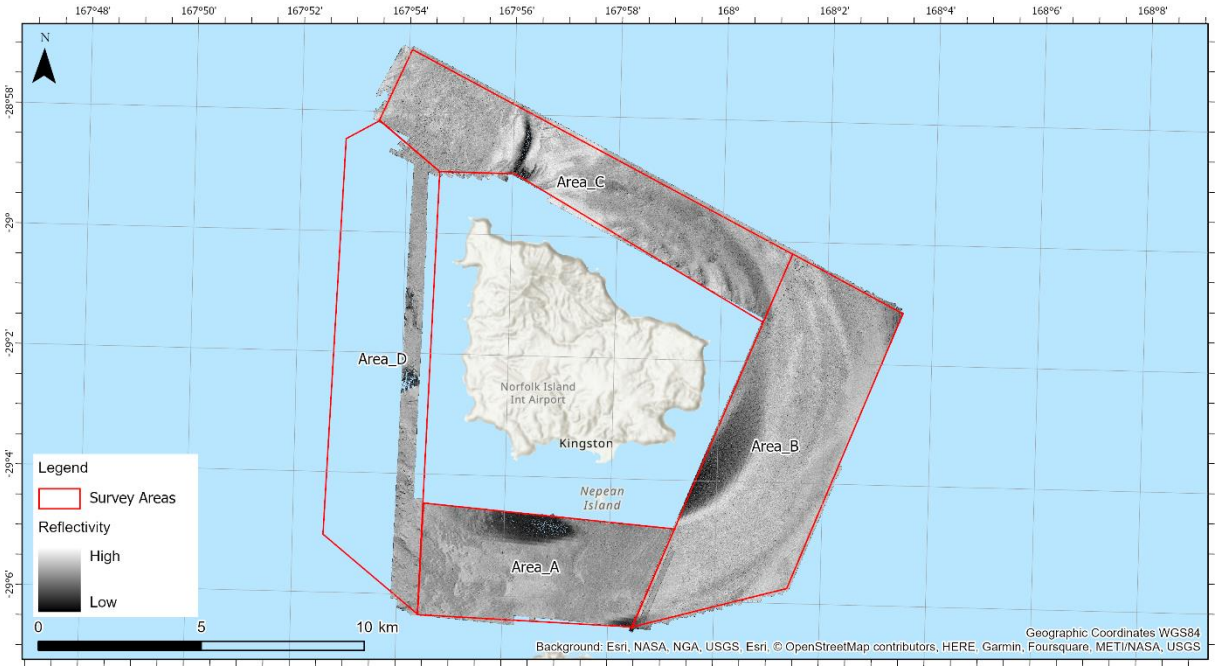

Figure 4-6: Backscatter Imagery

4.3 Sub-bottom profiler

SBP data was acquired using the iXblue Delph Acquisition software in XTF format. Data files are then processed in Delph Interpretation, where the following data quality control and light processing are performed::

- Heave correction applied;
- Bottom picking to apply swell filter (when necessary) and water column removal;
- TIFF export – raw profiles;
- Convert XTF to SEGY.

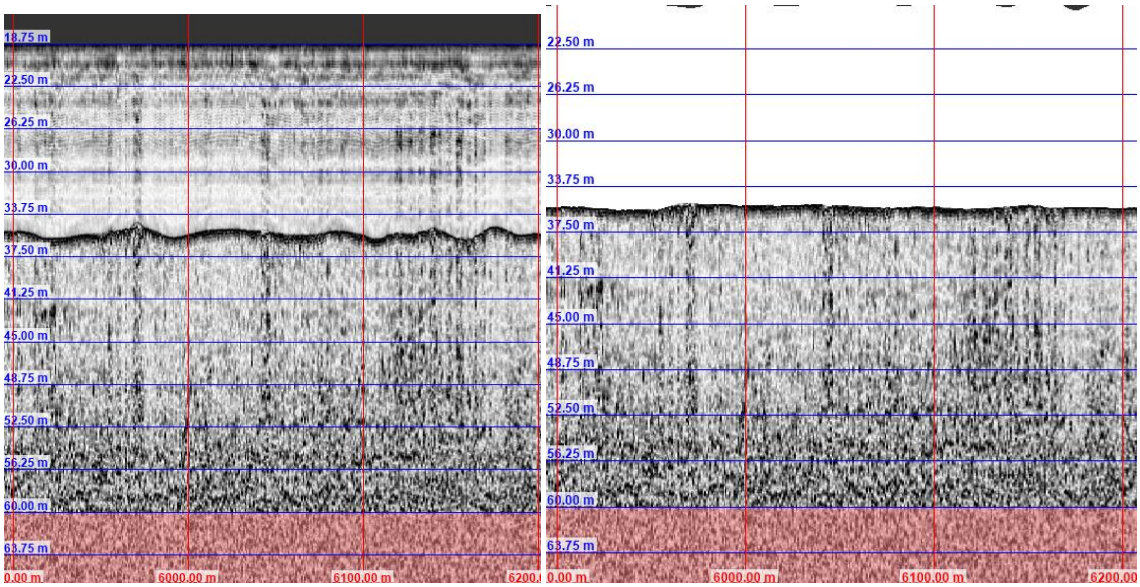

Figure 4-7: Profile extracts of before (left) and after (right) heave correction and water column removal

4.4 Baited Remote Underwater Videos

Of the 44 BRUVS deployed around Norfolk Island, 42 deployments were successfully analysed. The deployments occurred in a depth range between 12–48 m. The habitats sampled consisted of mainly stony coral dominated infralittoral reef or soft sediment (Figure 4-8; Figure 4-9). Encrusting stony corals made up the majority of the stony coral cover, followed by foliose and plate forms, and digitate forms. Soft sediment cover was predominantly made up of fine sand with some biogenic pebble cover in deeper areas (Figure 4-8). Records of the canopy forming kelp *Ecklonia radiata* at Norfolk Island were also observed from the BRUVS footage (NF_165 and NF_175) which is the northern-most extent of its range.

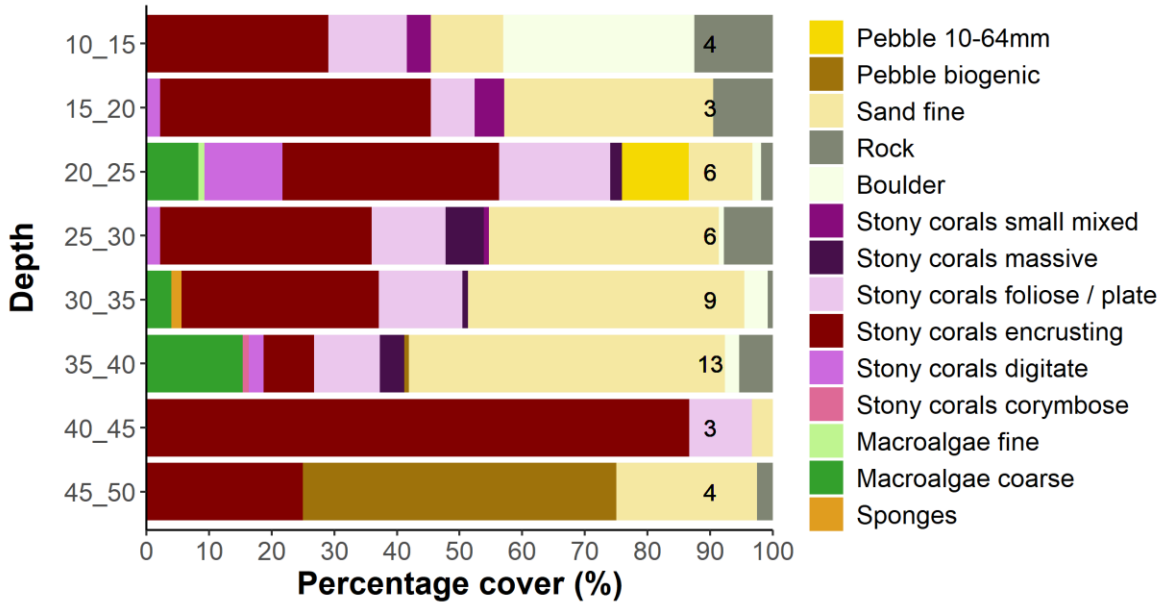

Figure 4-8: Percentage cover of each habitat type observed in the BRUVS footage by depth zone.

Habitat examples | Fish assemblage examples

Figure 4-9: Screenshots from the BRUVS deployments showing examples of habitats and fish assemblages observed

From the BRUVS, 3,094 individuals were observed across 76 taxa within 35 families (Figure 4-9). Individuals from family Pomacentridae comprised of over 50 % of the total observations alone, while the next highest percentage came from Labridae at only 9 % (Figure 4-10). The Norfolk chromis *Chromis norfolkensis*, were the most abundant taxa observed followed by southern demoiselle *Chrysiptera notialis*, and one-spot puller *Chromis hypsilepis* (Figure 4-10). Across all deployments, the taxa observed were quite variable with the most widespread taxa, luculent wrasse *Pseudolabrus luculentus*, occurring on 69 % of deployments, followed by grey moray *Gymnothorax nubilus* and redthroat emperor *Lethrinus miniatus* on 61 % of deployments. All other species occurred on less than 50 % of deployments. Large-bodied sharks and fishes contributed most to the biomass observed, with sharks in the Carcharhinidae family comprising of over 46 % of observations, followed by individuals in the Carangidae family at 27 %. The tiger shark *Galeocerdo cuvier* had the highest biomass observed, followed by yellowtail kingfish *Seriola lalandi* (Figure 4-10).

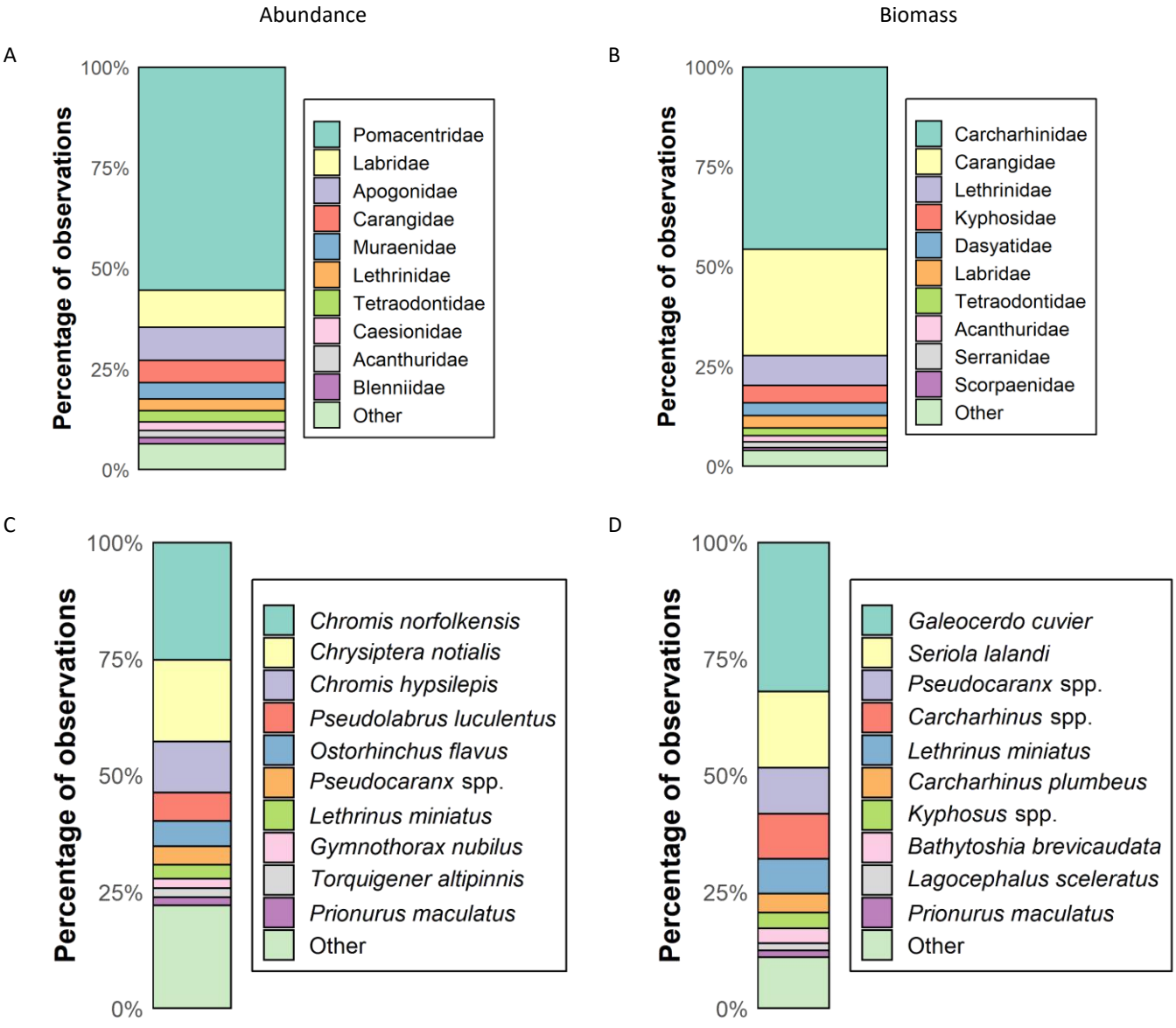

Figure 4-10: Percentage contribution of each family to observations for abundance (A) and biomass (B) and percentage contribution of each species to abundance (C) and biomass (D).

Species richness and total abundance differed significantly by habitat type, but total biomass did not (Figure 4-11). Higher abundance and richness were observed in infralittoral reef habitats compared to soft sediment habitats. The fish assemblage also differed significantly by habitat type (Table 22, Figure 4-11). Only two species out of the top ten contributing to differences between habitat types had higher abundances on the soft sediment compared to infralittoral reef, the highfin toadfish *Torquigener altipinnis* and the silver toadfish *Lagocephalus sceleratus*. The remaining eight species had higher abundances on infralittoral reef habitats (Table 23).

Species richness and total biomass differed significantly by depth, while total abundance did not (Figure 4-11). Lower species richness was observed in the 30–40 m and 40+ m classes compared to the 10–20 m and 20–30 m and the 40+ m class had the highest biomass compared to all other depth classes (Figure 4-11). Similar to habitat type, the fish assemblage was also significantly different in different depth classes (Table 22, Figure 4-11). The shallowest two depth classes 10–20 m and 20–30 m, differed to the two deepest classes 30–40 m and 40+ m (Table 22). The shallowest depth class had higher abundances of luculent wrasse *Pseudolabrus luculentus*, banded scalyfin *Parma polylepis*, and southern demoiselle *Chrysiptera notialis* compared to deeper classes, which had higher abundances of highfin toadfish *Torquigener altipinnis*, grey moray *Gymnothorax nubilus*, yellowtail kingfish *Seriola lalandi*, and redthroat emperor *Lethrinus miniatus* (Table 24). The 20–30 m depth class had higher abundances of yellow-banded wirrah *Acanthistius cinctus* and whaler sharks *Carcharhinus* spp. (Table 24 and Table 22).

The spatial distribution of richness, abundance, and biomass showed that all were higher in the rocky reef areas while lower richness, abundance, and biomass occurred in the lower relief, sedimentary areas (Figure 4-12, Figure 4-13, Figure 413). Additionally, higher richness was found in the regions around the northwest point of Norfolk Island and northeast and north of Philip Island (Figure 4-12). Biomass and abundance have similar patterns but with slightly greater biomass in the deeper depths compared moving offshore of the islands compared to abundance (Figure 4).

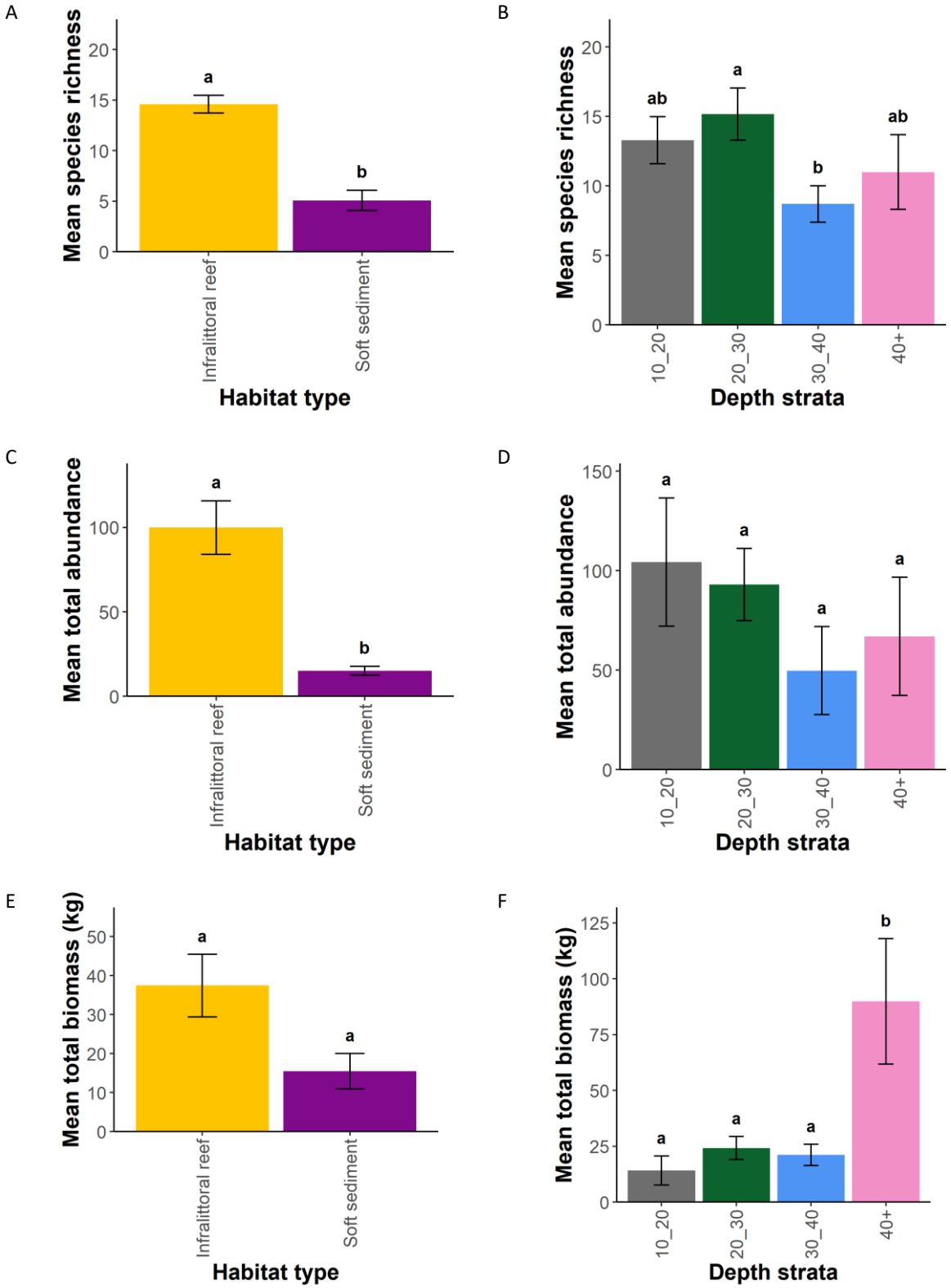

Figure 4-11: Mean species richness by habitat type (A) and depth (B), mean total abundance by habitat type (C) and depth (D), and mean total biomass by habitat type (E) and depth (F).

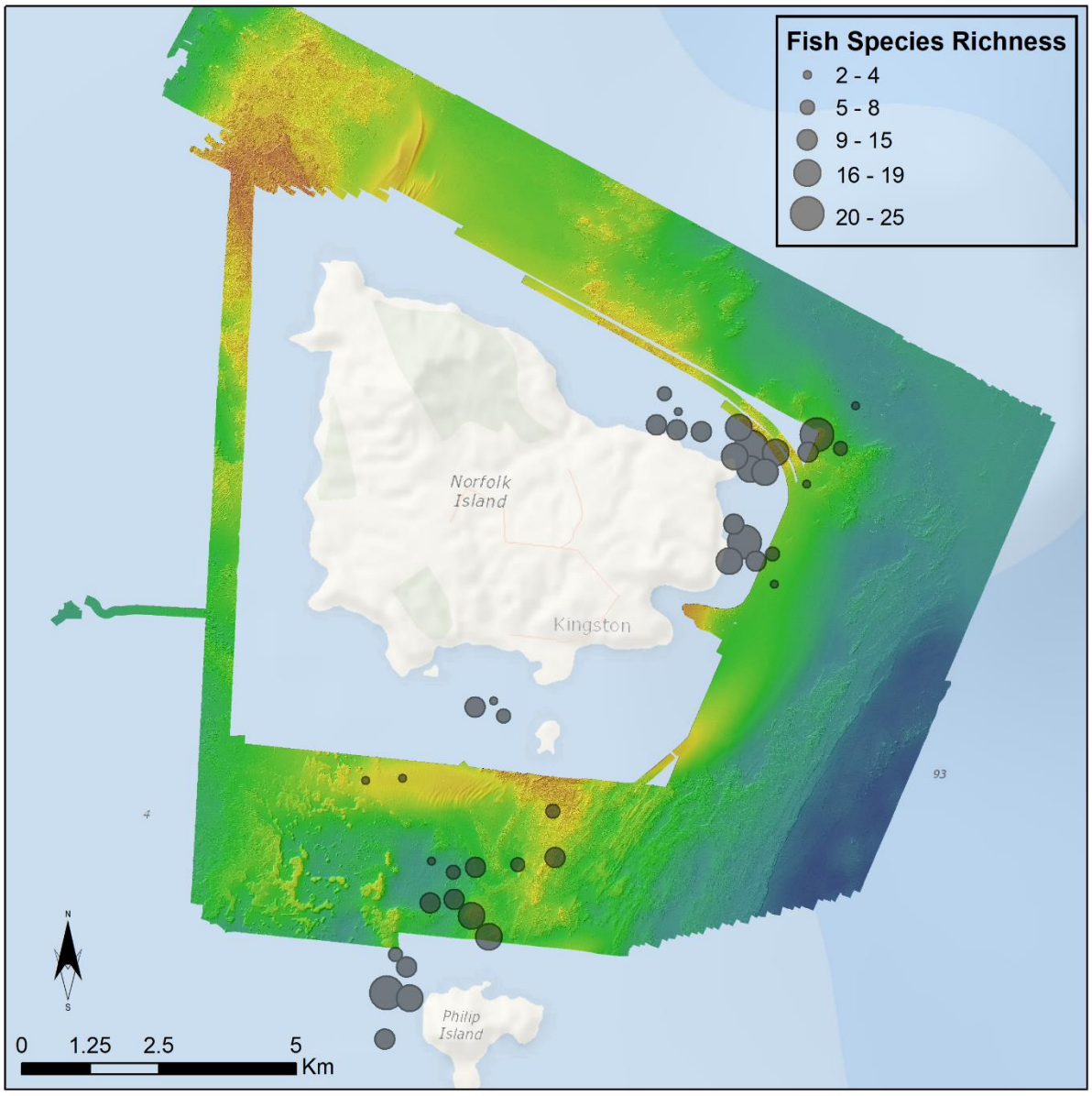

Figure 4-12: Bathymetric map of Norfolk Island with the fish species richness derived from the BRUVS overlaid as a bubble plot. The larger circles represent greater species richness (number of species), while the smaller bubbles represent lower fish species richness.

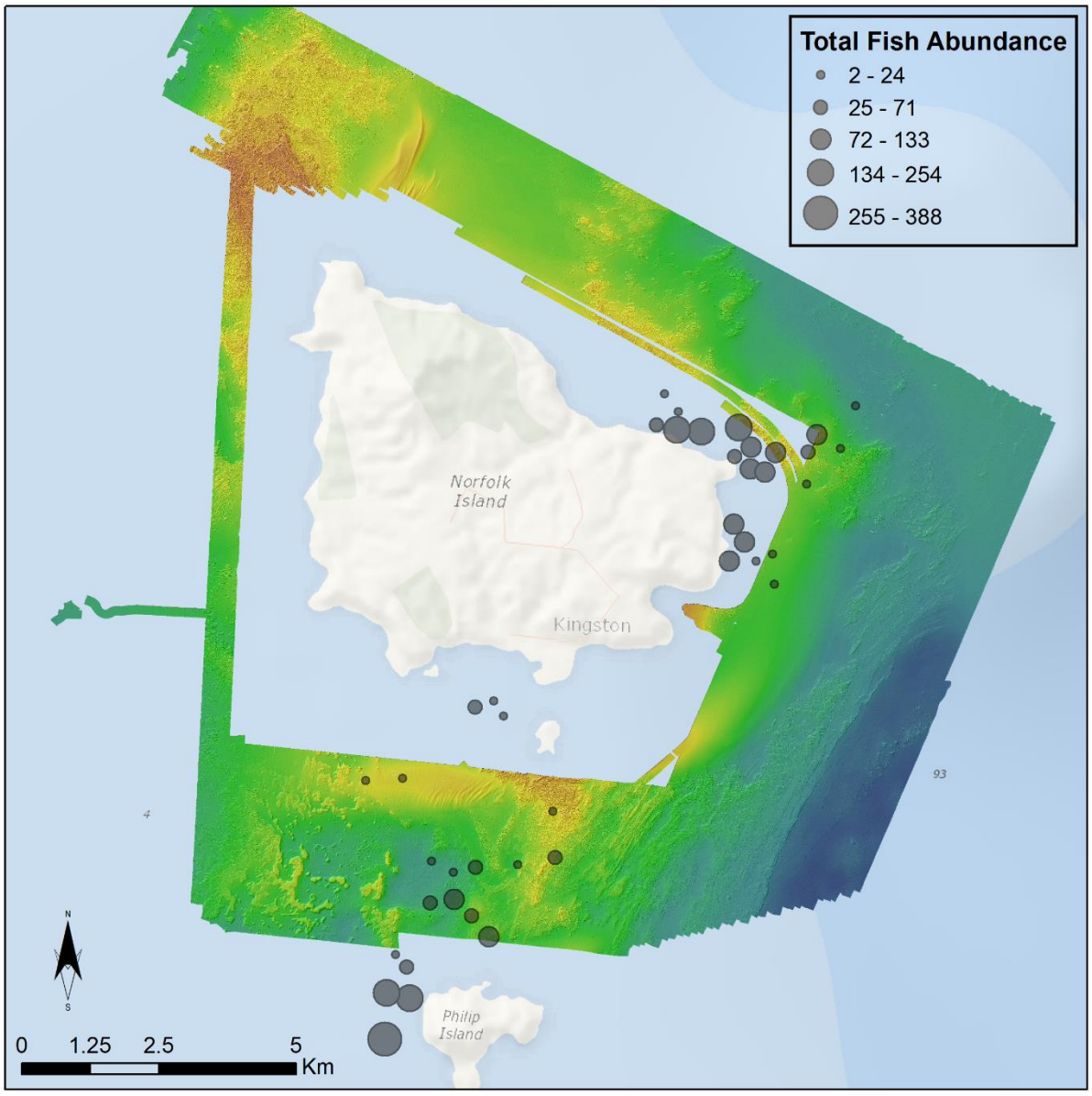

Figure 4-13: Bathymetric map of Norfolk Island with the total fish abundance derived from the BRUVS overlaid as a bubble plot. The larger circles represent greater abundance (number of individuals), while the smaller bubbles represent lower fish abundance.

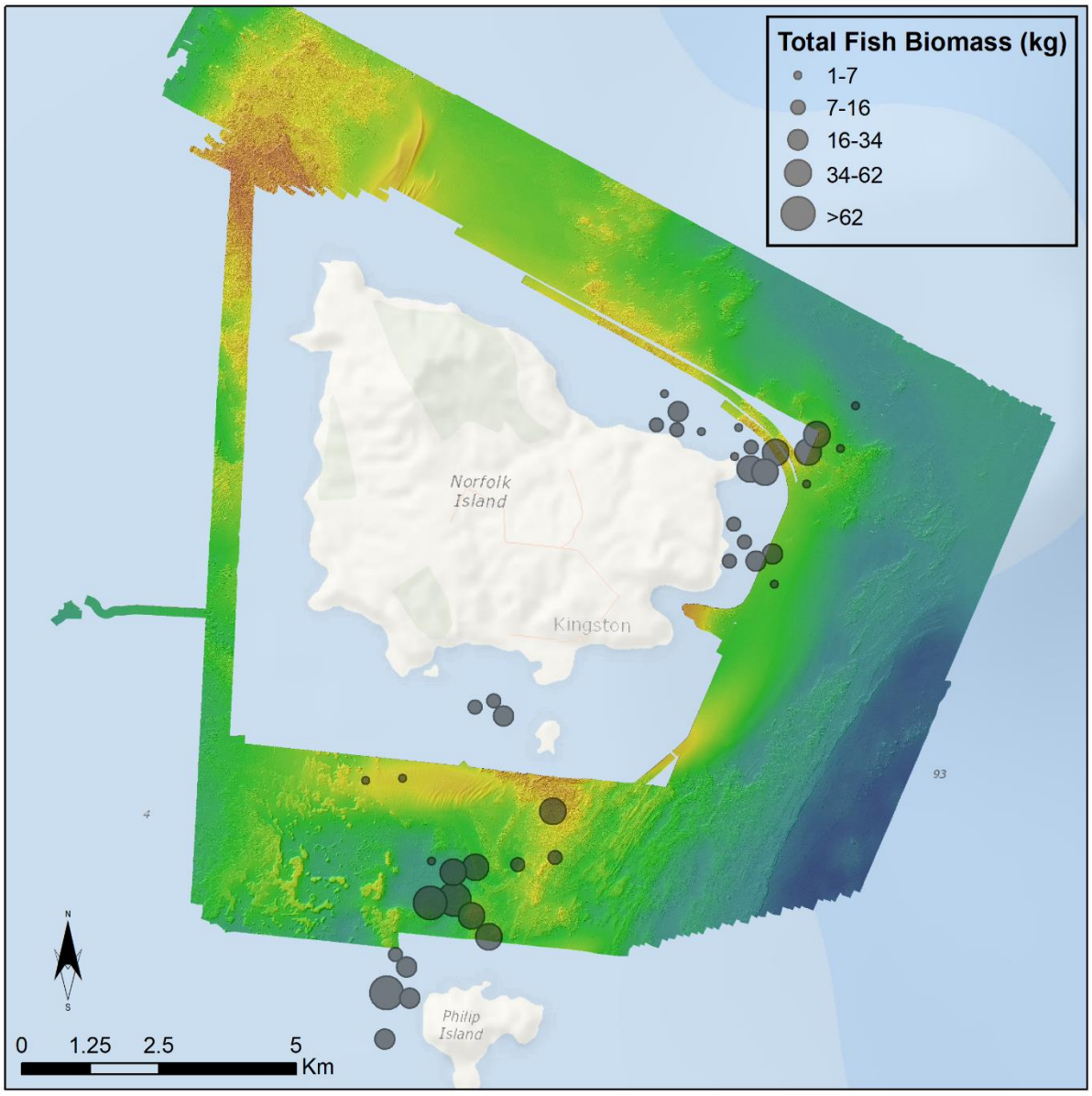

Figure 4-14: Bathymetric map of Norfolk Island with the fish biomass derived from the BRUVS overlaid as a bubble plot. The larger circles represent greater biomass in kilograms, while the smaller bubbles represent lower fish biomass.

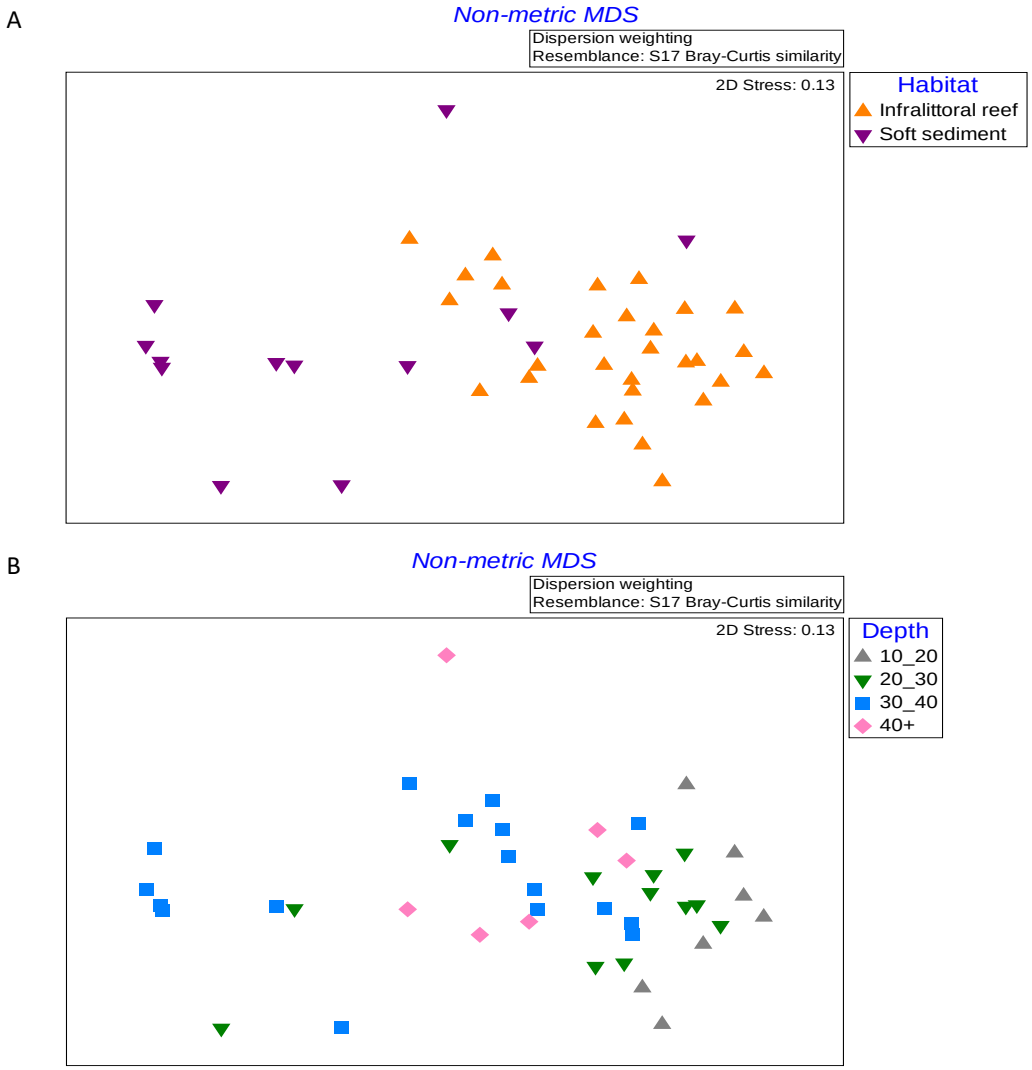

Figure 4-15: nMDS plot showing the factor A) habitat and B) depth for the BRUVS deployments at Norfolk Island. Each symbol represents one BRUVS deployment and the spacing signifies similarity between deployments.

Table 22: Comparison of fish assemblages across depth and habitat classes.

Factor	df	MS	Pseudo-*F*	*P*	Pairs	t	*P*
Habitat	1	22390	7.48	**0.001**			
					10–20 vs 20–30	1.11	0.2
					10–20 vs 30–40	1.88	**0.001**
					10–20 vs 40+	1.77	**0.001**
Depth	3	7051.3	2.21	**0.001**	20–30 vs 30–40	1.50	**0.037**
					20–30 vs 40+	1.38	**0.039**
					30–40 vs 40+	1.16	0.218

Table 23: Results from the SIMPER analysis showing the top species contributing to differences between habitat types.

Taxa	Average abundance			Average dissimilarity	Diss/SD	% contribution
	Infralittoral reef		Soft sediment			
Torquigener altipinnis	0.01	<	1.72	8.73	0.82	9.59
Pseudolabrus luculentus	1.58	>	0.30	6.75	**1.27**	7.42
Acanthistius cinctus	1.00	>	0.00	4.53	0.82	4.98
Gymnothorax nubilus	0.69	>	0.40	4.11	0.83	4.52
Carcharhinus spp.	0.59	>	0.31	3.85	0.90	4.23
Seriola lalandi	0.79	>	0.08	3.67	0.91	4.03
Lethrinus miniatus	0.72	>	0.20	3.58	0.85	3.93
Lagocephalus sceleratus	0.07	<	0.62	3.30	0.95	3.63
Notolabrus inscriptus	0.66	>	0.08	2.95	0.91	3.24
Chrysiptera notialis	0.57	>	0.00	2.55	0.74	2.80

Table 24: Results from the SIMPER analysis showing the top species contributing to differences between depth classes.

Taxa	Average Abundance			Average dissimilarity	Diss/SD	% contribution
	10–20		30–40			
Torquigener altipinnis	0.00	<	1.22	6.69	0.62	7.59
Pseudolabrus luculentus	1.57	>	0.65	6.25	1.45	7.09
Parma polylepis	0.86	>	0.00	3.94	1.19	4.47
Chrysiptera notialis	0.80	>	0.12	3.81	0.89	4.32
Carcharhinus spp.	0.43	~	0.47	3.72	0.69	4.22
	10–20		40+			
Gymnothorax nubilus	0.11	<	1.20	5.10	1.02	5.91
Pseudolabrus luculentus	1.57	>	0.61	5.08	1.09	5.88
Seriola lalandi	0.53	<	1.24	4.56	1.18	5.28
Lethrinus miniatus	0.04	<	0.98	4.07	1.27	4.72
Parma polylepis	0.86	>	0.00	3.71	1.12	4.30
	20–30		30–40			
Pseudolabrus luculentus	2.00	>	0.65	7.18	1.23	8.62
Torquigener altipinnis	0.16	<	1.22	6.42	0.66	7.70
Acanthistius cinctus	1.17	>	0.53	4.78	0.95	5.74
Gymnothorax nubilus	0.70	>	0.52	3.53	0.81	4.23
Carcharhinus spp.	0.67	>	0.47	3.10	0.94	3.72
	20–30		40+			
Pseudolabrus luculentus	2.00	<	0.61	6.52	1.18	8.04
Gymnothorax nubilus	0.70	<	1.20	5.05	0.98	6.23
Acanthistius cinctus	1.17	>	0.67	4.51	0.97	5.56
Seriola lalandi	0.40	<	1.24	3.93	1.09	4.84
Lethrinus miniatus	0.36	<	0.98	3.01	0.97	3.70

There were four variables included in the top model to explain the variation in the fish assemblage, depth, % cover of fine sand, % cover of biogenic pebbles, and % cover of coarse macroalgae (Figure #). According to the dbRDA, the first axis, correlated best % cover of fine sand, explained 20 % of the variation observed within the assemblage, while the second axis, correlated best with % cover of coarse macroalgae, explained 10 % of the variation.

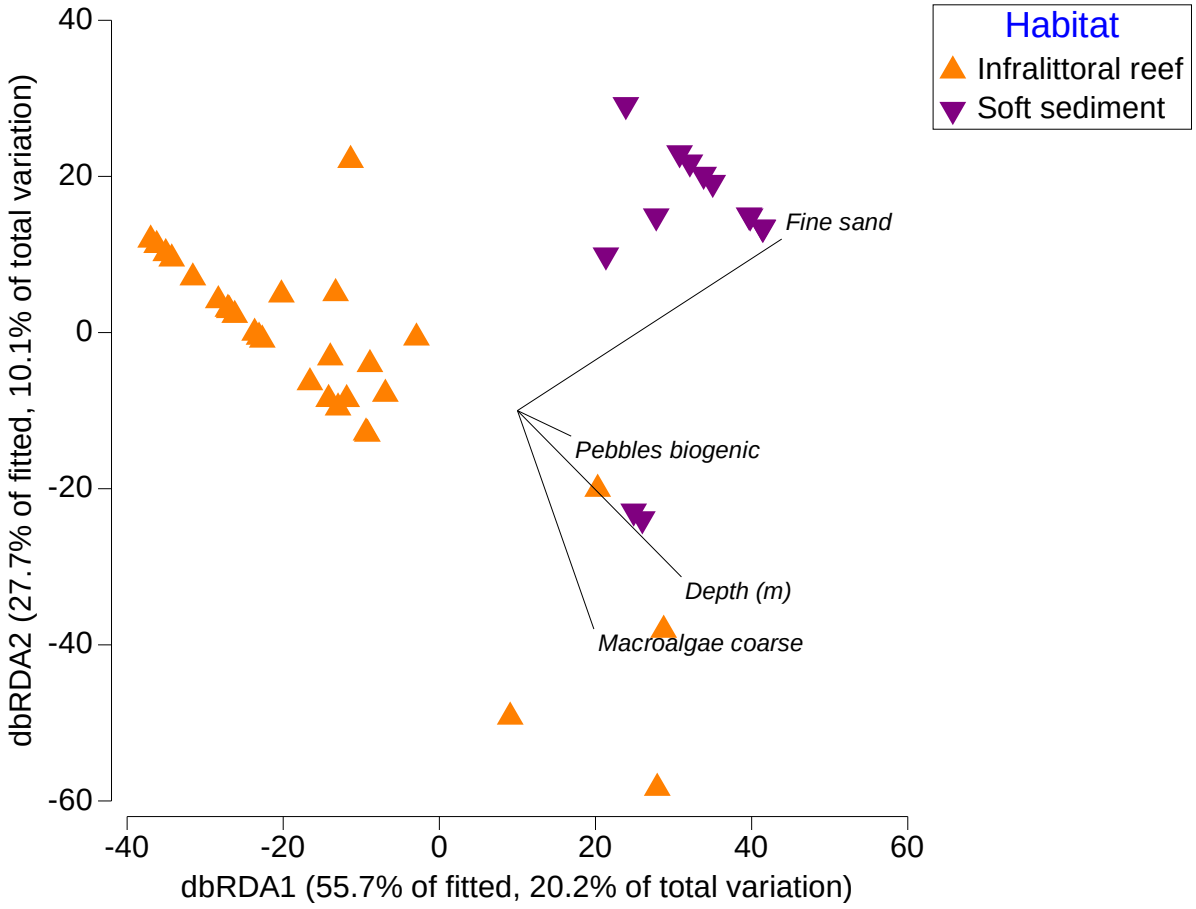

Figure 4-16: Distance based redundancy analysis plots showing the influence of environmental variables (% cover of fine sand, biogenic pebbles and coarse branching macroalgae, and depth (m)) based on the top model output from DISTLM for the BRUVS fish assemblage.

Individual fish were observed across a range of sizes (Figure 4-17). Whaler sharks *Carcharhinus* spp. were among the largest individuals observed followed by kingfish *Seriola lalandi*. Schools of small damselfish and cardinalfish were also readily observed such as *Ostorhinchus flavus* and *Chromis norfolkensis.*

Carcharhinus spp.

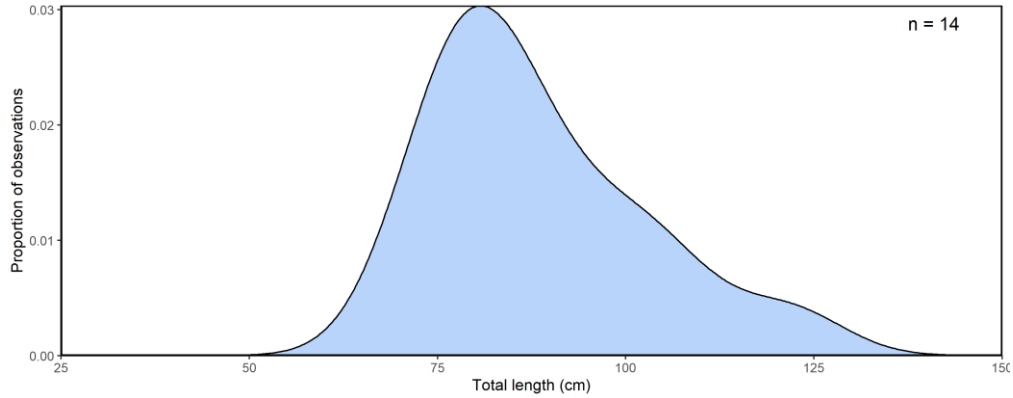

Chromis hypsilepis

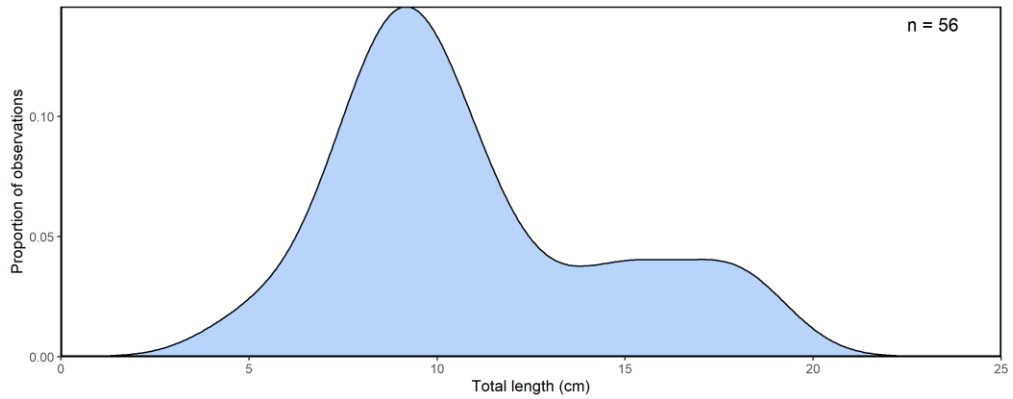

Chromis norfolkensis

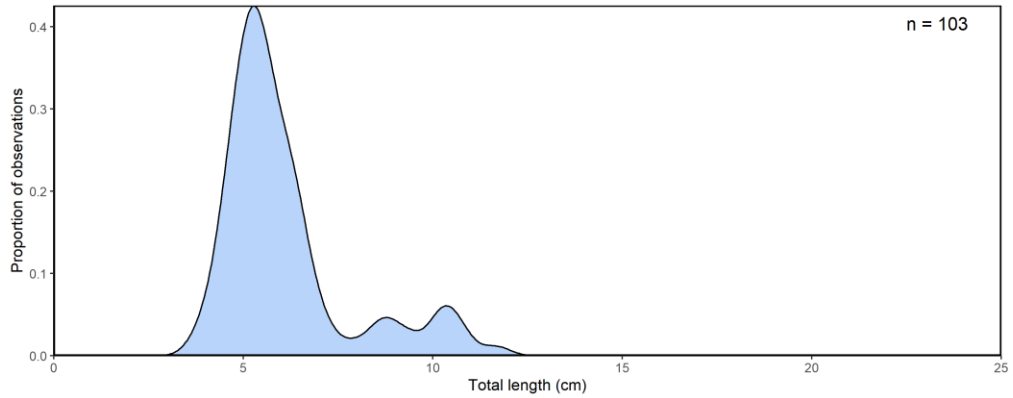

Chrysiptera notialis

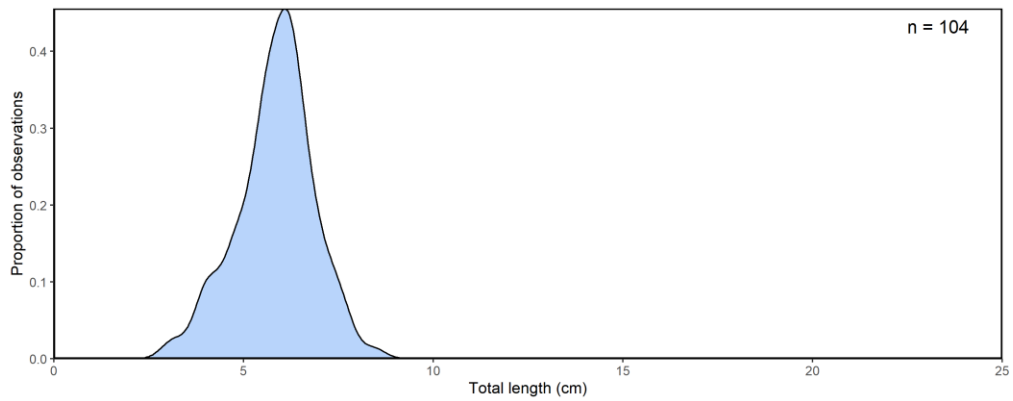

Lethrinus miniatus

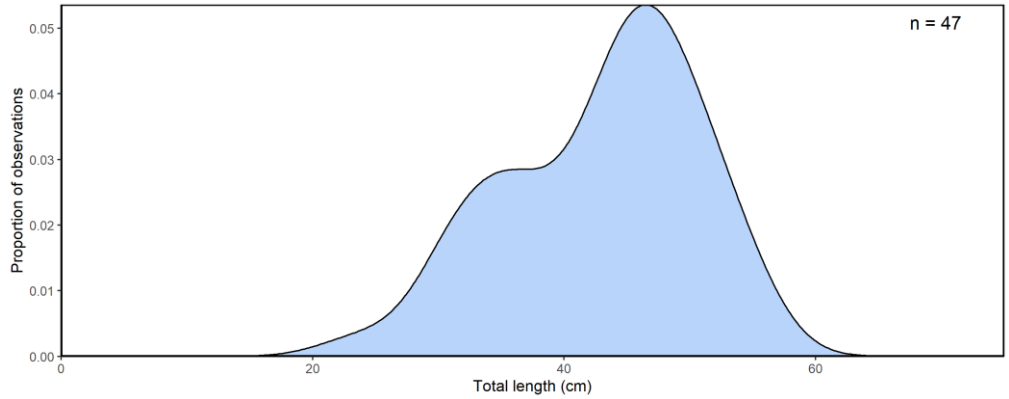

Ostorhinchus flavus

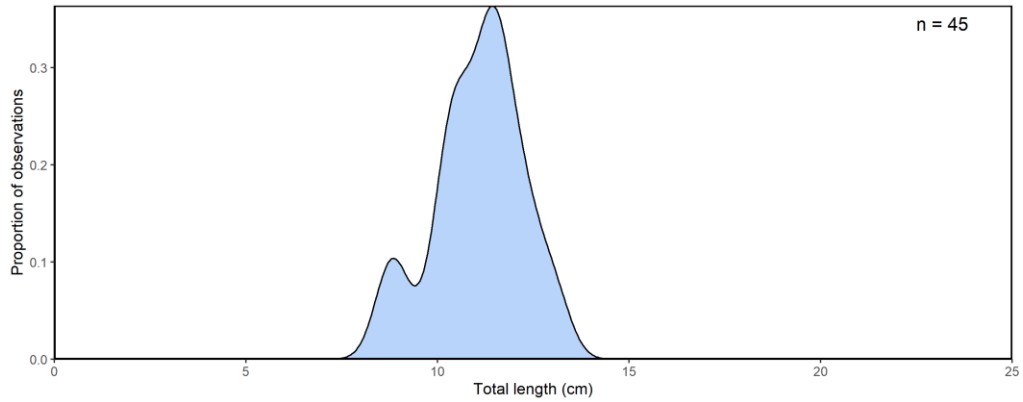

Pseudocaranx spp.

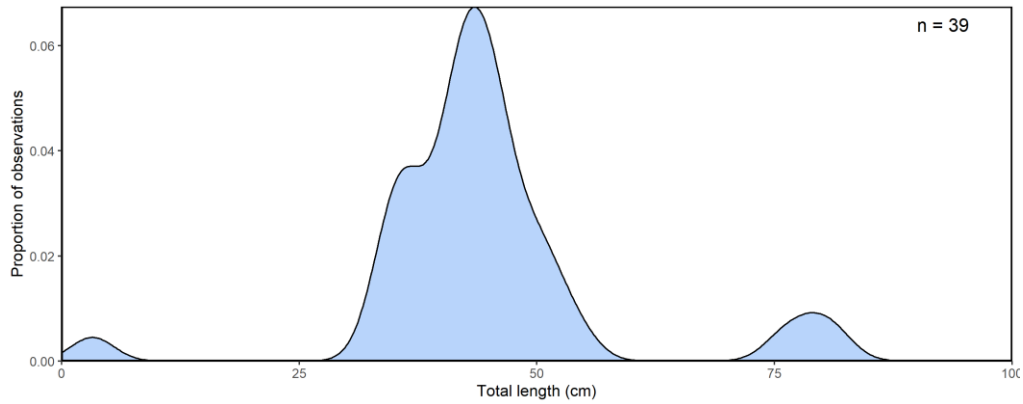

Pseudolabrus luculentus

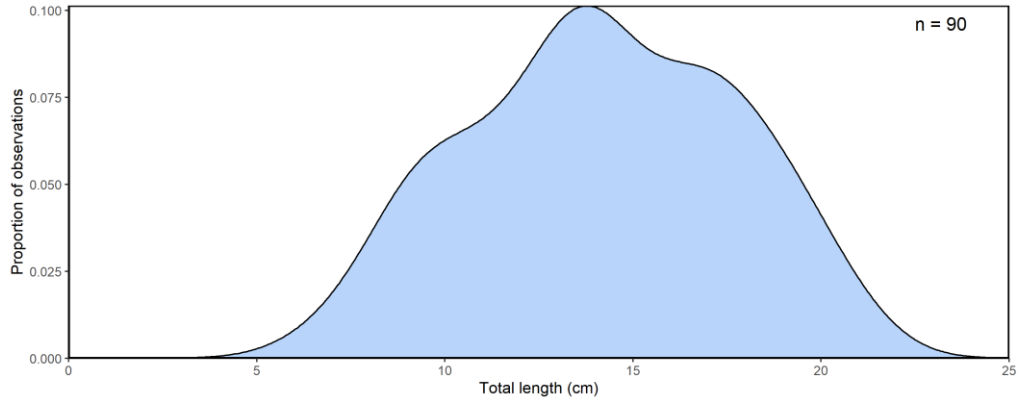

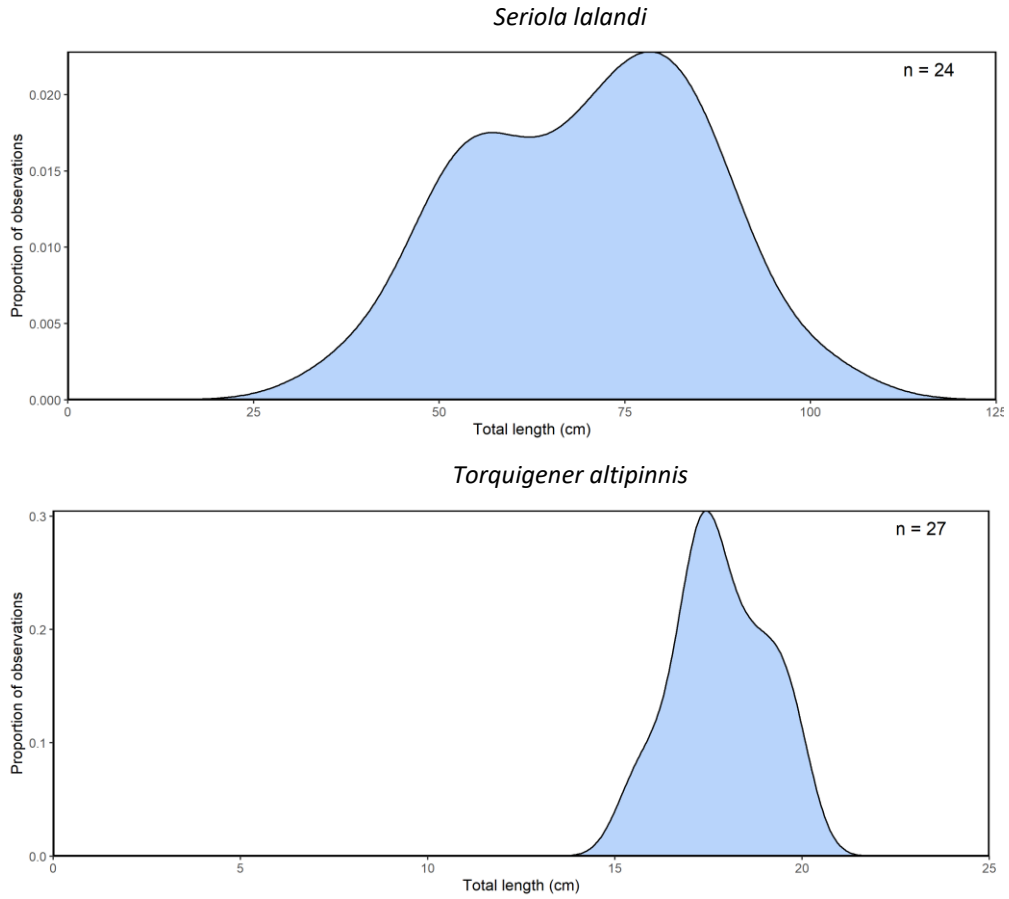

Figure 4-17: Size frequency plots for species with more than 20 measurements available and for whaler sharks Carcharhinus spp.

4.5 Coastal Mapping

Photogrammetry data processing was performed with Agisoft Metashape Professional 1.7.4. Processing consisted of:

- Digital Elevation Model: Resolution / Accuracy positioning (Table 25 and full processing reports in separated digital deliverables);
- Photography projection on the DEM;
- 10cm resolution RGB mosaic.

Table 25: Average camera location error and DEM Resolution

Sites	X error (m)	Y error (m)	Z error (m)	XY error (m)	Total error (m)	DEM Resolution (cm/pix)	DEM point density (points/m$^{2)}$
Captain Cook Lookout	4.249	5.602	3.292	7.031	7.763	15.1	44.1
Anson Bay	2.694	3.439	1.970	4.368	4.792	7.01	203
Puppy's Point	6.803	22.818	2.934	23.811	23.991	6.22	258
Headstone Bay	1.958	4.558	2.804	4.961	5.699	6.19	261
Slaughter Bay and Bumbora Beach	2.125	1.096	1.379	2.391	2.760	4.15	579
Ball Bay	1.334	1.621	1.409	2.099	2.528	64.4	2.41
Emily Bay and Cemetery Bay	1.694	1.306	2.287	2.139	3.131	6.44	241

Please note, no specifications were provided to assess the compliancy of the data.

5. Description and Interpretation of Results

5.1 Coastal Geomorphology by Drone Photogrammetry

Based on the High-resolution DEMs and 3D imagery obtained from Drone photogrammetry, seven coastal sites around Norfolk Island are analysed to provide main characteristics of the three sides of the island (Figure 5-1).

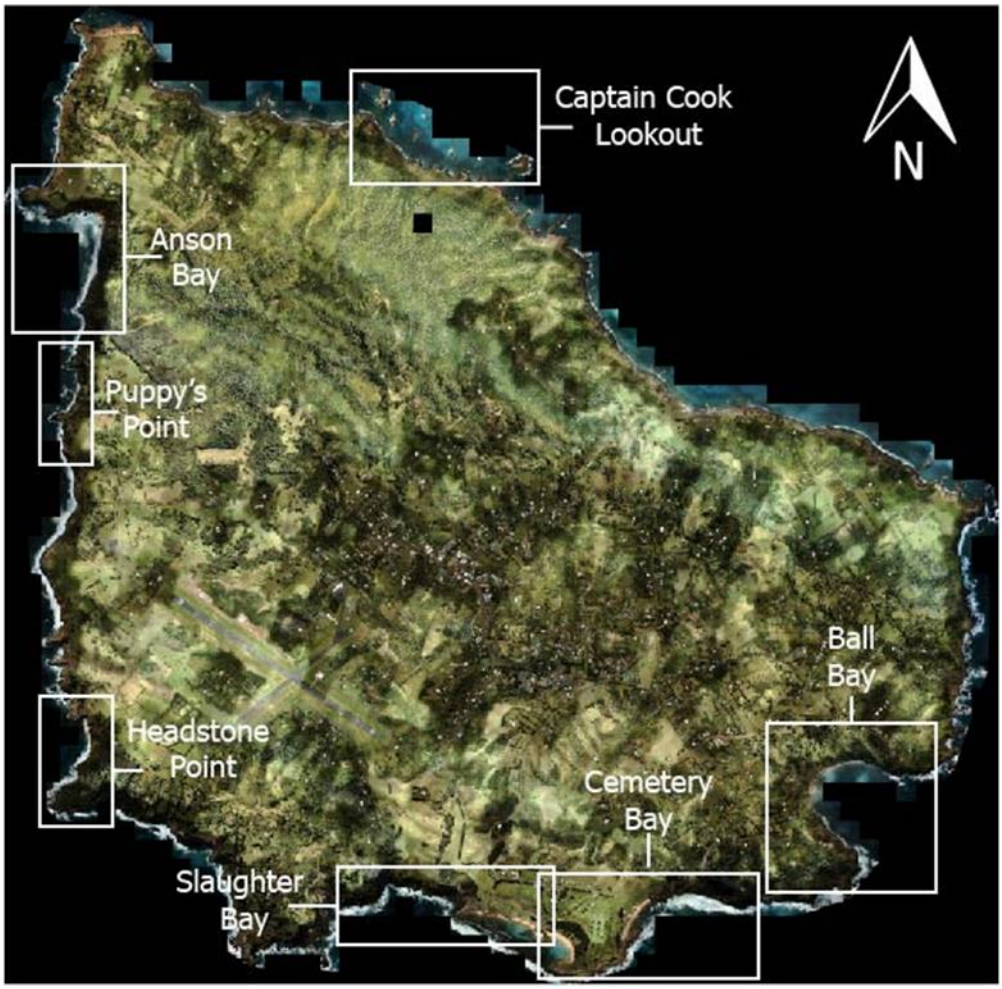

Figure 5-1: Sites of November 2021 iXblue drone photogrammetry surveys. Base map from Gallant and Petheram (2020)

The description of the sites indicates the geological formations composing the coastline, an estimation of type of morphology defined, the mass movement types and status when observed and the main geomorphologic highlights that characterise the survey area.

5.1.1 Captain Cook Lookout

Captain Cook Lookout is on the island's northern side, exposed to waves and wind. From this lookout, a view of Norfolk Island's north-facing cliffs and offshore stacks was captured by drone. This section of the coast is formed from both Duncombe Bay Basalt, Cascade Basalt and yellow tuff (Bird, 2010; Jones and McDougall, 1973). The coastline surveyed is made up of cliffs fronted by rocky beaches (90 %) and shore platforms (10 %), with 19 offshore platforms and six stacks (Figure 5-2).

The rocky beaches wrap around the base of the cliff continuously for 500 m, with an average width of 25 m. Though only a few sections of the shore platform were captured by the drone survey, these are front sections of protruding headland. The largest has a width of 65 m from the base of the cliff, thinning to 16 m. Off the coast, rocky sediment can be seen building up to a distance of 170 km off the base of the cliffs.

Offshore stacks rise out of the ocean. Some of these stacks, such as Elephant Rock, Bird Rock and Cathedral Rock, are made from eroded columnar basalt and have dramatic hexagonal columns (Bird, 2010). Platforms have formed on the seaward side of some of the stacks. These platforms are, on average, 50 m wide but extend up to 70 m towards the ocean in some locations. These platforms are horizontal (Figure 5-3). Offshore platforms that do not have stacks may be the remains of past stack locations which have now eroded to sea level.

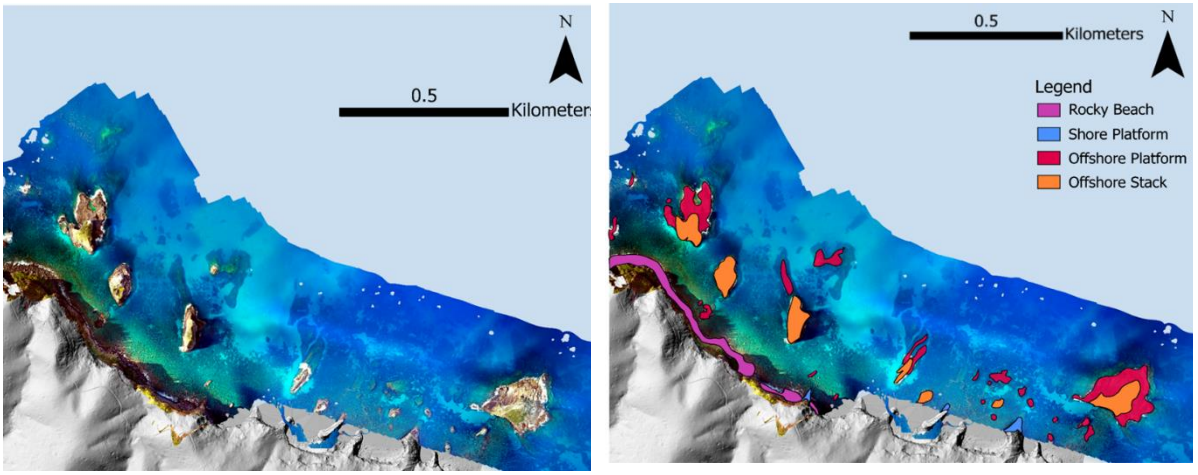

Figure 5-2: Orthophotography of Captain Cook Lookout and surrounds. Hill shade data from 1 m lidar data (Gallant and Petheram, 2020). Left: Georeferenced drone imagery collected on 21/11/2021. Right: Geomorphic map of Captain Cook Lookout and surrounds recognising coastal morphology and offshore formation of platforms and stack.

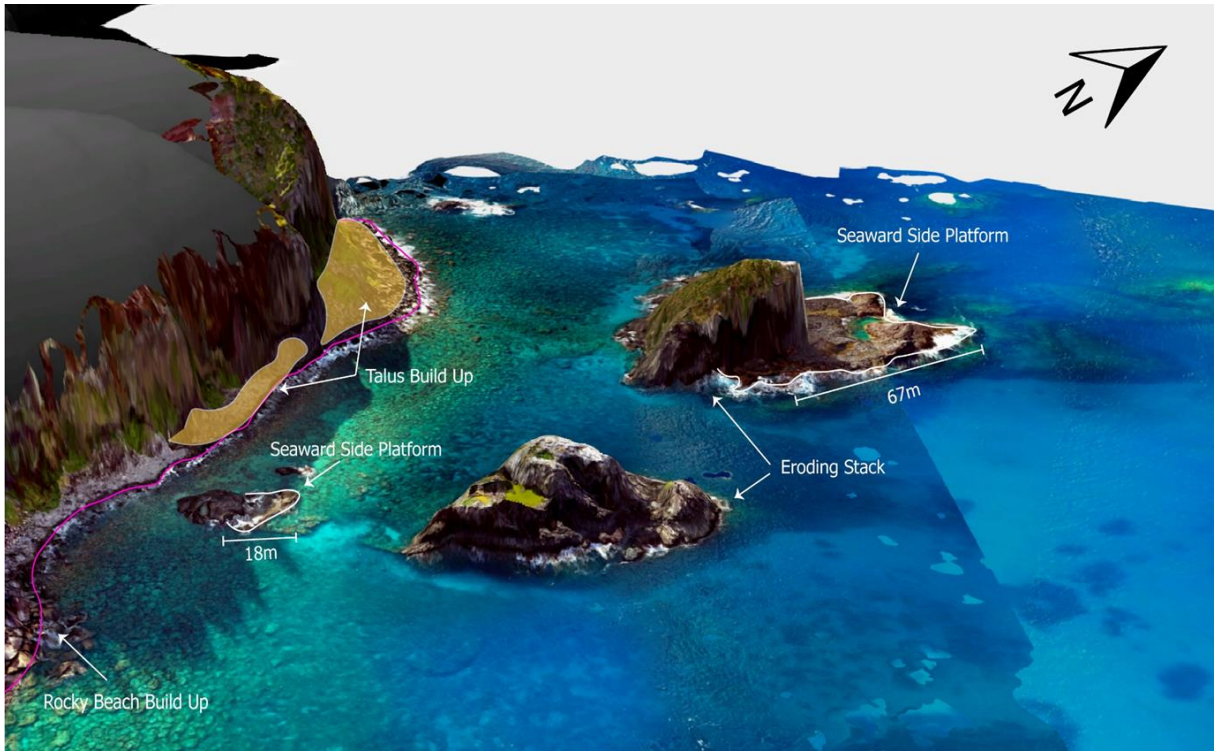

Figure 5-3: Oblique view of Captain Cook drone photogrammetry viewing the base of the cliffs and the sea stacks. The cliffs show build-up of talus slopes at their base, before transitioning into rocky beach and continuing clast deposits into the ocean. The stacks show clear horizontal platforms forming on their seaward side.

5.1.2 Anson Bay

Anson Bay is a southwest facing beach on the northeastern side of the island, accessible from a zig-zag track off Anson Bay Rd. The Cascade Basalt forms a thick layer of columnar basalt, which dips 30° south, sandwiched between yellow tuff below and highly weathered grey tuff above (Bird, 2010). The coastline is made up of a rocky beach (50%), shore platform (43%) and calcareous sandy beach (7%) (Figure 5-4).

Anson Bay has a sandy beach made of calcareous marine sand with shell fragments (Bird, 2010). The beach is 50 m wide and 160 m long. The southern section of Anson Bay is made up of a rocky beach extending 240 m down the coast before terminating where the columnar basalt reaches the ocean. The rocky beach is 40 m wide at its thickest before thinning to 20 m near where the columnar basalt meets the ocean. This rocky beach continues further south out of the extent of drone imagery.

Around the headland north of Anson Bay, a shore platform extends 62 m from the base of the cliff. The platform wraps around the exposed section of the headland, thinning to 18 m on the northern and southern sides. Offshore platforms sit around 40 m away from the shore platform or the northern headland. The largest being 28 x 25 m.

Within the slopes of Anson Bay, evidence of past mass movement is evident, mostly concentrated around the zig-zag track to the beach. The largest of these shows a scarp of 65 m wide and chute of 87 m.

When exploring the data in 3D, evidence of cave formation and undercutting can be seen. Figure 5-5 shows the northern section of Anson Bay, where gouges have been removed from the platform and the cliff, as the start of the undercutting erosive process around the headland.

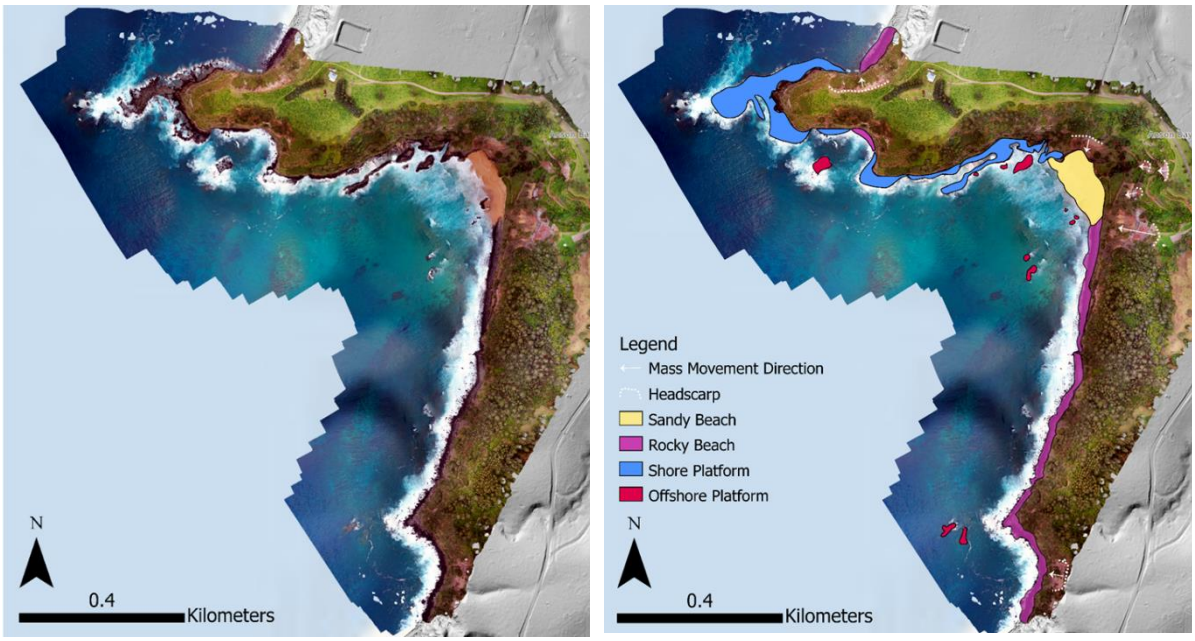

Figure 5-4: Orthophotography of Anson Bay. Hill shade data from 1 m lidar data (Gallant and Petheram, 2020). Left: Georeferenced drone imagery collected on 22/11/2021. Right: Geomorphic map of Anson Bay and surrounds recognising coastal morphology and regions of mass movement.

Figure 5-5: 3D drone photogrammetry of the northern end of Anson Bay. The cliff shows evidence of undercutting and formation of small cave between sections of shore platform.

5.1.3 Puppy's Point

North of Headstone Point and south of Anson Bay, Puppy's Point is a coastal cliff section on Norfolk Island's western side. This section of the coast consists mostly of cliffs fronted by rocky beaches (68 %) and shore platforms (78%), as well as a couple of offshore platforms and a stack (Figure 5-6).

Much of this coastline overlaps rocky beaches and shore platforms, with rocky beaches forming the base of a talus slope on top of shore platforms.

Headstone Point is a basalt headland on the island's western side, north of Rocky Point Reserve. Built into Steels Point Basalt, the coastline is made up of shore platforms (63 %), rocky beaches (25 %), offshore platforms and cliffs which terminate at sea level (12.7 %) (Figure 5-8).

Shore platforms at Puppy's Point are concentrated around exposed basalt headlands. These platforms, 85 m at their widest, are continuous in the northern section of the surveyed region (likely connecting up to Anson Bay).

Seven offshore platforms were identified off the coast of Puppy's Point. The largest of which extends horizontally off a sea stack. As observed at Captain Cook's lookout, the platforms around this stack are on the seaward side, forming a 30 m platform to the west of the stack.

Seven locations of the mass movement were identified along the cliffs. These are mostly concentrated around Puppy's Point carpark and lookout. All scarps were found at the summit of the cliffs. The largest is 74 m wide along its head scarp and an erosional chute extending half the cliff's height. The photogrammetry has captured some of these landslide events in detail (Figure 5-7) with erosion scarps and possible old talus slopes suggesting past mass movement events. These older talus slopes have now been vegetated.

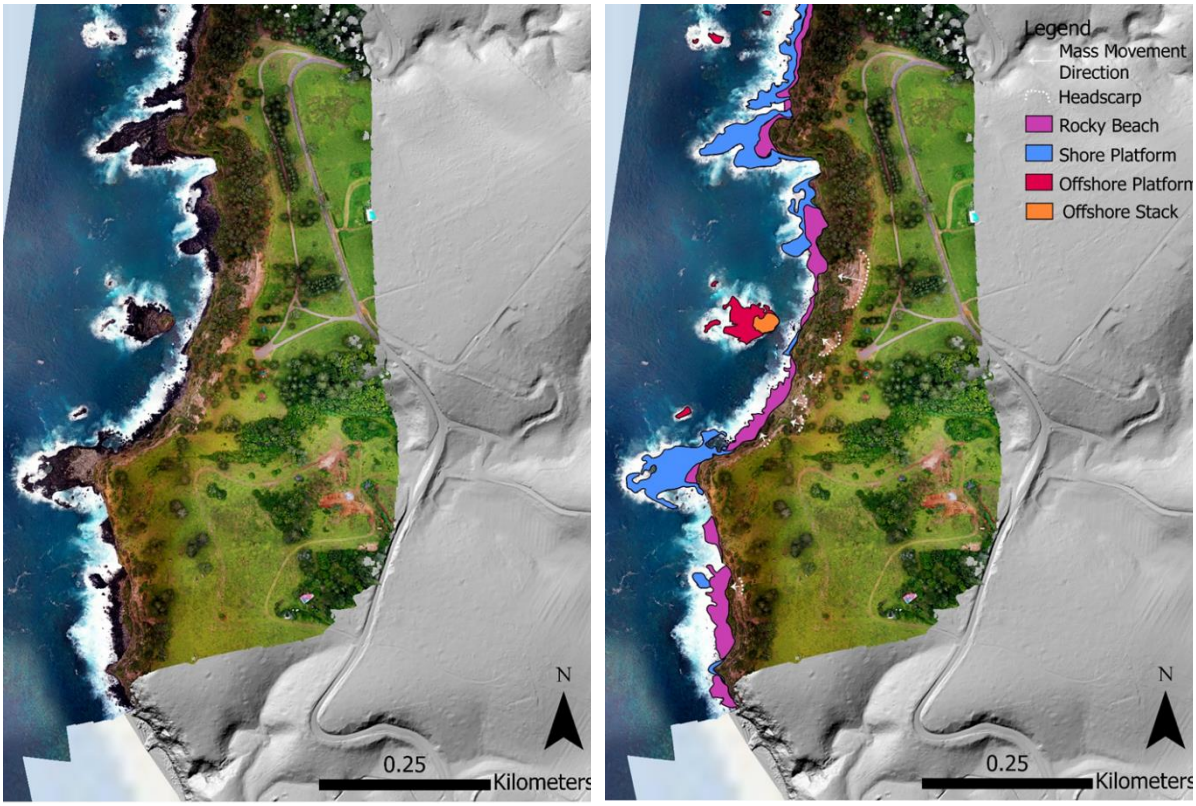

Figure 5-6: Orthophotography of Puppy's Point and surrounds. Hill shade data from 1 m lidar data (Gallant and Petheram, 2020). Left: Georeferenced drone imagery collected on 23/11/2021. Right: Geomorphic map of Puppy's and surrounds recognising coastal morphology, offshore stack and regions of mass movement.

Figure 5-9 shows a section of the cliff between Headstone Po and Headstone Point. The high-resolution photogrammetry shows regions where caves are formed by wave undercutting. As the coast is made up of undercutting cliff and rocky beaches, this suggests a cyclic retreat process occurring along this section of Norfolk Island, whereas a section of cliff is undercut, it collapses, forming boulder beaches that protect that section of the cliff from further erosion. However, a new section of the cliff will now be undercut until it collapses or until the rocky beach is reworked and transported away.: Orthophotography of Puppy's Point and surrounds. Hill shade data from 1 m lidar data (Gallant and Petheram, 2020). Left: Georeferenced drone imagery collected on 23/11/2021. Right: Geomorphic map of Puppy's and surrounds recognising coastal morphology, offshore stack and regions of mass movement.

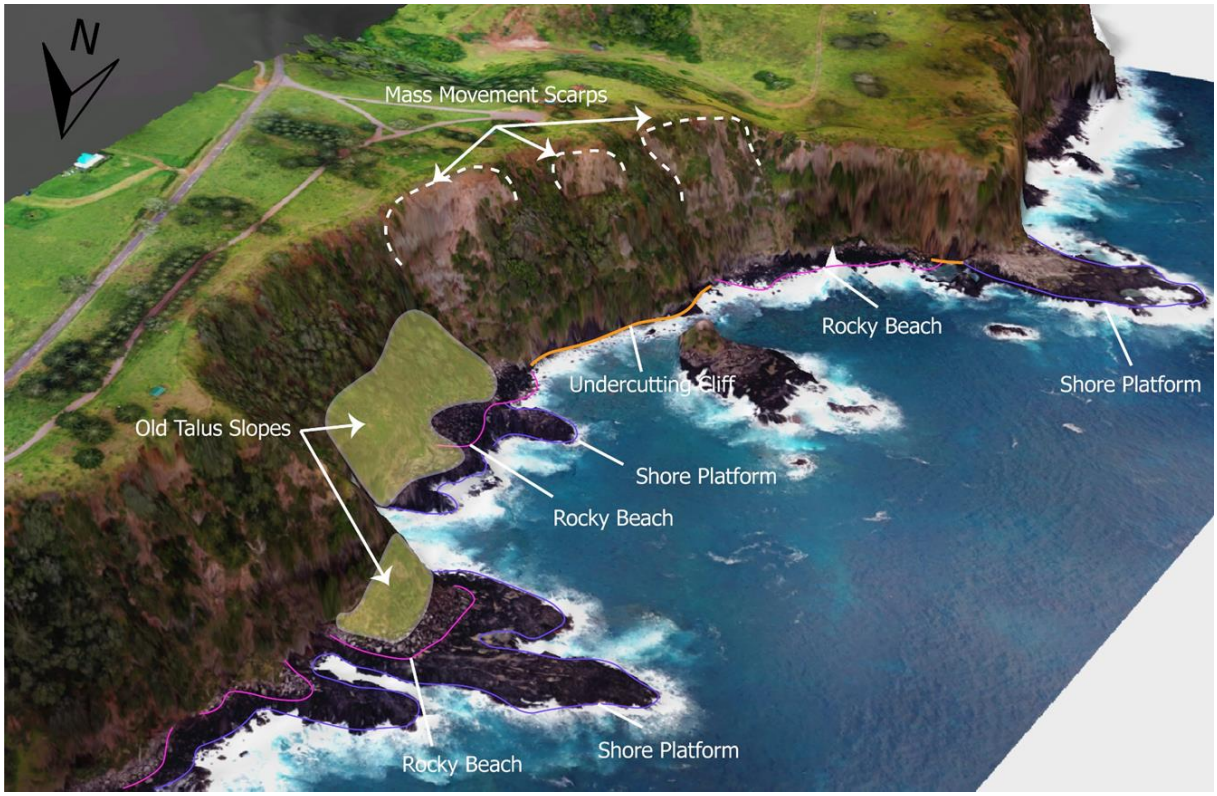

Figure 5-7: 3D drone photogrammetry of Puppy's Point showing mass wasting scarps and old talus slope build up. Platform is alternating shore platform, rocky beach and undercutting cliff.

5.1.4 Headstone Point

Headstone Point is a basalt headland on the island's western side, north of Rocky Point Reserve. Built into Steels Point Basalt, the coastline is made up of shore platforms (63 %), rocky beaches (25 %), offshore platforms and cliffs which terminate at sea level (12.7 %) (Figure 5-8).

The rocky beaches front the cliffs at Rocky Point, forming within small embayments of the protruding headland. These beaches are, on average, 20 m wide and broken up by shore platforms.

Around Headstone Point, shore platforms extend discontinuously around the base of the cliffs. These have an average width of 12 m, however, one section of the platform extends 63 m from the base of the cliff. These platforms are not laterally continuous but rather separated by sections of a cliff dropping into the ocean or boulder beaches within small headland embayments.

Around Rock Point, at least 20 individual offshore platforms can be identified, concentrated near the point of the headland. The largest of these platforms was 45 x 32 m. Two offshore platforms can be seen in the northern section of the image, around Headstone Point, which may have previously been attached to the wide shore platform extending from the base of the cliffs.

Only two mass movement scarps were identified at the summits of the cliffs. These scarps were 30 m wide with no obvious sediment lobes or deposits.

Figure 5-9 shows a section of the cliff between Rocky Point and Headstone Point. The high-resolution photogrammetry shows regions where caves are formed by wave undercutting. As the coast is made up of undercutting cliff and rocky beaches, this suggests a cyclic retreat process occurring along this section of Norfolk Island, whereas a section of cliff is undercut, it collapses, forming boulder beaches that protect that section of the cliff from further erosion. However, a new section of the cliff will now be undercut until it collapses or until the rocky beach is reworked and transported away.

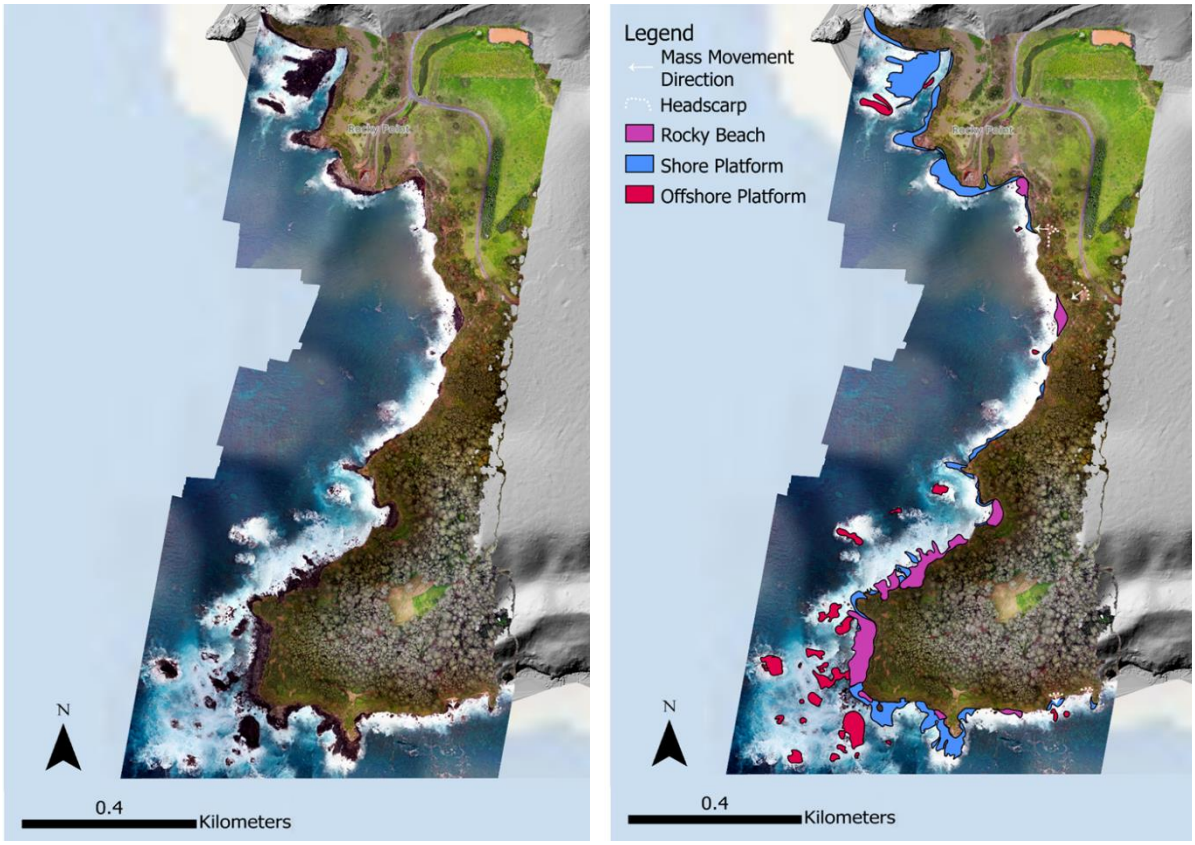

Figure 5-8: Orthophotography of Headstone Point and surrounds. Hill shade data from 1 m lidar data (Gallant and Petheram, 2020). Left: Georeferenced drone imagery collected on 23/11/2021. Right: Geomorphic map of Headstone Point and surrounds recognising coastal morphology, and regions of mass movement.

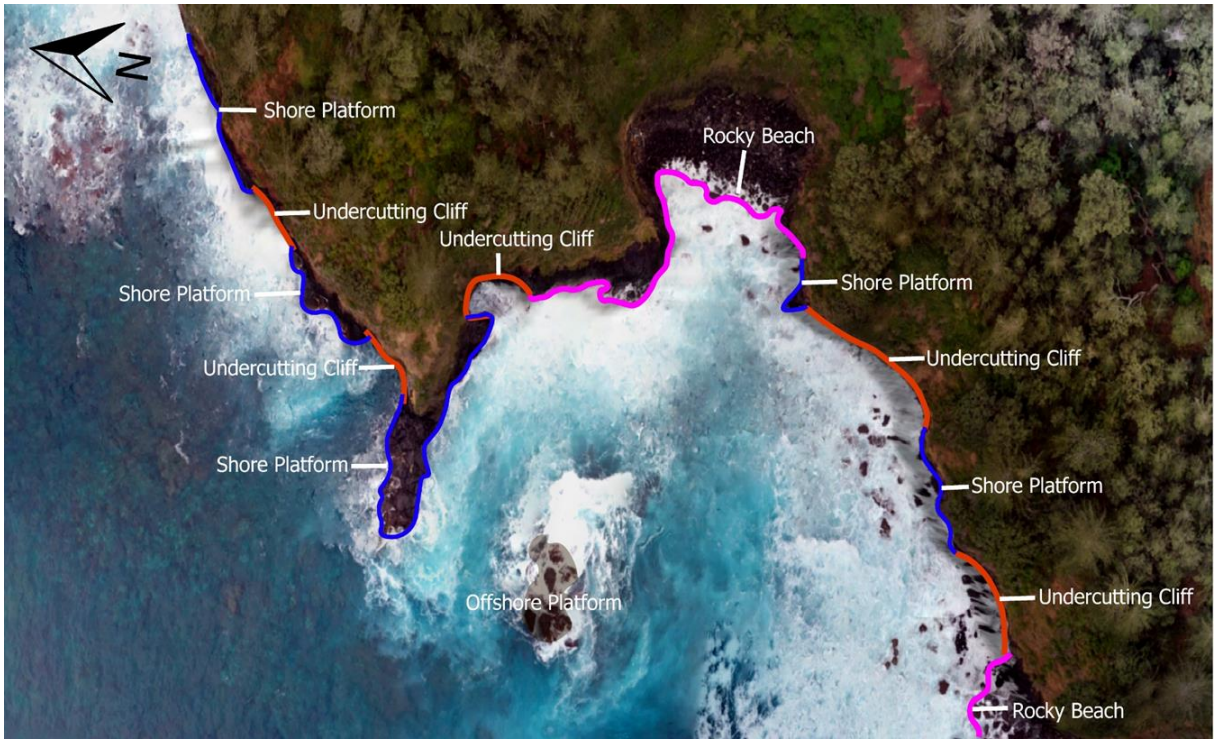

Figure 5-9: Section of Rocky Point/ Headstone Point cliff which cyclic pattern of shore platform formation, cliff undercutting and then rocky beach formation.

5.1.5 Slaughter Bay and Bumbora Beach

Slaughter Bay and Bumbora Beach are on the southern coast of Norfolk Island and look out towards Nepean and Phillip islands. Bumbora is formed into Steels Point Basalt, whilst Slaughter Bay has formed into calcarenite; the transition between them is marked by the cliff to the left of the Kingston Pier. This was the largest region surveyed, with the coastal morphology consisting of rocky beaches (43 %), sandy beaches (21 %), shore platforms (32 %) and hard engineering (3 %), as well as offshore platforms and coral reefs (Figure 5-10).

Slaughter Bay makes up the largest continuous sandy beach on Norfolk Island, 640 m long and width ranging between 40 and 8 m. It is part of the KAVHA region of the island, with many of the heritage buildings built up on the back of Slaughter Bay. Slaughter Bay beach is calcareous. A smaller beach can be seen at Bumbora, 15 m in width and overtopped with rocky clasts.

Around Bumbora and the Steels Point Basalt cliffs, rocky beaches front the cliffs, some on top of shore platforms. These beaches are, on average, 15 m wide, however, they extend up to 30 m in width. Rocky beaches are more commonly found within the Steels Point Basalt cliff region. However, some are found in Slaughter Bay around the calcarenite. These rocky beaches are found on top of the sandy beach of Slaughter Bay and are less dense in clasts than their basalt counterparts.

The shore platforms are found around the base of the cliffs in the western region of the study site. They vary in width from 5 m to 43 m, occurring in continuous stretches. On Slaughter Bay, calcarenite platforms are near the low tide mark, each between 30 – 75 m long and 10 m wide. These calcarenite platforms can be found 85 m offshore, where, like at Emily Bay, they force waves to break early, forming a protected region of the coast. The calcarenite extends 830 m from the edge of Kingston Pier, across the mouth of Slaughter Bay and Emily Bay, to Point Hunter.

Within this protected area of Slaughter Bay, a coral reef, or a reef garden (Bird, 2010), has formed. The reef area covers at least 21,351 m2 and is concentrated near the offshore calcarenite platforms.

The Kingston region has had the most coastal modification of all surveyed sites on Norfolk Island. There is a 75 m seawall to the west to the west of Kingston Pier, as well as a 350 m long seawall at the back of Slaughter Bay. Kingston Pier itself acts as a groyne to sediment in Slaughter Bay.

Mass movement can be seen around the basalt cliffs of Kingston. To the west of Kingston, a large active slip exists, which appears to be the largest from all the surveyed sites with a 67m scarp and 47 m descent to the ocean. However, other scarps can be seen along the cliffs west of Kingston. These landslides have erosional chutes extending at least half of the cliff height; however, very little talus slope or flow deposit remains at the base of the cliffs (Figure 5-11). Rather, either cliffs plunge into the ocean or are terminated by short intermittent shore platforms. The pattern of undercutting cliff and shore platform alternation is similar to that observed up the western coast of the island at Headstone Point and Puppy's Point.

It is off the coast of these basalt cliffs that the concentration of offshore basalt offshore platforms and the only stack is found within this survey region. Like those observed at Captain Cook Lookout, this stack exhibits a horizontal seaward platform, extending 13m from the base of the stack to the sea. Other offshore platforms suggest that at least two other stacks existed before being eroded to sea level. No offshore stacks exist around Slaughter Bay.

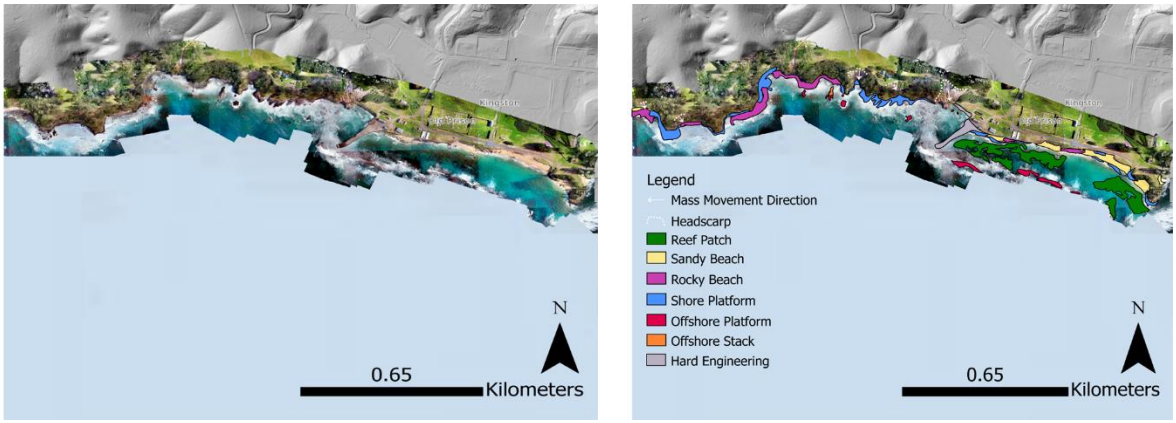

Figure 5-10: Orthophotography of Bumbora and Slaughter Bay. Hill shade data from 1 m lidar data (Gallant and Petheram, 2020). Left: Georeferenced drone imagery collected on 22/11/2021. Right: Geomorphic map of Bumbora and Slaughter Bay and surrounds recognising coastal morphology, offshore platforms, reef growth and regions of mass movement.

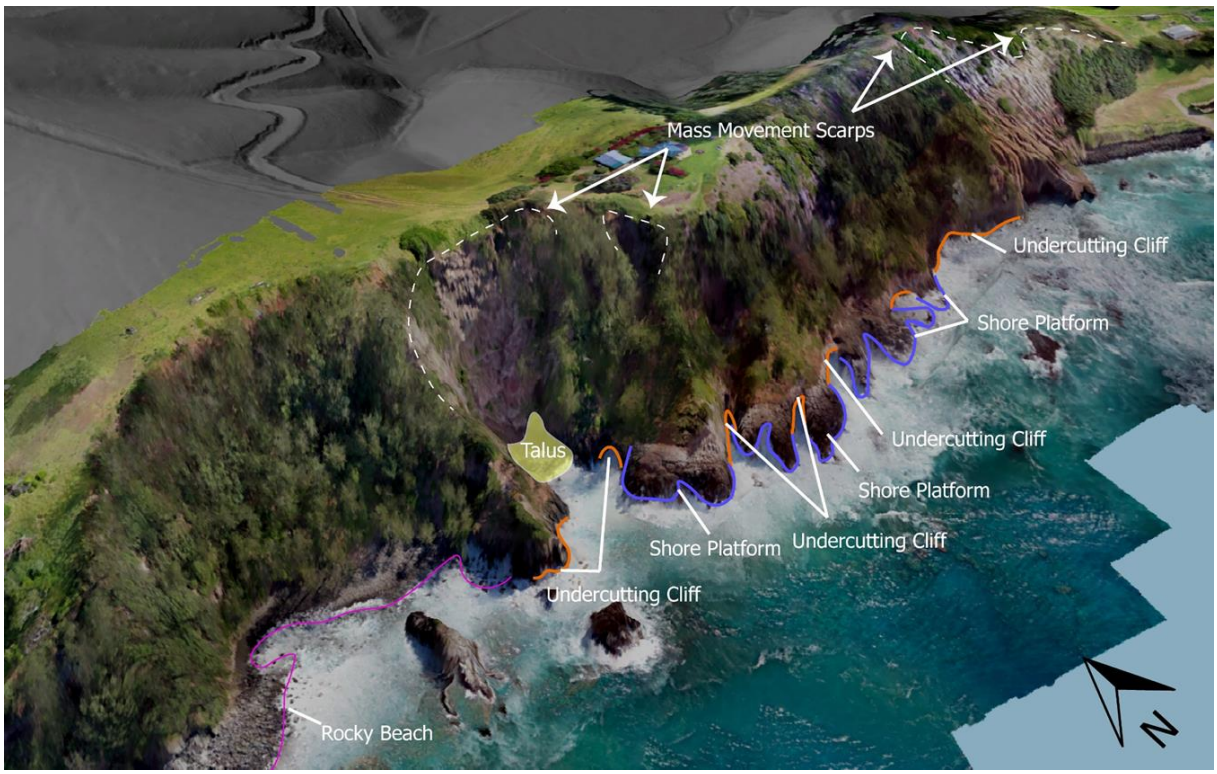

Figure 5-11: 3D drone photogrammetry of basalt cliffs west of Kingston Jetty. Large mass movement scarps can be seen on the summit of the cliffs, whilst at the base, cliffs alternate between undercutting and shore platform formation.

5.1.6 Ball Bay

Ball Bay is sheltered on the southeastern side of the island and is formed into Ball Bay Basalt (Jones and McDougall, 1973). The bay has a rocky coastline comprising rocky beaches (80 %), shore platforms (20 %) and offshore platforms (2 %) (Figure 5-12). The shore platform and rocky beach regions overlap, with rocky beach deposits forming directly on the exposed platform.

The rocky beaches range in width between 24 m and 14 m wide, decreasing in size at the head of the bay (Bird, 2010). However, the drone photogrammetry shows rounded clasts within the waters of Ball Bay for up to 250 m off the shore. These may be reworked in storm events.

Shore platforms extend along the exposed northern and southern points of the bay. In the northern section, platforms are, on average, 20 m wide, with rocky sediment collecting on top of the platforms, at the base of the cliffs, or between platform sections. The shore platform around the southern point of Ball Bay is discontinuous, broken up by rocky beaches formed within embayments. At its widest, this platform is 63 m but undulating in elevation. This platform has evidence of rock pool formation and clear jointing patterns on the platforms (Figure 5-13).

The slope of the cliffs and hills descending into Ball Bay is gentler than in many other sections of the island. However, on the slopes of Ball Bay, mass movement and upper soil erosion is an issue (Norfolk Island Regional Council, 2020; Petheram et al., 2020). In the drone photogrammetry, head scarps show mass movement towards the ocean. Some scarps are poised at the summit of the cliffs or the join of two hanging valleys (Bird, 2010). At the base of some of the mass movement scraps, talus slopes have built up (Figure 5-13).

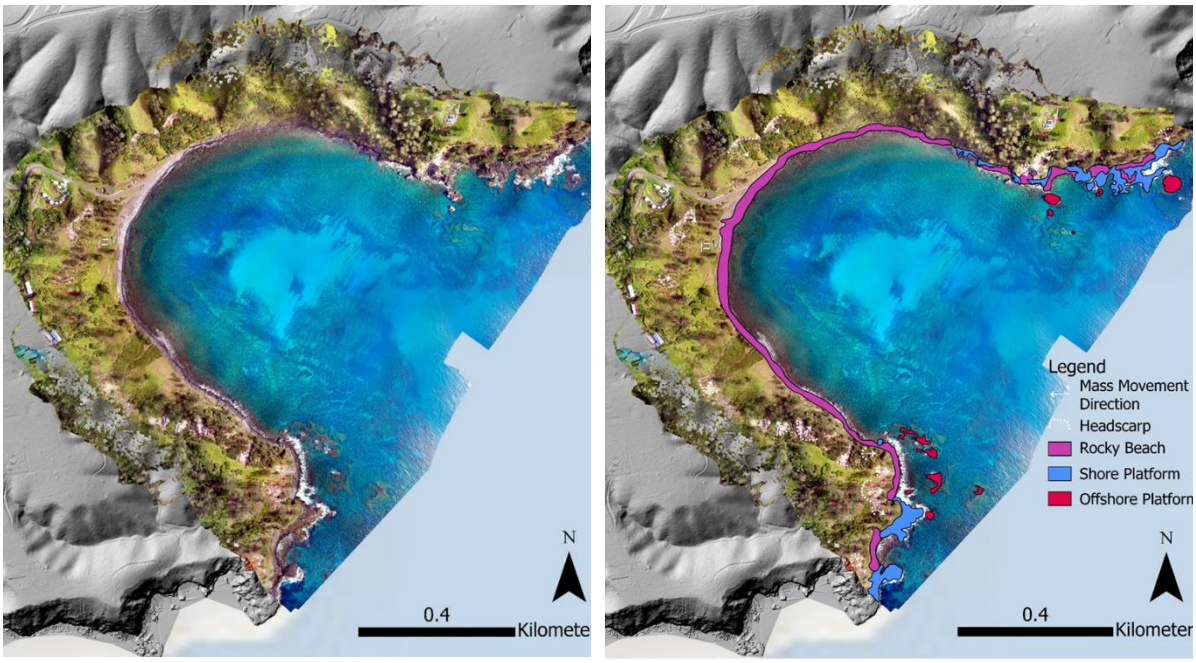

Figure 5-12: Orthophotography of Ball Bay. Hill shade data from 1 m lidar data (Gallant and Petheram, 2020). Left: Georeferenced drone imagery collected on 16/11/2021. Right: Geomorphic map of Ball Bay and surrounds recognising coastal morphology and regions of mass movement.

Figure 5-13: 3D view of mass movements and platforms on the southwestern mouth of Ball Bay. Drone photogrammetry shows locations of talus slope build up the base of mass movement scarps. The platform in the lefthand side of the image shows natural formation of rock pools.

5.1.7 Cemetery and Emily Bay

Cemetery Bay and Emily Bay are calcareous beaches on the island's southern side. Between the two extends Point Hunter. The beaches are between Steels Point Basalt cliffs to the east and calcarenite exposures to the west. The calcarenite is eolianite, a calcium carbonate cemented bioclastic dune rock deposited in Quaternary coastal environments (Fairbridge and Johnson, 1978). At Norfolk Island, the eolianite is mostly comprised of corals, shells, carbonaceous clay and basalt pebbles deposited by the wind (Abell, 1976). Cemetery Bay backs onto the Norfolk Island cemetery and the golf course. This region is a part of the Kingston and Arthur's Vale Historical Area (KAVHA), which runs from Cemetery Bay to the Kingston Pier. This section of the coast comprises sandy beaches, rocky beaches, shore platforms with offshore platforms and reef patches (Figure 5-14). There are many sections of overlapping rocky beaches (48 %), sandy beaches (31%) and shore platforms (22 %).

Emily Beach and Cemetery Bay are made of calcareous sand (Bird, 2010), likely from eroding calcarenite. Cemetery Beach itself is 375 m long and 35 m wide. Small dunes have developed with vegetation at the back of the beach. Emily Bay is a sheltered bay within the Kingston region, with Point Hunter at its eastern edge. The beach, 315 m long and 40 m wide, is sheltered from wave energy by the calcarenite platform and reefs present at the mouth of the bay.

Two main lithologies make up the rocky beaches: calcarenite and basalt. The rocky basalt beach, found in the east of the surveyed region, is the most laterally extensive, 900 m in length, on average 15 m in width, and continuing outside the surveyed region. The rocky beaches line the front of Steels Point cliffs, where rockfall and clasts can be seen in the ocean extending up to 170 m away from the base of the cliffs. The rocky beaches formed from calcarenite are less laterally continuous (150- 260 m) and line the southeast-facing section of Point Hunter. These overlap with sections of shore platform.

The shore platforms also vary based on lithology. In the calcarenite region of Point Hunter and Emily Bay, shore platforms dominate over rocky beaches and are most extensive at the exposed head of Point Hunter and the mouth of Emily Bay. These are, on average, 30 m wide. In some sections, rocky beaches have formed on top of the platform at Point Hunter. In the east of the surveyed region, the Steels Point Basalt section of Cemetery Bay, small exposures of platforms can be seen, 15 m wide, between sections of rocky beach.

Around Point Hunter, eroded offshore platforms force waves to break early, forming a non-continuous boundary around the calcarenite. These platforms break wave energy, allowing for sheltered reef growth in Emily and Slaugther Bays. In Emily Bay, reef patches cover ~19,500 m2 of the seafloor, concentrated around the mouth of the bay.

Mass movement scarps can be seen around the cliff section of Cemetery Bay, with landslide chutes pointing towards the ocean. Like Ball Bay, many of these scarps sit at the top of cliffs and hanging valleys. The largest of these scarps is 110 m long and 30 m tall. No distinct talus slope has been built up as a result of these events, however, the rocky beach, and clast build up around the base of the cliffs (Figure 5-15) does suggest eroded and reworked sediment stored near the coastline.

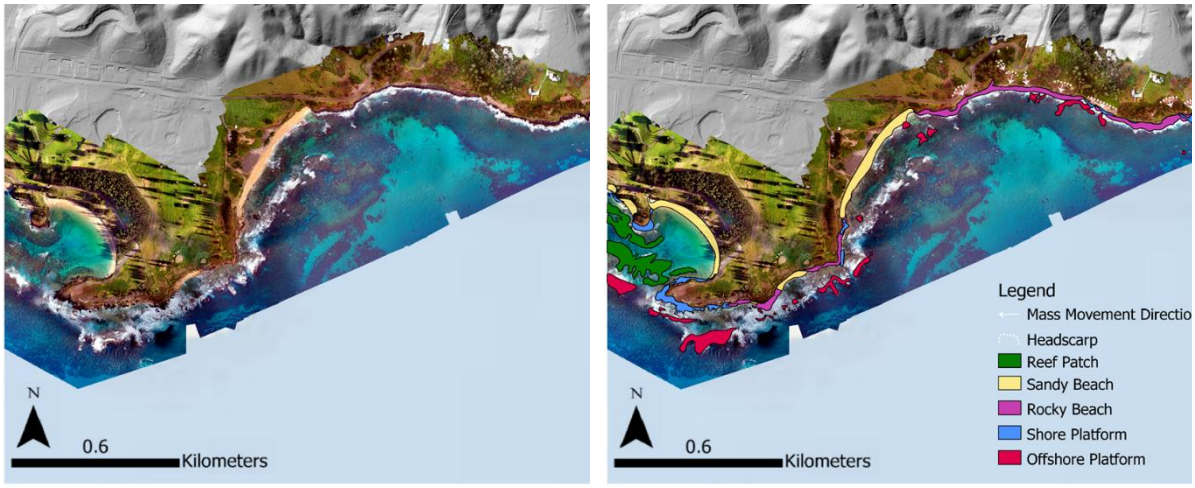

Figure 5-14: Orthophotography of Cemetery Bay and Emily Bay. Hill shade data from 1 m lidar data (Gallant and Petheram, 2020). Left: Georeferenced drone imagery collected on 21/11/2021. Right: Geomorphic map of Cemetery Bay, Emily Bay and surrounds recognising coastal morphology, reef growth and regions of mass movement.

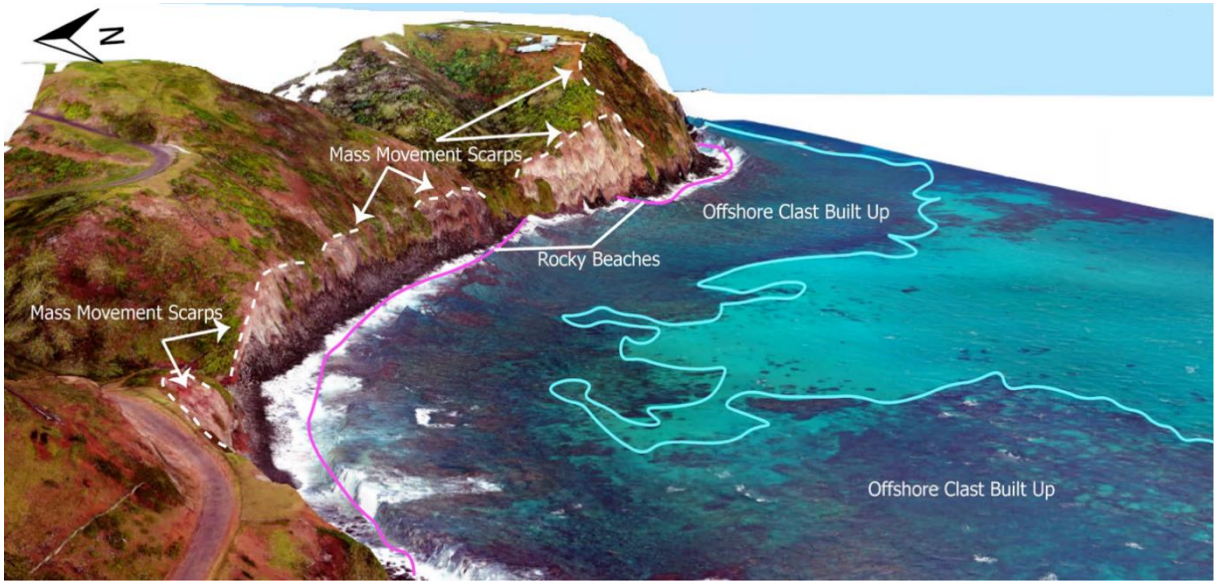

Figure 5-15: 3D drone photogrammetry image of the eastern cliffs of Cemetery Bay. Extent of rocky beach and offshore sediment can be seen in conjunction with mass movements scarps.

5.1.8 Conclusion

The photogrammetry of seven representative sites around Norfolk Island, allow the characterisation of three coastlines of the island (North-East, West and South). The geomorphology is highly constrained by the geological formation encountered on site, their response to weathering processes (waves and wind erosion) affected by the exposure of the site, and their magnitude of mass wasting.

The North facing section of Norfolk Island, represented by Captain Cook Lookout, is represented by offshore stacks (such as Elephant and Bird Rock), dramatic cliffs and onshore and offshore platforms with pockets of rocky beaches.

The West side, represented by Anson Bay, Puppy's Point and Headstone Point, is exposed to Westerlies and Eastward waves. For these three sites, the predominant morphology is shore platforms made of Basalt, and rocky beach. The cliffs are shaped by cyclic retreat process, making caves, boulder beaches and undercut sections. Some mass movements are observed in the imagery, mainly on the top section of the cliffs.

The South side, represented by Slaughter Bay, Emily Bay and Cemetery Bay, and Ball Bay, shows two geological formations, a sedimentary rock (calcarenite) and a volcanic rock (basalt). Although the rocky beach and cliff remain the main morphologies, the South side of the island also offers the best sandy beaches. Natural waves breakers (such as Point Hunter in Cemetery Bay or calcarenite platform in Slaughter Bay) create calmer environments, such environment may have facilitated the reef growth within Slaughter Bay. On shore, several localised mass movements are observed, the largest being in the Kingston Region, where the weathered basalt prone to failure.

Table 26: Percentage of coastal geomorphology cover as sited by drone photogrammetry

Norfolk Island	Survey Sites	Shore Platform (%)	Rocky Beach (%)	Sandy Beach (%)	Undercutting Cliff (%)
North Side	**Captain Cook Lookout**	18	79	0	3
West Side	**Anson Bay**	43	51	6	0
	Puppy's Point	54	43	0	3
	Headstone Point	62	20	13	5
South Side	**Slaughter Bay**	33	44	23	0
	Cemetery bay	21	48	31	0
	Ball Bay	26	74	0	0
	Total	37	51	10	2

5.2 Morpho-bathymetry

The surveyed shelf surrounding Norfolk varies in depth, between -12 m and -60 m, with an average depth of 41 m. The shelf itself deepens going away from Norfolk Island. This section of the report explores the morphology of the surveyed Norfolk Island seafloor using geospatial methods and ground truthing with BRUV images. The backscatter imagery is then used to provide an interpretation of the spatial variation of the seabed nature over the whole survey area.

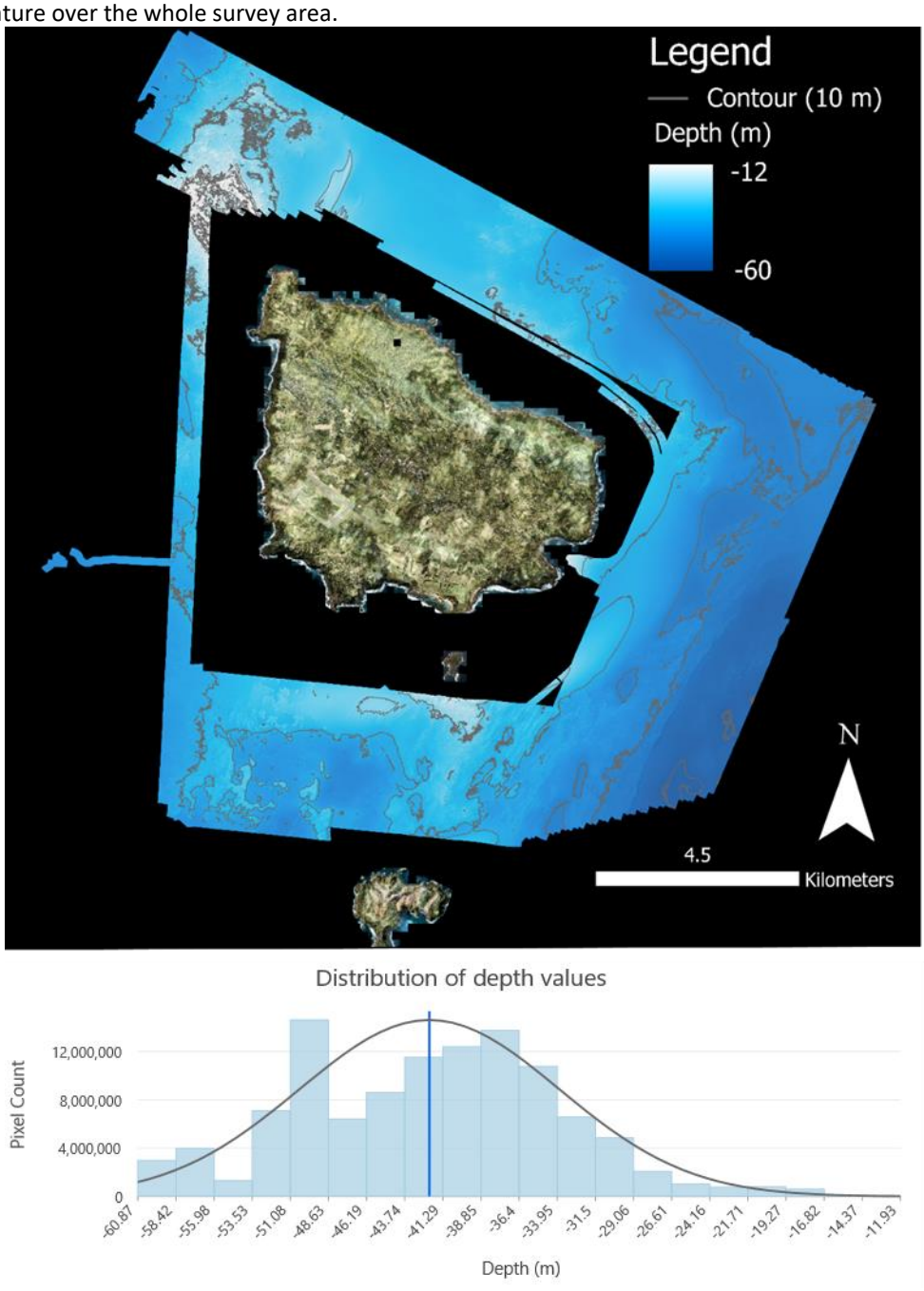

Figure 5-16: MBES bathymetry surrounding Norfolk Island with 10 m contours. The histogram shows the distribution of depth values, with an average depth of -41 m at the blue line

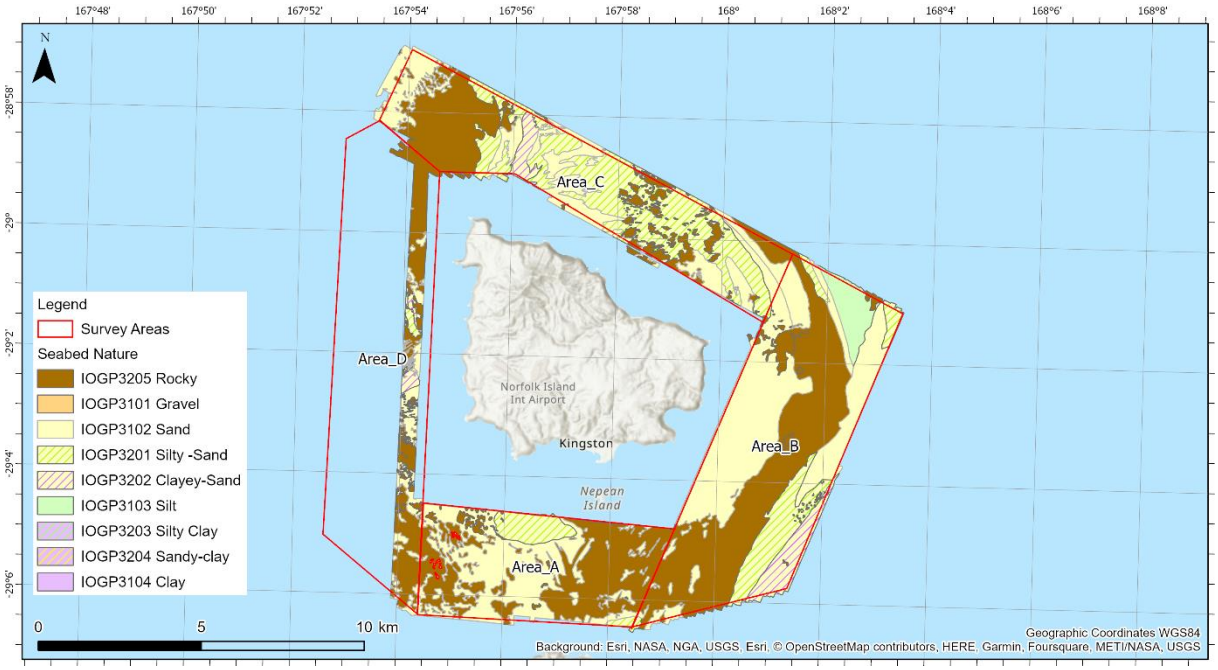

Figure 5-17: Seabed Nature from backscatter interpretation

5.2.1 Geomorphometric analysis – Benthic Terrain Modeller toolbox

Using bathymetry, terrain derivatives have been generated across the surveyed seafloor. Terrain derivative analysis was carried out using Benthic Terrain Modeller 3.0 (BTM) in ArcGIS Pro (10.3.2). This set of python GIS toolboxes uses descriptive and quantitative terrain parameters such as slope, ruggedness and bathymetric position index to classify bathymetry into a defined set of classes (Lundblad et al., 2006; Rinehart et al., 2004; Walbridge et al., 2018). Finally, utilising a user-defined dictionary, the BTM toolbox assists in a terrain-based supervised classification.

Initial terrain derivates were generated from the bathymetry, including slope, ruggedness, and broad and fine bathymetric position index (Figure 5-18). The parameters used to generate these calculations and figures can be found in the appendix 9.1.

The slope of the surveyed region varies between 0 and 78° degrees, with an average slope of 2.5 ° (Figure 5-18). Sections of steeper slopes can be found in the southern and northeastern regions, whilst gentler slopes (flatter) can be found within the northern and eastern regions. The sections of the steeper slope, however, are localised, distinguishing areas of more rugged terrain. The slope figures share some similarities with the ruggedness of Norfolk Shelf.

Ruggedness, also known as rugosity, or surface roughness, explores terrain heterogeneity by comparing a draped surface distance to a linear distance (Walbridge et al., 2018). The Vector Ruggedness Measure (VRM) is a quantitative measure of terrain heterogeneity. Like its terrestrial equivalent, the terrain ruggedness index, VRM standardises ruggedness measurements to allow for comparisons across different landscapes (Riley et al., 1999). VRM values closer to 0 show no variation, while those near one show complete variation. In a typical spread of natural data, VRM values are small, < 0.4 (Walbridge et al., 2018). The VRM values on the Norfolk shelf vary between 0 and 0.024, with an average of 0.00269, all small, showing minimal variation (Figure 2). However, rougher surfaces can be seen, often in similar locations to higher slopes, around the northwest, southeast and northern sections of Norfolk Island. South of Nepean Island, these ruggedness features show linearity, often running parallel to the coast of Norfolk Island.

Bathymetric Position Index (BPI) is based on the Topographic Position Index, originally used by Weiss (2001), to measure topographic slopes and automate the classification of landforms. Walbridge et al. (2018) applied this to the bathymetric environment creating the BPI as a part of the BTM toolbox.

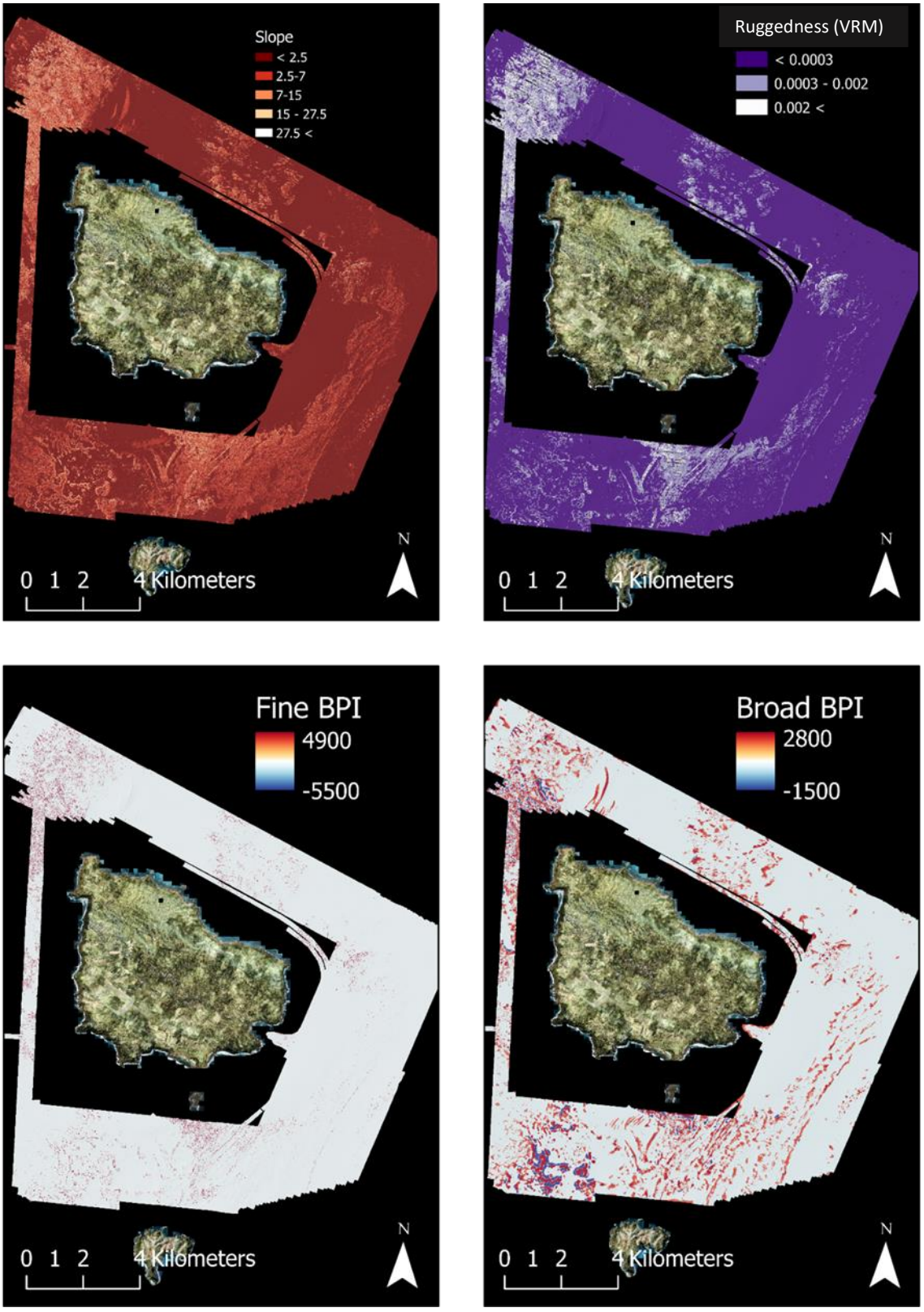

Figure 5-18: Terrain derivatives from MBES bathymetry around Norfolk Island including (from left to right, top to bottom), slope, Vector Ruggedness Measure, fine bathymetric position index and broad bathymetric position index.

BPI assesses the elevation change of grid cells within a DEM relative to a specific neighbourhood around that cell. If a BPI value is positive, the cell is, on average, higher in elevation than its surrounding cells. If a BPI value is negative, the cell is lower on average than its surrounding cells. The BTM toolbox allows multiple calculations to be completed at a fine and broad scale to compare the relative change of elevations at a regional or more localised scale within the bathymetry.

The fine BPI of Norfolk Island MBES bathymetry shows positive elevation change in red and negative in blue (Figure 2). The mean value of fine BPI is 0.54, with values between -5507 and 4869, suggesting that the overall seafloor is flat with areas of sudden increase or decrease in depth. Regions of increased BPI are localised in the northeastern and southern sections of surveyed regions. In particular, the southeastern region shows a linear pattern from southwest to the northeast of fine BPI positive values, showing ridge-like features.

The broad BPI identifies larger-scale morphologies by comparing terrain variation across a larger spatial area. The broad BPI has less variation in values than the fine BPI, with values between -1593 and 2756. The average value is 0.63, which like the fine BPI, suggests that the terrain is flat. Some bathymetric lows, or negative BPI values, occur in the southwestern and northwestern sections, both immediately adjacent to some positive BPI values. These variations are subtle, but significant across the flat Norfolk Shelf.

The terrain derivatives, slope VRM, fine and broad BPI, as well as the bathymetry itself, describe the seafloor variations across Norfolk bathymetry. The bathymetry is flat and smooth, gradually decreasing depth. It also shows localised regions where the seafloor is steeper, rougher and with small features increasing but occasionally decreasing in depth. These regions are focused within the bathymetry's northwestern, southwestern, and southeastern sections, and some show linearity in features, often running parallel to the Norfolk shoreline.

5.2.2 Localised Transects of Interest

A series of transects or profiles have been extracted from the bathymetry based on areas of variability from Figure 5-18 to explore in further detail (Figure 5-19). Some of these profiles correspond with the location of BRUVs deployments providing an opportunity to ground truth the seafloor observations.

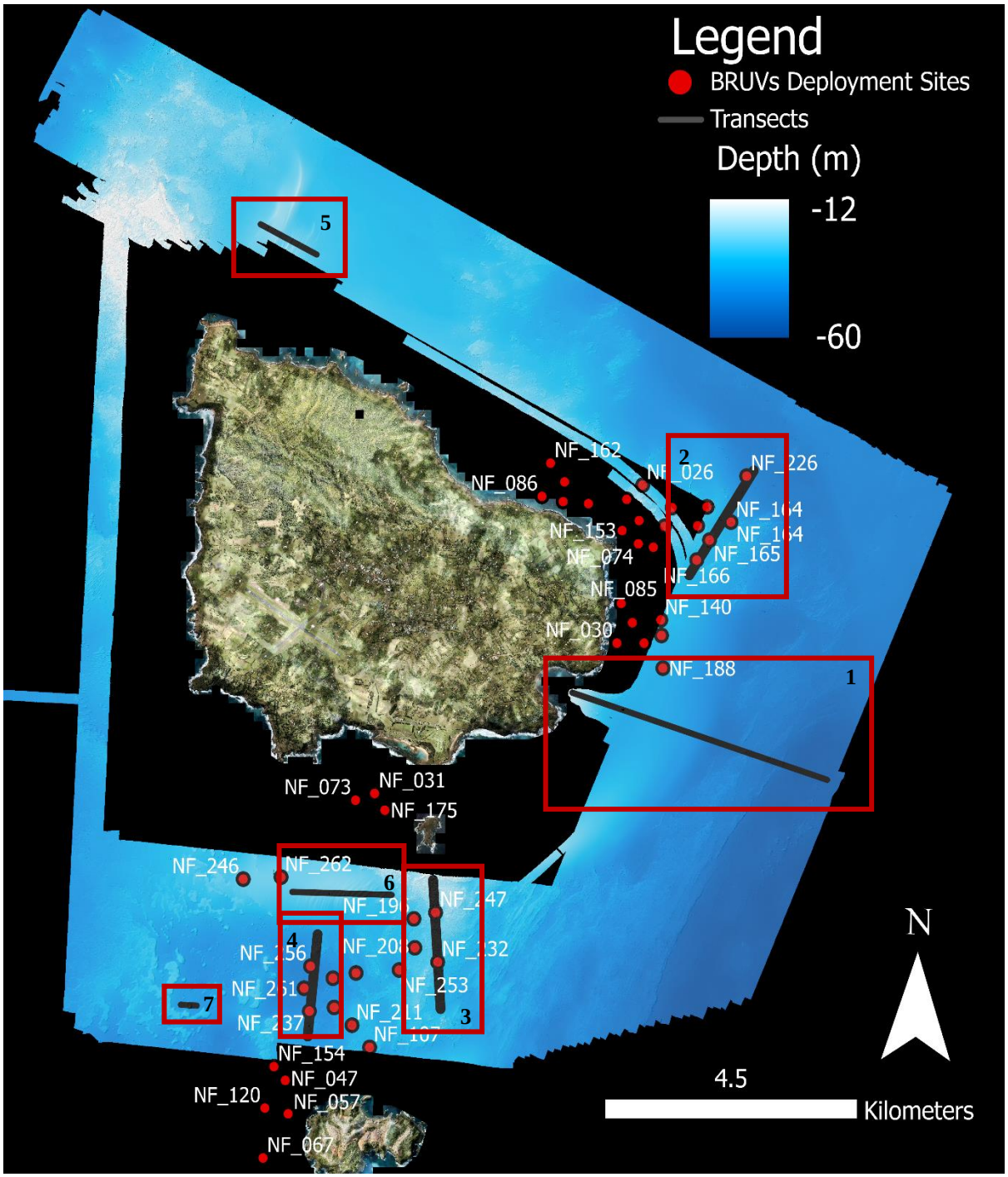

Figure 5-19: Locations of transects and BRUVs deployments have been throughout Norfolk Island. Red boxes and numbers refer to the transects explored below, while white labels correspond to a specific BRUV deployment.

5.2.2.1 TRANSECT 1

Measured from the mouth of Ball Bay to for 4000 m across the shelf, Transect 1 shows the largest continuous section of bathymetry on the Norfolk Shelf (Figure 5-20). Running from northwest to southeast, the depth of the profile gradually changes from -20 m deep within the mouth of Ball Bay to -60 m deep. The profile has a gradual slope for ~500 m out of the mouth of Ball Bay until it flattens out for 1 km. Here the profile becomes slightly convex. This rounded section of the seafloor is in the bathymetry as a subtle increase in elevation (~5 m) and extends north and south around the eastern region of Norfolk Island. At 3 km along the profile, a rougher surface can be seen with localised surface variation ranging on a scale of up to 5 m. Overall, the profile moving away from Norfolk Island shows two main sections of elevation decent, from 0 to 1 km and from 2.4 to 2.8 km. With the exception of the rough features at ~ 50 m depth, the majority of the profile appears to be over softer, smooth sand. No BRUVs deployments were taken near the profile, however, the closest one (NF_188), which is 900 m north of the profile, shows the seafloor made up of unconsolidated sand.

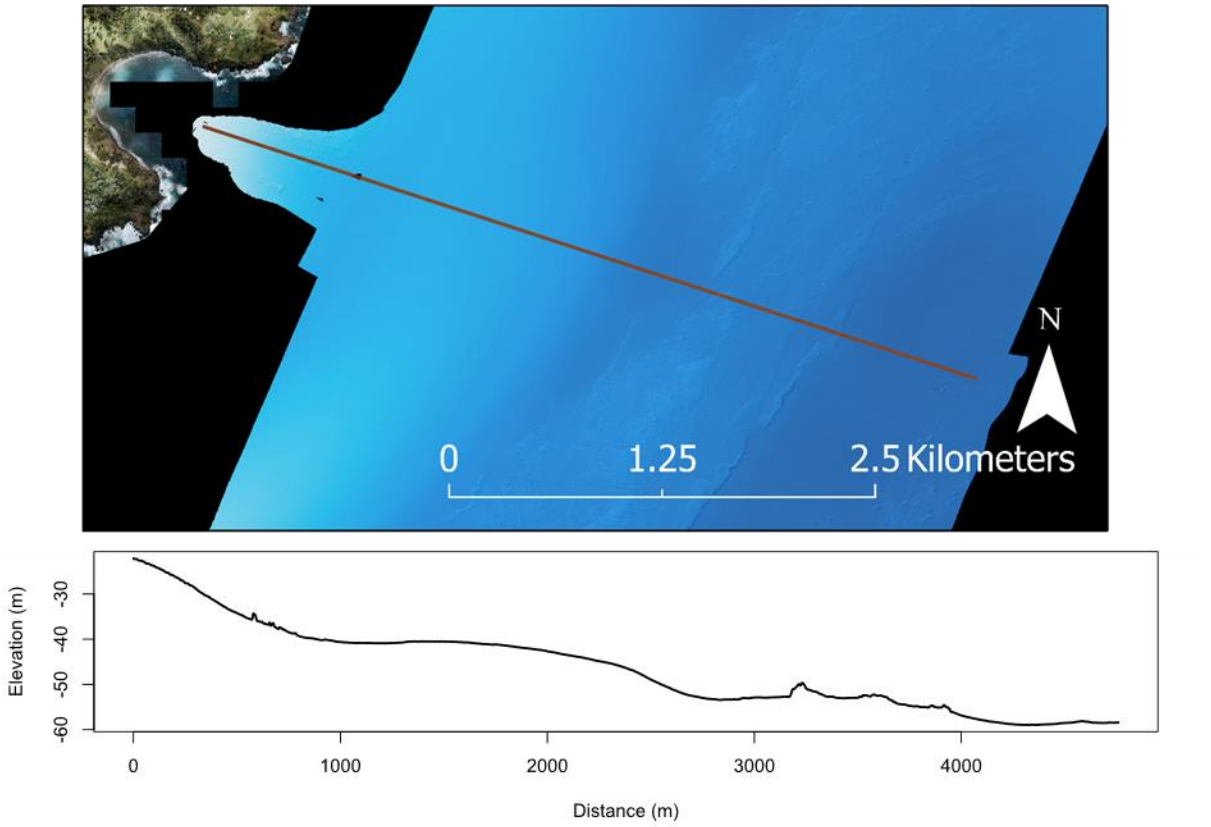

Figure 5-20: Transect 1 bathymetry and profile in the eastern section of the Norfolk Shelf from Ball Bay.

5.2.2.2 TRANSECT 2

Transect 2 is a profile 2.9 km long measured from southwest to northeast (Figure 5-21). The transect is measured in the eastern section of the bathymetry and passes successful two BRUVs deployment sites. The profile begins at -38 m depth, extending for ~600 m before passing over a rougher, undulating surface, likely a rocky outcrop, rising to -35 m. BRUV NF_166 at 350 m along the transect shows unconsolidated sandy sediment formed into linear features on the seafloor. After 1.2 km, the seafloor gradually descends 10 m to over -50 m depth, where NF_226 shows an unconsolidated sandy seafloor as a substrate, organised into linear ripples. This descent likely continues outside of the surveyed region.

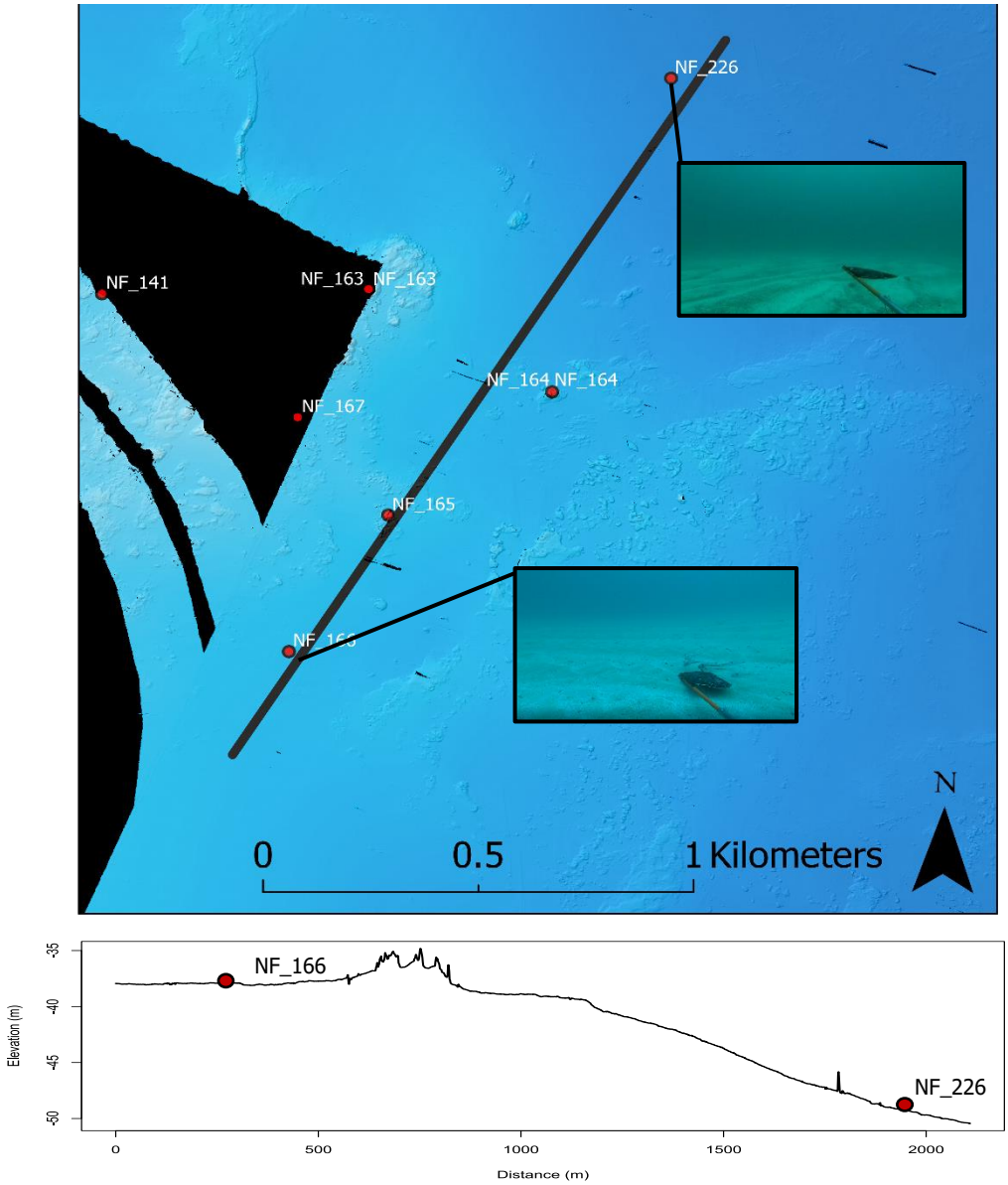

Figure 5-21: Transect 2 bathymetry and profile in the eastern section of the Norfolk Shelf.

5.2.2.3 TRANSECT 3

Transect 3 is a 2 km profile that runs from north to south, just south of Nepean Island and passes through two individual BRUVs deployment sites (Figure 5-22). The transect decreases with depth, and may have calcarenite exposures related to Nepean Island. The transect is undulating and passes over both consolidated, closest near Nepean and unconsolidated seafloor in the south of the profile. Over the profile, the seafloor descends from -25 m to -40m. However, the vertical variation within the profile is up to 3 m. At BRUV deployment NF_247, 550 m along the transect, the seafloor is unconsolidated, made up of a mixture of sandy substrates, larger cobble-sized clasts, and seagrass growth. The distribution of clasts, likely volcanic rock or carbonate, creates the bumpy morphology on the seafloor. Further along the transect, NF_232, at 1300 m, shows a deep water coral and sand on a rokcy outcrop. It is likely that within this region, the rocky substrates produce a location for corals to grow. As a result, the existence of both volcanic clasts and with a coral veneer forms a rough morphology. This transect is also diectly south of Nepean Island, which is a calcarenite body.

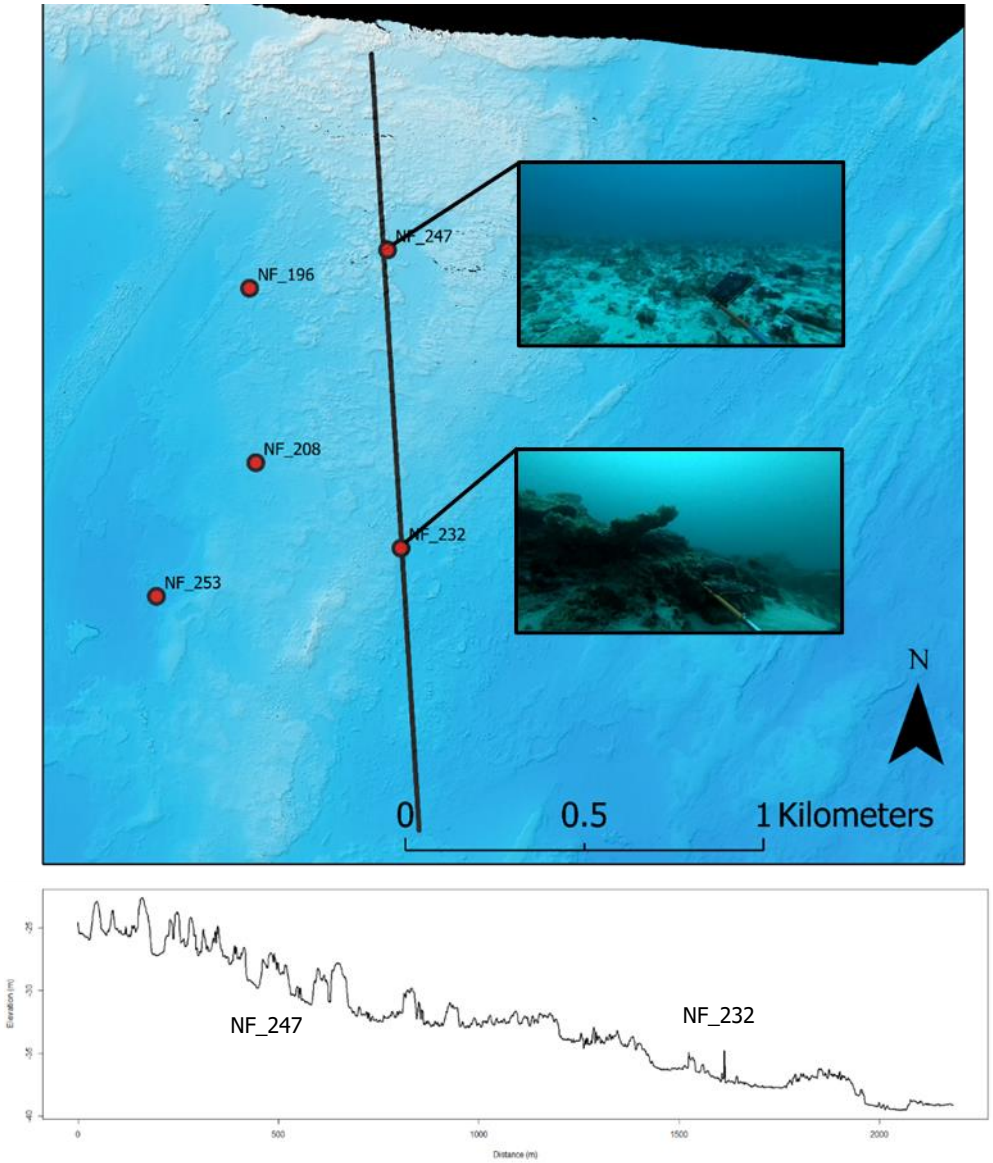

Figure 5-22: Transect 3 bathymetry and profile in the southern section of the Norfolk Shelf, south of Nepean Island.

5.2.2.4 TRANSECT 4

Transect 4, measured in the southwestern region, is 1.7 km long and is adjacent to three individual BRUVs sites (Figure 5-23). The transect, measured from north to south, traverses a bowl-like depression. The transect varies from -40 m at the edges of the depression to -49m at the deepest point. The transect starts with ~2 m of relative relief as it passes over a rough and undulating section of the seafloor for ~300 m. The seafloor then gradually descends into the depression over ~300 m, passing over NF_256. Here the seafloor is unconsolidated with a mixture of sand and gravels. No ripples of sediment can be seen here. The transect becomes rockier again closer to the south, near Phillip Island.

From 600 to 850 m, the depression is at its lowest, -49 m, and passes adjacent to the NF_261 BRUV point. Here the seafloor is unconsolidated with a dominance of sand and some seagrass growth. The sand shows some organisation with small ripples developing around seagrass growth locations. At around 1000 m, the gradient increases as the seafloor rises symmetrically up to -44 m. Here it flattens for ~200 m before continuing to ascend. NF_237 shows unconsolidated with sand, seagrass and smaller gravels/cobbles at this point of the transect. The sand is organised in linear ridges, possibly tied to the locations of the seagrass. After rising back to -40 m in depth, the seafloor gradually descends again.

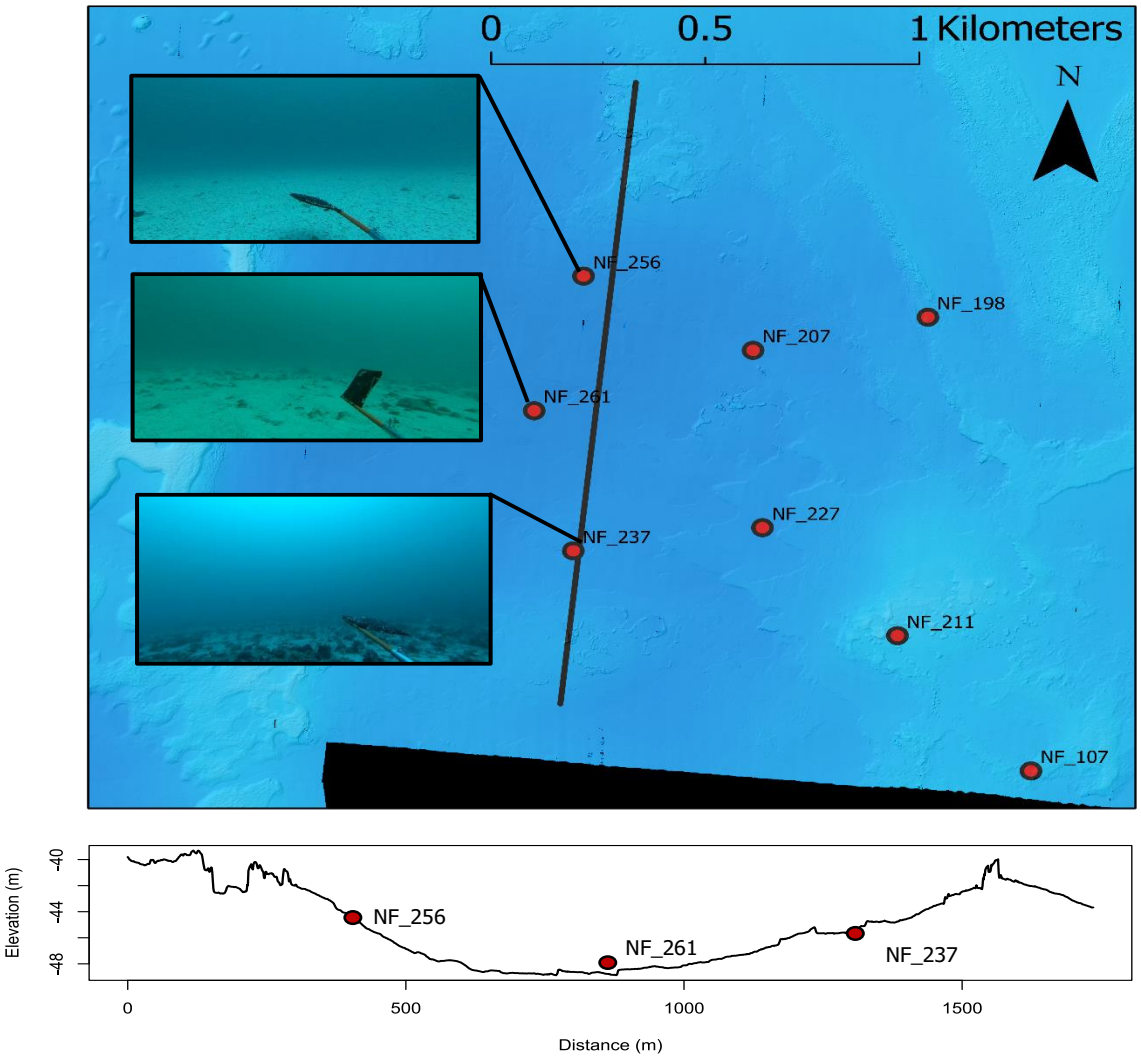

Figure 5-23: Transect 4 bathymetry and profile in the southern section of the Norfolk Shelf, southwest of Nepean Island.

5.2.2.5 TRANSECT 5

Transect 5 is a 1.1 km profile running from northwest to southeast (Figure 5-24). This transect was measured perpendicular to a ridge feature observed on the seafloor. The height of relief varies between 4 m in the eastern section of the sand ridges and less than a metre in the western. The whole ripple region is localised, ~1 km wide (perpendicular to wave direction) and at least 1.5 km long (parallel to ridge direction). This feature is likely to continue south towards Norfolk Island, outside the surveyed region. No BRUVs were deployed over this site, though it is likely that this section of the seafloor is made up of unconsolidated soft sediments such as sand.

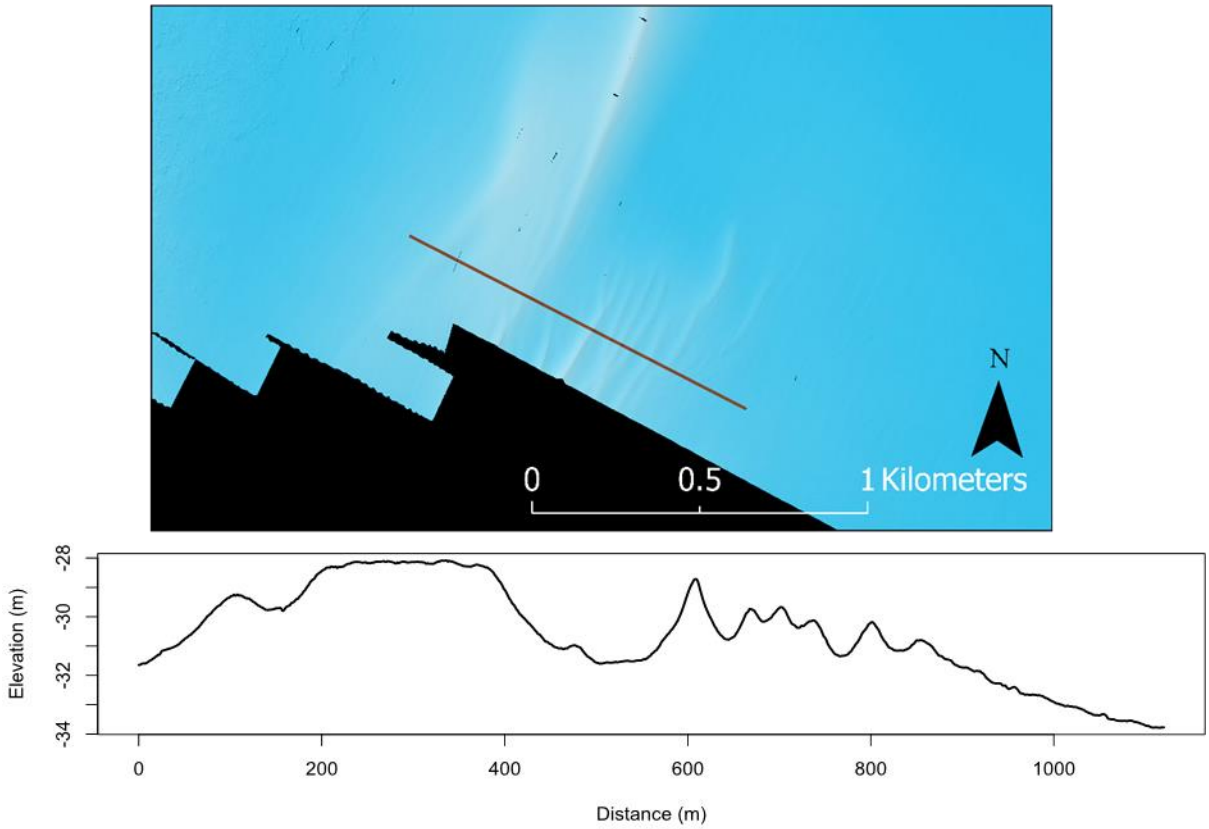

Figure 5-24: Transect 5 bathymetry and profile in the northern section of the Norfolk Shelf

5.2.2.6 TRANSECT 6

Transect 6 (Figure 5-25) is a 1.7 km profile from west to east across a sand ridge feature located in the southern part of the survey, between Nepean Island and Phillip Island. The sand ridges range from half a metre to 2 metres in relative relief. The ridges are symmetrical, with no dominant skewing in one direction. These ridges are ~1.5 km in length from west to east and ~600 m from north to south. No other such features are seen in the southern section of the bathymetry. BRUV completed 300 m to the northwest (NF_262) shows unconsolidated sandy substrate making up the seafloor.

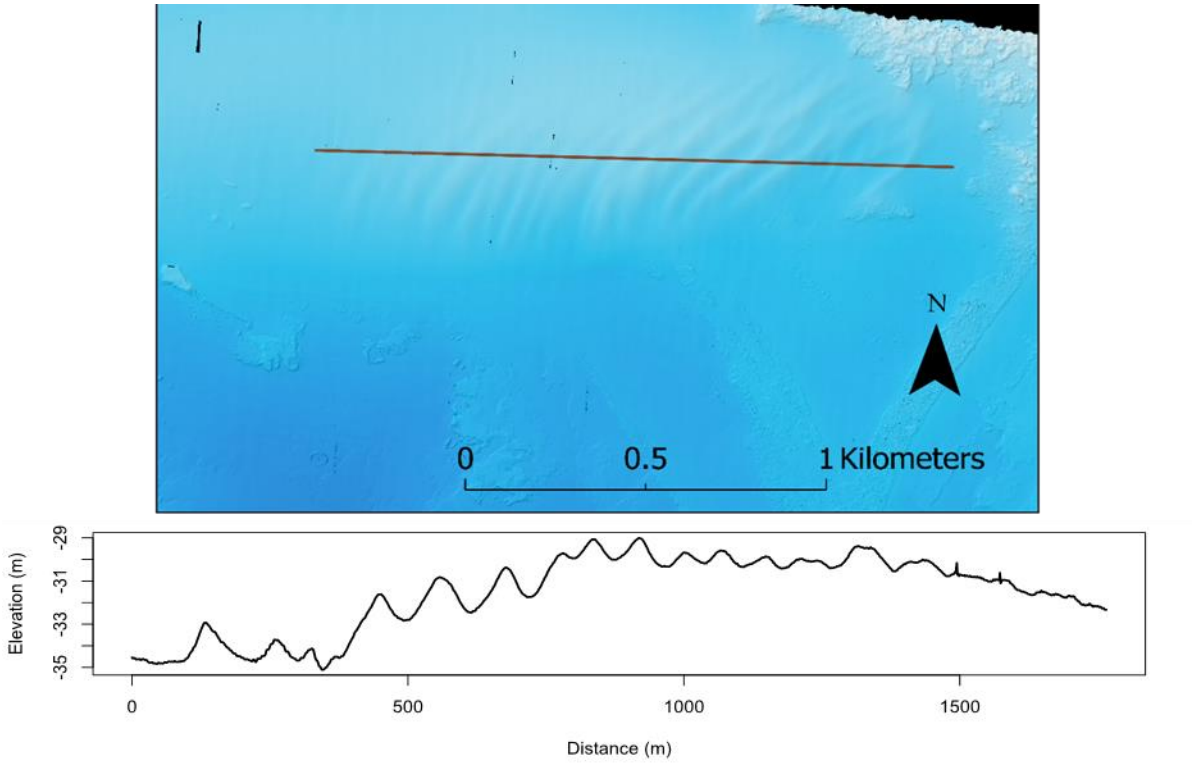

Figure 5-25: Transect 6 bathymetry and profile in the southern section of the Norfolk Shelf, southwest of Nepean Island.

5.2.2.7 TRANSECT 7

The smallest transect, 300 m from west to east, Transect 7, was taken across distinct circular feature in the southwestern region of the survey (Figure 5-26). This feature is remarkably symmetrical with two elevated rims, the western rising to -40m and the eastern to -39 m. The inside of the rim is a 60 m wide bowl at an elevation of -41 m. No other feature like this has been seen from the bathymetry collected by the survey. No BRUVs deployments were taken adjacent to the features.

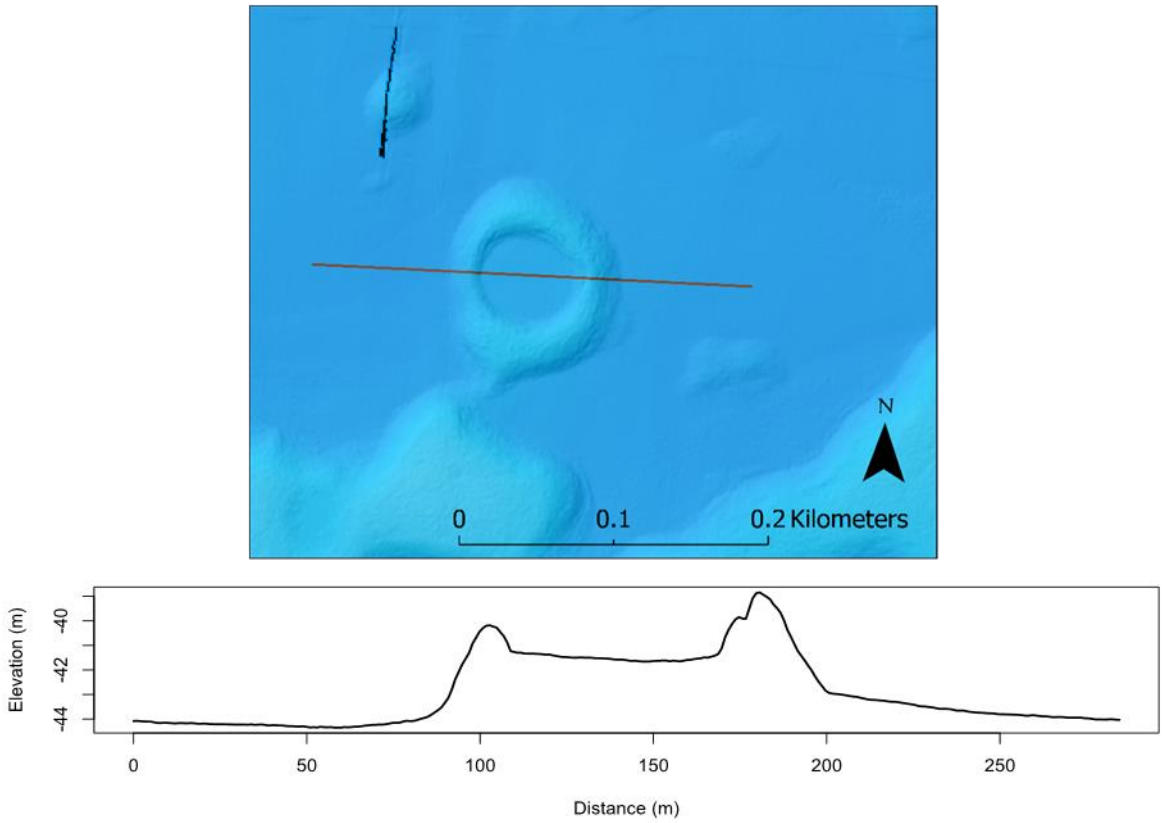

Figure 5-26: Transect 7 bathymetry and profile in the southern section of the Norfolk Shelf, southwest of Nepean Island

5.2.3 Baited Remote Underwater Videos to assist geomorphological classification

Though the BRUVs data does not cover all the bathymetry areas and is focused in the south and northeast, it can assist in the seafloor and geomorphological classification of the Norfolk Shelf.

At each BRUVs deployment, camera footage and still images were used to classify the seafloor based on its substrate (Figure 5-27). 68 % of the BRUVs sites showed unconsolidated seafloor made up of sand, gravels or cobbles. 32% of the seafloor was consolidated and comprised of coral cover or rock (volcanic or calcarenite) outcrops. 47 % of the seafloor was dominated by sand as its primary substrate. 28 % of the seafloor had deepwater coral cover as the primary seafloor substrate. Sands and gravels were also found in 54 % of the BRUVs sites as secondary substrates. From the BRUVs, the seafloor around Norfolk is mostly unconsolidated and made out of the sand with some cobbles and gravels. In localised areas, there are consolidated exposures of deep water corals and rocky outcrops, with some secondary substrates of sands and gravels. These corals veneer rock outcrops.

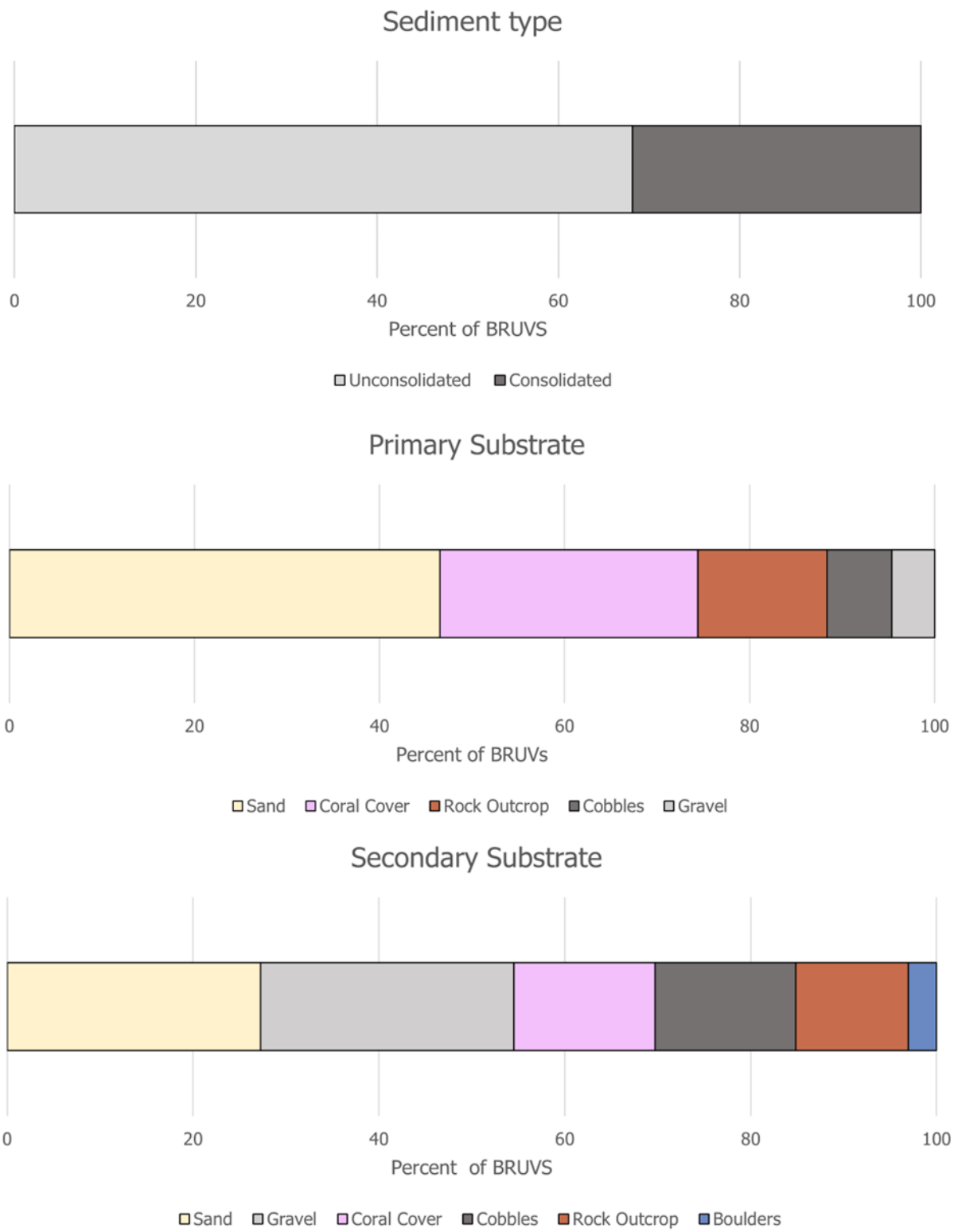

Figure 5-27: The percentage of BRUVs sites showing specific seafloor substrates. The top graph shows the percentage of unconsolidated to consolidated seafloor. The middle graph shows the percentage of primary seafloor substrates, and the bottom shows the percentage of the second substrate.

5.2.4 Geomorphic Classification of the Seafloor

Using the BTM toolbox and a user-set classification dictionary (Table 27), the seafloor of Norfolk Island has been classified into various categories based on slope, broadscale BPI, fine-scale BPI and depth (Figure 5-28). In some locations, BRUVs data has been used to ground truth the observations. The morphology terms follow those defined by Dove et al. (2020) and IHO (2019).

Table 27: Seafloor feature class definitions

Seafloor Feature	Definition	Substrate
Steep Slope	An inclined surface, in this case over 15°, showing regions of sudden change.	
Ridge	An elongated area of elevation with varying size and gradient (Dove et al., 2020; IHO, 2019).	Consolidated. Coral or volcanic rock outcrops.
Depression	This general term is used for a closed contour bathymetric low (Dove et al., 2020).	
Hummocks	This is a ground of small knolls or mounds occurring in low elevation and close proximity (Dove et al., 2020).	Consolidated. Coral or volcanic rock outcrops.
Plane	This is a flat or a sub-horizontal surface (Dove et al., 2020).	Unconsolidated. Sands, cobbles or gravel.

Table 28: Area and seafloor coverage (%) of feature classes based on BTM classification

Class	Zone	Area (m^2)	Coverage of Seafloor (%)
Steep Slope	1	2,578,902	2.37
Plane	2	91,799,108	84.34
Depression	3	1,562,279	1.44
Ridge	4	3,144,051	2.89
Hummocks	5	9,711,985	8.93

The seafloor surrounding Norfolk Island is dominantly a plane made of unconsolidated sandy sediments with low gradient and relative relief variation. Throughout the northwestern and south/southeastern sections of Norfolk Island, hummocky features can be seen, which have increased slope, positive fine BPI values and correlates with regions of higher ruggedness. Based on the BRUVs, this aligns with regions of rock outcrops (either vocalic or calcarenite) which form a substrate that deepwater corals can grow on. In the southwest, a section of the seafloor comprises ridges and depressions bound by steeper slopes. These have been defined as ridges of some form, which include sand ridge. Regions of depression are only found in association with these ridge features, an example of such can be seen in Transect 4.

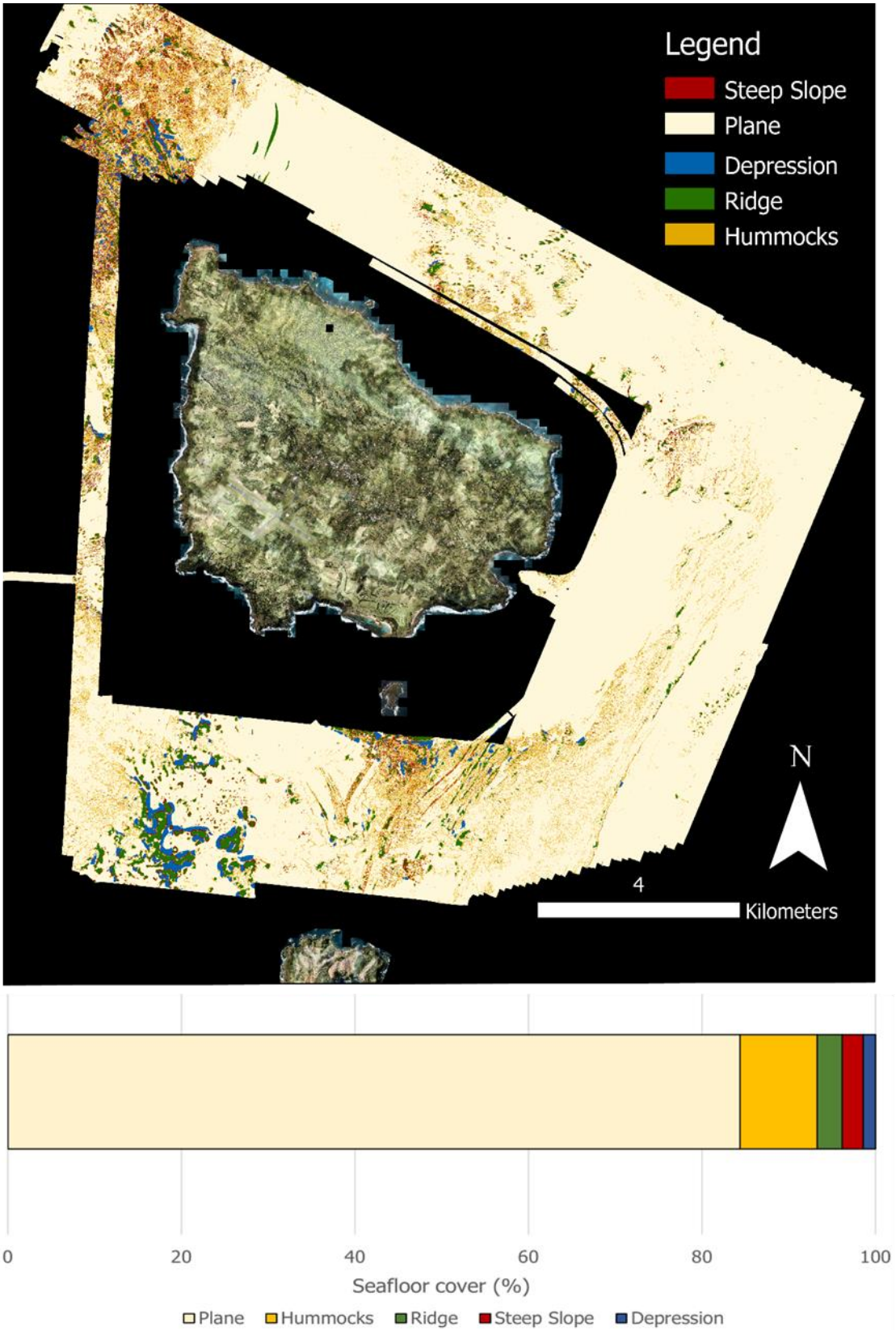

Figure 5-28: BTM classification of Norfolk Island bathymetry and percent of seafloor class cover based on classification dictionary (Table 28).

5.3 Seabed Nature Cartography

Beam Intensity feature available with the multibeam echosounder provides the seabed reflectance, knowns as backscatter imagery. The result is illustrated by a grey scale picture of the seabed, with high reflectivity represented by light (white) facies and low reflectivity by dark (black) facies. Intensity is defined by the seabed type. Rocks/ corals or coarse sediment are prone to reflect more than fine and soft sediments that tend to absorb. The backscatter imagery also highlights features such as rides and rock fractures. Figure 5-29 illustrates the seabed nature map interpreted from the backscatter imagery collected over Norfolk Shelf.

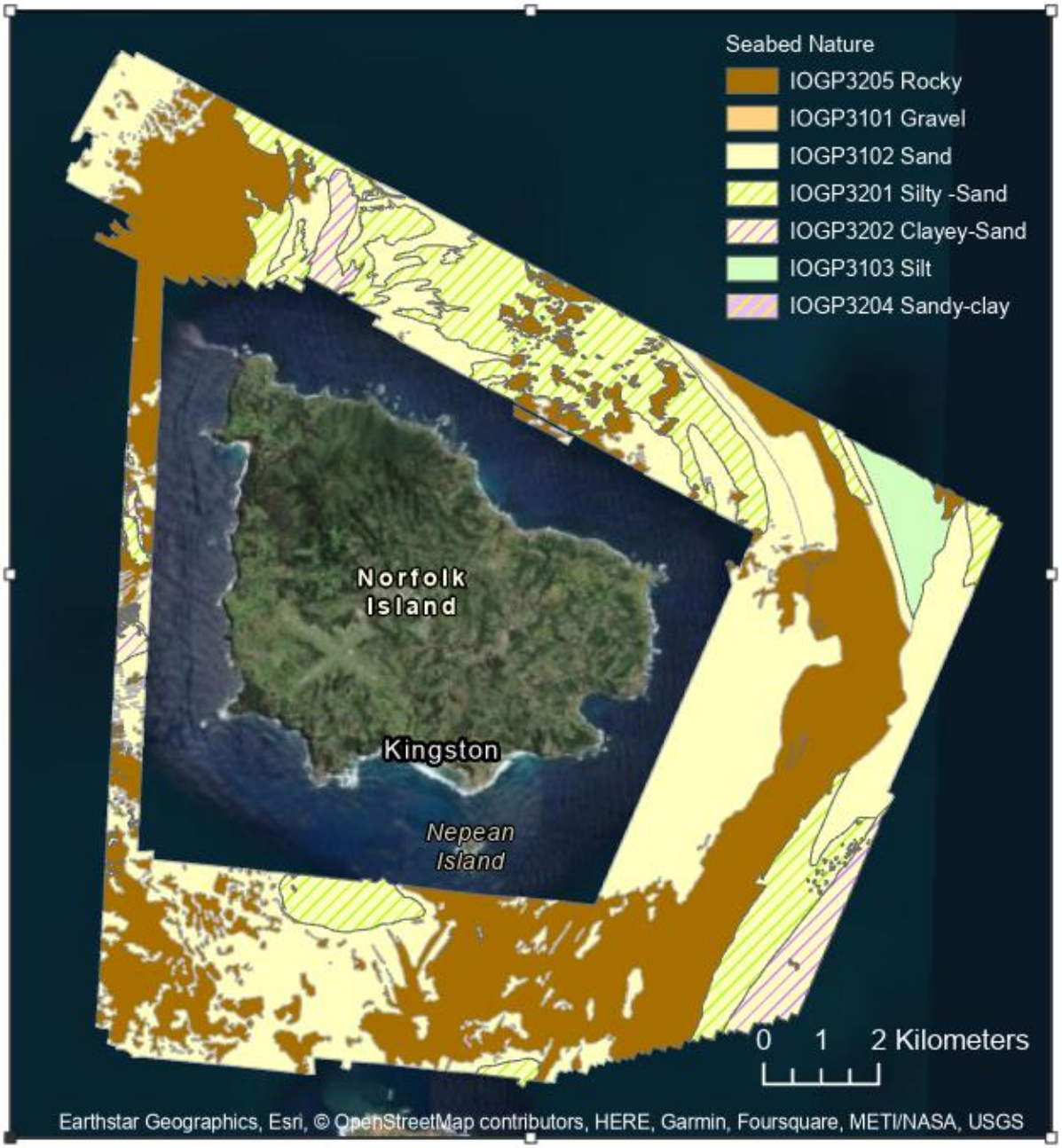

Figure 5-29: Norfolk Sheld seabed nature map - hypothesis

The analysis of Norfolk Shelf backscatter imagery allows to describe sub-categories from the consolidated and unconsolidated seafloor previously defined by the section 5.2. The spatial repartition for gravel, sand, silty sand, clayey sand, silt and sandy clay suggested here remains hypothetic and deserve to be confirmed by ground truthing.

5.3.1 Consolidated Seafloor Types

Consolidated Seafloor has a high to medium reflective (white to grey) facies with heterogeneity which is associated to high values of ruggedness. High reflective (white) facies are generally bared rock, whilst reflective (grey) facies suggest indurated bottom colonised by living material (kelp, corals, algae). It is possible to distinguish the relief and the fractures that characterises the rocky formations (Figure 5-30).

Consolidated seafloor is found in the Northwest corner of the survey area, as a large S-N ridge in the East, as well as between Nepean Island and Philip Island in the South. The examples below illustrate the main facies encountered over the consolidated seafloor and their hypothetic interpretation:

- In northern area, the rocky facies is characterised by SW-NE to W-E structures (Figure 5-30, box A). In advanced analysis, this could help defining the local bedrock formation.
- In the eastern shelf, the heterogenous facies refers to the ridge mentioned in the previous section. Its contours area well delimited by a linear contacts on each side, 5km long on the island side and 7km long on the offshore side. That emphasises the regional extend of the rocky section of the eastern shelf (Figure 5-30, box B);
- In southern area, consolidated seafloor shows rounded relief, forming large and isolated patches. This typical shape is similar to coral structures (Figure 5-30, box C)

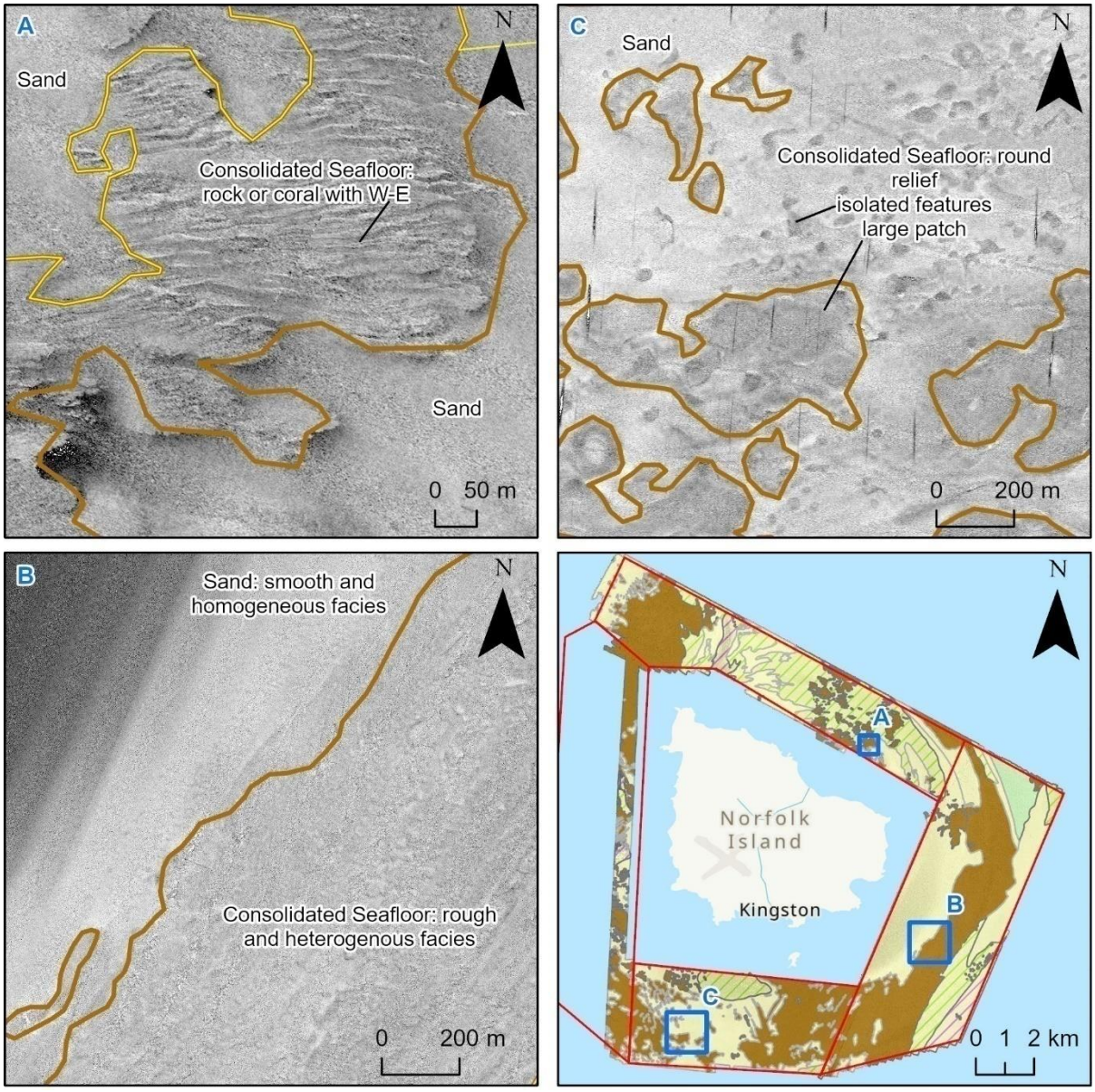

Figure 5-30: Example of consolidated seafloor of the Norfolk Shelf

5.3.2 Unconsolidated Seafloor Types

Unconsolidated seafloor is characterised by smooth aspect and homogeneous facies. The reflectivity level varies and is directly linked to main fraction of grain size and or presence of living organisms (algae, corals…). Some specific features, driven by local hydrodynamic or the effect of the underlaying bedrock structure, can be observed in the backscatter imagery.

- In northern region, unconsolidated seafloor is marked by variability of the reflectivity levels that can be delimited and interpreted as different sediment types. The more reflective (whiter) facies is defined as sand and seems to be covered by a finer grain-size deposits (slightly greyer). Those have some W-E shadows that suggests the mobility of the sediment (Figure 5-31). The bathymetry does not highlight significative depth variation.

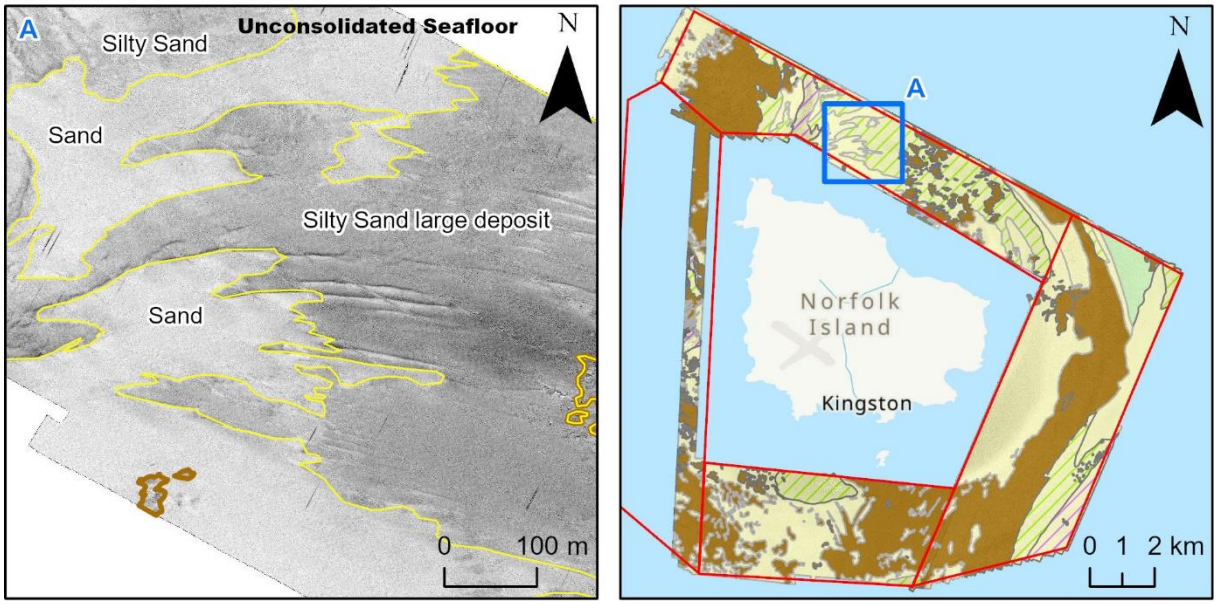

Figure 5-31: Sand and mobile sediment in the northern section of the Norfolk Shelf

- In the eastern area of the Norfolk Shelf, the deposits are driven by the regional rocky ridge. Sandy deposits are found on each side of the ridge. The interpretation suggests that finer sediment are in the East side of the ridge, where the depth is more important and most favourable to finer grain-size deposits.
- Localised in the western region, a homogeneous and low reflective (dark) facies is observed as different kind of features: isolated patch in between rocks (Figure 5-32, box A), large asymmetric patch (Figure 5-32, box B), or thin elongated S-N strip (Figure 5-32, box C). Current interpretation is very fine deposits (clayey sand to sandy clay) shaped by local hydrodynamic condition specific to the West coast of Norfolk Island;

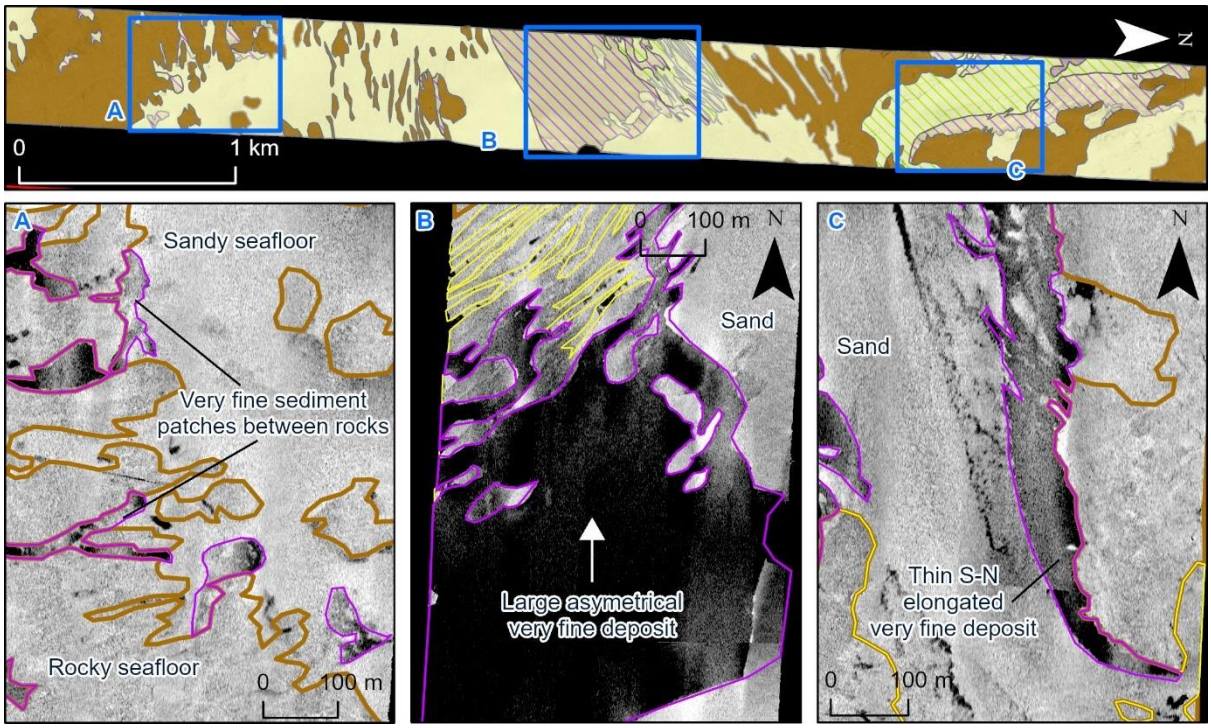

Figure 5-32: Very fine sediment deposits in West Norfolk Shelf

- As mentioned previously, some sand ridges locally shape the mobile sediment cover in the northern (section 5.2.2.5) and southern regions of Norfolk Shelf. The Figure 5-33 illustrates these features as observed in the backscatter imagery. The low reflectivity of the sediment suggests that sand ridges are made of fine sediment (Figure 5-33).

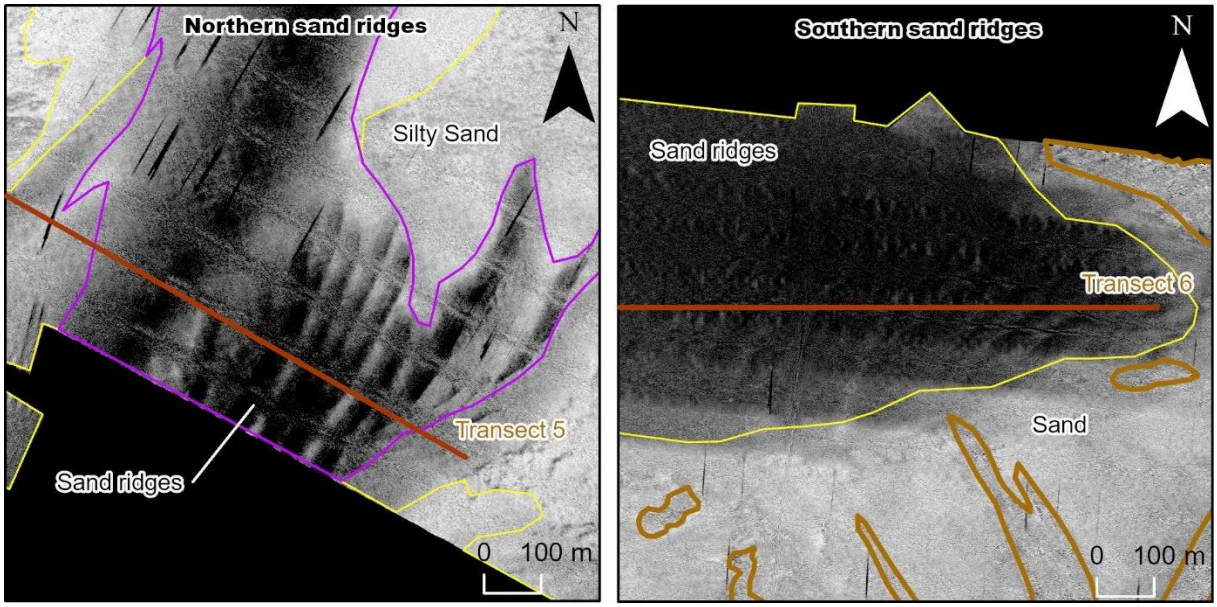

Figure 5-33: Sand ridges as observed in backscatter imagery (left Northern area, right southern area)

5.4 Fish communities

The BRUVS data collected in this project around Norfolk Island provides a glimpse of the fish communities present and also can serve as a baseline dataset for future surveys to determine if there are changes in these communities through time. Across the 42 BRUVS successfully deployed, over 3,000 individual fish were observed, covering 76 taxa within 35 families. The reefs surrounding Norfolk Island are at the southern extreme of coral reef formation and, therefore, support a mix of tropical and temperate species. Previous studies have shown the endemism in this region can vary from 22-36% due to isolation of the reefs (de Forges et al. 2000). However, there hasn't been a significant amount of biodiversity surveys done in this region, especially in the deeper reefs adjacent to the island. Recently and dating back to 2009, surveys were completed by Reef Life Survey focussed on the shallow subtidal reefs around Norfolk Island where they found variation in the biodiversity across sites around Norfolk and Philip Islands (Heather et al. 2022). Therefore, the BRUV deployments in depths greater than diver depths helps to fill a knowledge gap of the fish communities in this region.

The most common species observed in the BRUVS surveys, Chromis norfolkensis, was not identified in the shallower water surveys done by Reef Life Survey (Heather et al. 2022), showing how the BRUVS surveys allow the observations of abundant species outside the depth range of divers. C. norfolkensis is a planktivore that is typically found adjacent to reef habitat in 5-40 m water depths (Allen & Allen 2021). The other two most common species from the BRUVS, Chrysiptera notialis and Chromis hypsilepis were abundant in the RLS surveys (Heather et al. 2022). Two Vulnerable, blotched fantail ray Taeniurops meyeni and sandbar shark Carcharhinus plumbeus, and one Near Threatened species, tiger shark Galeocerdo cuvier, were observed on the BRUVS footage. These species were sighted one, three, and two times respectively.

Both habitat type and depth had a significant effect on the species observed via BRUVS. The highest diversity occurred in intermediate depth (20–30 m) on infralittoral reef habitats, likely due to the prevalence of reef-associated species such as wrasse and damselfish species and the high number of reef deployments within this depth range. Abundance was also highest on reef habitats, but not affected by depth. Large sharks and rays and yellowtail kingfish contributed to the high biomass seen in deep (40+ m) deployments.

6. Conclusion and Recommendations

The coastal and nearshore survey performed in 2021, results in the first high resolution marine dataset of Norfolk Island. The project combines information about the coast, the seabed and the water surrounding the island.

Drone photogrammetry was collected at seven locations throughout Norfolk Island. Geomorphic interpretation was able to recognise variation in the coastal geomorphology of Norfolk Island based on the region of the Island. Sites in the North, represented by Captain Cook Lookout have dramatic cliffs, onshore and offshore platforms and offshore stacks (such as Elephant and Bird Rock). The Western side of the Island, represented by Anson Bay, Puppy's Point and Headstone Point, is exposed to Westerlies and Eastward waves. The basalt geology contributes to formation of cliffs, rocky beaches within embayments and seacaves. These features follow a alternate pattern up the coast suggesting cyclic retreat process of cliff undercutting, seacave formation, and collapse to form rocky beach. In contrast, the southern side of Norfolk Island, represented by Slaughter Bay, Emily Bay and Cemetery Bay, and Ball Bay, is formed from volcanic basalt, and calcarenite. The calcarenite forms offshore platforms and breakwaters in which to protect both the sandy beaches of Slaughter Bay, Emily Bay and Cemetery Bay, but also the coral communities within Slaughter Bay. Mass wasting scarps are common throughout Norfolk Island coastlines, with the largest to the west of the Kingston Jetty.

Seafloor geomorphology was interpreted by applying the Benthic Terrain Modeller toolbox to the multibeam bathymetric data set of the Norfolk Island seafloor. Using a series of terrain derivatives such as slope, ruggedness, and bathymetric position index and ground truth with seabed reflectance and BRUVS images, the seafloor of Norfolk Shelf was defined into Plane, Hummocks, Ridges, Depression and Steep Slopes. The vast majority of the seafloor is classified as plane, with low gradient, sandy or clay base and gradual descent to depth. Other sections showed outcropping rocks veneered by deep water corals creating a hummocky morphology. Sand ridges and depressions were also identified.

The analysis of the seafloor reflectance allows to define sub-categories of the unconsolidated and consolidated seafloor. For example, the northern region shows rocky seabed characterised by fractures, whilst the southern region displays round shape patches interpreted as indurated seabed colonised by corals. The most extended rocky platform is the regional ridge with well delimited contours observed East of Norfolk Island. The unconsolidated seafloor has a variable acoustic response that suggest a wide range of grain-size sediment, from coarse sand to very fine deposits. Local hydrodynamic conditions (waves, tide, deep currents) differently affect the deposits pattern in each region. The spatial repartition of the unconsolidated sediment and their nature (gravel, sand, silty sand, clayey sand, silt and sandy clay) suggested by the seabed nature map remain a hypothetic interpretation and deserve further ground truthing followed by grain-size analysis.

Where BRUVs where deployed, in the northeast and south of the island, over 3,000 individual fish were observed, covering 76 taxa within 35 families. Both habitat type and depth had a significant effect on the species observed via BRUVS. The highest diversity occurred in intermediate depth (20–30 m) on infralittoral reef habitats. The BRUVS results provide a foundation for which future work can build upon. We recommend including additional sampling sites especially along the west and northwest of the island and extending sampling into deeper mesophotic areas. Pelagic deployments may also be beneficial to better capture the shark and pelagic fish population around the island. This and future work may be important to track changes within a presumed climate hotspot that straddles the extremes for both temperate and tropical species.

7. Digital Deliverables

Items	Folder	File Name/ Format
Drone photogrammetry processing reports	Norfolk_Aerial_Photogrammetry_Processing_Reports.zip	Anson_Bay_report.pdf Ball_Bay_report.pdf Capt_Cook_report.pdf Cemetery_Emily.pdf Headstone_report.pdf Puppys_report.pdf Slaughter_Bay_Bumbora_report.pdf
Photogrammetry images	AMPNorfolk_OI_WGS84_R1.gdb	Raster NFK_AnsonBay_10cm_WGS84 NFK_BallBay_10cm_WGS84 NFK_Cook_10cm_WGS84 NFK_EmSl_10cm_WGS84 NFK_Headstone_10cm_WGS84 NFK_Puppy_10cm_WGS84 NFK_SlBa_10cm_WGS84 NFK_BallBay_10cm_WGS84
Bathymetry	AMPNorfolk_OI_WGS84_R1.gdb	Raster NFK_Bathy_1m_WGS84
Backscatter Imagery	AMPNorfolk_OI_WGS84_R1.gdb	Raster NFK_BS_1m_WGS84
Seabed Nature	AMPNorfolk_OI_WGS84_R1.gdb	Feature Class NFK_SeabedNature_WGS84

8. References

Abell, R.S., 1976. A groundwater investigation on Norfolk Island.

Allen, G.R. & Allen, M.G. 2021. Two new species of Chromis (Teleostei: Pomacentridae) from northwestern Australia and the southwestern Pacific Ocean, previously part of C. fumea (Tanaka, 1917). Journal of the Ocean Science Foundation 38: 78–103. https://doi.org/10.5281/zenodo.5601971

Bird, E., 2010. Norfolk Island. Encyclopedia of the World's Coastal Landforms 1247–1254. https://doi.org/10.1007/978-1-4020-8639-7_227

Birt MJ, Harvey ES, Langlois TJ (2012) Within and between day variability in temperate reef fish assemblages: Learned response to baited video. J Exp Mar Biol Ecol 416–417:92-100

Bond T, Partridge JC, Taylor MD, Langlois TJ, Malseed BE, Smith LD, McLean DL (2018) Fish associated with a subsea pipeline and adjacent seafloor of the North West Shelf of Western Australia. Mar Environ Res 141:53-65

Cappo M, Speare P, De'ath G (2004) Comparison of baited remote underwater video stations (BRUVS) and prawn (shrimp) trawls for assessments of fish biodiversity in inter-reefal areas of the Great Barrier Reef Marine Park. J Exp Mar Biol Ecol 302:123-152

Cappo M, Stowar M, Syms C, Johansson C, Cooper T (2011) Fish-habitat associations in the region offshore from James Price Point– a rapid assessment using Baited Remote Underwater Video Stations (BRUVS). J R Soc West Aust 94:303-321

Clarke TM, Whitmarsh SK, Fairweather PG, Huveneers C (2019) Overlap in fish assemblages observed using pelagic and benthic baited remote underwater video stations Mar Freshwat Res 70:870-880

Dove, D., Gafeira, J., Dolan, A., Stewart, M. F. J., Arosio, H., & Scott, R. (2020). *A two-part seabed geomorphology classification scheme: (v.2) Part 1: morphology features glossary*. https://doi.org/10.5281/ZENODO.4075248

Fairbridge, R.W., Johnson, D.L., 1978. Eolianite, in: The Encyclopedia of Sedimentology. pp. 279–282.

Froese R, Pauly D (2010) FishBase. Fisheries Centre, University of British Columbia

Gallant, J., Petheram, C., 2020. Norfolk Island lidar. v1. https://doi.org/10.25919/5e4a0e4e93d4c

Harvey ES, Cappo M, Kendrick GA, McLean DL (2013a) Coastal fish assemblages reflect geological and oceanographic gradients within an Australian zootone. PLoS ONE 8:e80955

Harvey E, Cappo M, Shortis M, Robson S, Buchanan J, Speare P (2003) The accuracy and precision of underwater measurements of length and maximum body depth of southern bluefin tuna (Thunnus maccoyii) with a stereo-video camera system. Fish Res 63:315-326

Heather FJ, Stuart-Smith RD, Cooper AT, and Edgar GJ (2022) Reef Life Survey Assessment of Marine Biodiversity in Norfolk Marine Park. Reef Life Survey Foundation Incorporated.

IHO. (2019). *Standardisation of Undersea Feature Names. Guidelines proposal form terminology. Edition 4.2.0*. https://iho.int/uploads/user/pubs/bathy/B-6_e4%202%200_2019_EF_clean_3Oct2019.pdf

Jones, J.G., McDougall, I., 1973. Geological history of norfolk and philip islands, southwest pacific ocean. Journal of the Geological Society of Australia 20, 240–254. https://doi.org/10.1080/14400957308527916

Langlois T, Goetze J, Bond T, Monk J, Abesamis RA, Asher J, Barrett N, Bernard ATF, Bouchet PJ, Birt MJ, Cappo M, Currey-Randall LM, Fairclough DV, Fullwood LAF, Gibbons BA, Harasti D, Heupel MR, Hicks J, Holmes TH, Huveneers C, Ierodiaconou D, Jordan A, Knott NA, Malcolm HA, McLean D, Meekan M, Miller D, Mitchell PJ, Newman SJ, Radford B, Rolim FA, Saunders BJ, Stowar M, Smith ANH, Travers MJ, Wakefield CB, Whitmarsh SK, Williams J, Driessen D, Harvey ES (2020) A field and video-annotation guide for baited remote underwater stereo-video surveys of demersal fish assemblages. Methods Ecol Evol 00:1-9

Langlois T, Williams J, Monk J, Bouchet P, Currey L, Goetze J, Harasti D, Huveneers C, Ierodiaconou D, Malcolm H, Whitmarsh S (2018) Marine sampling field manual for benthic stereo BRUVS (Baited Remote Underwater

Videos). In: Przeslawski R, Foster S (eds) Field Manuals for Marine Sampling to Monitor Australian Waters. National Environmental Science Programme (NESP)

Logan JM, Young MA, Harvey ES, Schimel ACG, Ierodiaconou D (2017) Combining underwater video methods improves effectiveness of demersal fish assemblage surveys across habitats. Mar Ecol Prog Ser 582:181-200

Lundblad, E. R., Wright, D. J., Miller, J., Larkin, E. M., Rinehart, R., Naar, D. F., Donahue, B. T., Anderson, S. M., & Battista, T. (2006). A Benthic Terrain Classification Scheme for American Samoa. *Http://Dx.Doi.Org/10.1080/01490410600738021*, *29*(2), 89–111. https://doi.org/10.1080/01490410600738021

Norfolk Island Regional Council, 2020. Plan of Management- Ball Bay Reserve.

Petheram C, Taylor A, Hughes, J., Philip S, Tavener, N., Greenwood D, Taylor N, Pr, W., Raiber, M., Turnadge, C., Yang A, Seo L, Davies, P., Vanderzalm J, Davis A, Gallant, J., Ahmed W, Rogers L, Ticehurst, C., Marvanek S, Gerber, Bui, E., Grice T, Crosbie R, Metcalfe, S., Fitzpatrick, R., Schepen A, Levick, S., Nobbs C, Cahill K, Vaze J, 2020. Norfolk Island Water Resource Assessment. A report to the Australian Government from the CSIRO Norfolk Island Water Resource Assessment team. Australia. https://doi.org/10.25919/tg90-3x77

Richer de Forges, B., Koslow, J. A., & Poore, G. C. B. (2000). Diversity and endemism of the benthic seamount fauna in the southwest Pacific. Nature, 405(6789), 944-947.

Riley, S. J., DeGloria, S. D., & Elliot R. (1999). A terrain ruggedness index that quantifies topographic heterogeneity. *Intermountain Journal of Sciences*, *5*(1–4), 23–27.

Rinehart, R., Wright, D. J., Rinehart, R. W., Lundblad, E. R., Larkin, E. M., Murphy, J., & Cary-Kothera, L. (2004). *ArcGIS 8.x Benthic Terrain Modeler: Analysis in American Samoa*. https://www.researchgate.net/publication/237546675

Santana-Garcon J, Newman SJ, Langlois TJ, Harvey ES (2014) Effects of a spatial closure on highly mobile fish species: an assessment using pelagic stereo-BRUVs. J Exp Mar Biol Ecol 460:153-161

SeaGIS (2020) EventMeasure: User guide. SeaGIS Pty Ltd, Victoria

Walbridge, S., Slocum, N., Pobuda, M., & Wright, D. J. (2018). Unified Geomorphological Analysis Workflows with Benthic Terrain Modeler. *Geosciences*, *8*(3), 94. https://doi.org/10.3390/geosciences8030094

Weiss, A. (2001). Topographic position and landforms analysis. In *Poster presentation, ESRI user conference* (Vol. 200, p. 1). http://www.jennessent.com/downloads/TPI-poster-TNC_18x22.pdff

9. Appendix

9.1 Morpho-Bathymetry Appendix

BTM Input Parameters

Bathymetry Raster	AU420_NFK_c1m_Tide_Finalised.tif
Broad BPI inner radius	15
Broad BPI outer radius	150
Fine BPI inner radius	3
Fine BPI outer radius	15
Ruggedness Neighbourhood Size	7
Classification Dictionary	See BTM Classification Table (Table 4)

BTM Classification Dictionary for Norfolk Island bathymetry

Class	Zone	BroadBPI Lower	BroadBPI Upper	FineBPI Lower	FineBPI Upper	Slope Lower	Slope Upper
1	Steep Slope					15	
2	Plane	-100	150	-100	100		5
3	Depression	-1500	-100				
4	Ridge	150	2700				15
5	Hummocks			-50	200	2	15

9.2 Relative abundance and biomass of all species observed in the BRUVS deployments

Family	Taxon	Common Name	Total observed	Relative abundance (mean ±SE)	Total lengths	Mean length (cm) (±SE)	Total biomass observed (g)	Relative total biomass (g) (mean ±SE)
Acanthuridae	*Acanthurus albipectoralis*	Whitefin surgeonfish	1	0.02 ± 0.02	1	36.81 ± 0	704.74	16.78 ± 16.78
Acanthuridae	*Prionurus maculatus*	Spotted sawtail	55	1.31 ± 0.76	16	37.3 ± 1.18	37509.52	893.08 ± 535.83
Aplodactylidae	*Aplodactylus etheridgii*	Notch-head marblefish	1	0.02 ± 0.02	NA	NA	NA	NA
Apogonidae	*Cheilodipterus quinquelineatus*	Five-lined cardinalfish	2	0.05 ± 0.05	2	13.62 ± 0.17	57.76	1.38 ± 1.38
Apogonidae	*Ostorhinchus doederleini*	Fourline Cardinalfish	30	0.71 ± 0.33	14	10.3 ± 0.43	713.23	16.98 ± 7.42
Apogonidae	*Ostorhinchus flavus*	Yellow Cardinalfish	169	4.02 ± 1.64	45	11.07 ± 0.17	3220.84	76.69 ± 30.25
Apogonidae	*Ostorhinchus norfolcensis*	Norfolk cardinalfish	6	0.14 ± 0.09	3	14.83 ± 0.28	384.11	9.15 ± 5.51
Apogonidae	*Taeniamia leai*	Lea's cardinalfish	46	1.1 ± 0.68	16	7.81 ± 0.22	444.97	10.59 ± 6.37
Berycidae	*Centroberyx affinis*	Redfish	1	0.02 ± 0.02	NA	NA	NA	NA
Blenniidae	*Plagiotremus tapeinosoma*	Piano fangblenny	48	1.14 ± 0.48	14	6.13 ± 0.09	52.79	1.26 ± 0.52
Bothidae	*Bothidae* spp.	Flounder	5	0.12 ± 0.1	NA	NA	NA	NA
Caesionidae	*Caesionidae* spp.	Fusilier	13	0.31 ± 0.31	5	6.94 ± 0.36	60.93	1.45 ± 1.45
Caesionidae	*Pterocaesio trilineata*	Three-stripe fusilier	53	1.26 ± 0.87	15	11.78 ± 0.35	1291.61	30.75 ± 21.18
Carangidae	*Pseudocaranx* spp.	Trevally	123	2.93 ± 1.06	39	44.56 ± 2.06	203492.1	4845.05 ± 1649.71
Carangidae	*Seriola lalandi*	Yellow-tail kingfish	45	1.07 ± 0.26	24	69.9 ± 3.15	222282	5292.43 ± 1324.34
Carangidae	*Seriola rivoliana*	Highfin amberjack	2	0.05 ± 0.05	NA	NA	NA	NA
Carangidae	*Trachurus* spp.	Mackerel	2	0.05 ± 0.05	2	40.18 ± 0.89	2654.91	63.21 ± 63.21
Carcharhinidae	*Carcharhinus plumbeus*	Sandbar shark	3	0.07 ± 0.04	1	164.8 ± 0	92308.93	2197.83 ± 1237.58

Carcharhinidae	*Carcharhinus* spp.	Whaler shark	21	0.5 ± 0.1	14	88.48 ± 3.81	107552.5	2560.77 ± 581.79
Carcharhinidae	*Galeocerdo cuvier*	Tiger shark	2	0.05 ± 0.03	2	216.46 ± 26.55	244319.9	5817.14 ± 4335.59
Chaetodontidae	*Chaetodon guentheri*	Gunther's butterflyfish	2	0.05 ± 0.05	1	16.71 ± 0	218.63	5.21 ± 5.21
Cheilodactylidae	*Cheilodactylus ephippium*	Painted Morwong	2	0.05 ± 0.03	1	39.45 ± 0	1625.23	38.7 ± 27.03
Cirrhitidae	*Notocirrhitus splendens*	Splendid hawkfish	3	0.07 ± 0.04	2	18.83 ± 1.42	246.46	5.87 ± 3.37
Congridae	*Diploconger polystigmatus*	Headband conger	1	0.02 ± 0.02	1	42.56 ± 0	93.9	2.24 ± 2.24
Dasyatidae	*Bathytoshia brevicaudata*	Smooth stingray	2	0.05 ± 0.03	1	124.64 ± 0	49181.38	1170.99 ± 817.85
Dasyatidae	*Taeniurops meyeni*	Blotched fantail ray	1	0.02 ± 0.02	NA	NA	NA	NA
Paguroidea	Paguroidea spp.	Hermit crab	1	0.02 ± 0.02	NA	NA	NA	NA
Grammistidae	*Aulacocephalus temminckii*	Goldribbon soapfish	3	0.07 ± 0.05	1	24.83 ± 0	586.16	13.96 ± 10.3
Kyphosidae	*Girella cyanea*	Blue drummer	6	0.14 ± 0.1	4	42.91 ± 4.39	10106.52	240.63 ± 178.06
Kyphosidae	*Kyphosus* spp.	Drummer	21	0.5 ± 0.32	13	45.36 ± 1.43	41211.84	981.23 ± 642.51
Labracoglossidae	*Labracoglossa nitida*	Blue knifefish	4	0.1 ± 0.1	2	35.53 ± 2.5	2673.88	63.66 ± 63.66
Labridae	*Anampses elegans*	Elegant wrasse	15	0.36 ± 0.16	4	19.61 ± 3.67	1480.61	35.25 ± 15.12
Labridae	*Bodianus unimaculatus*	Eastern pigfish	1	0.02 ± 0.02	1	48.57 ± 0	1672.76	39.83 ± 39.83
Labridae	*Coris bulbifrons*	Doubleheader	5	0.12 ± 0.05	3	63.28 ± 5.34	16992.66	404.59 ± 179.11
Labridae	*Coris picta*	Comb wrasse	9	0.21 ± 0.15	5	24.53 ± 0.82	932.53	22.2 ± 14.96
Labridae	*Coris sandeyeri*	Eastern king wrasse	28	0.67 ± 0.44	13	12.97 ± 1.84	1095.57	26.09 ± 14.89
Labridae	*Cymolutes praetextatus*	Knife wrasse	3	0.07 ± 0.07	1	19.49 ± 0	123.32	2.94 ± 2.94
Labridae	*Iniistius jacksonensis*	Keelhead Razorfish	2	0.05 ± 0.05	1	24.01 ± 0	206.81	4.92 ± 4.92
Labridae	*Notolabrus inscriptus*	Inscribed wrasse	20	0.48 ± 0.1	14	31.67 ± 0.89	8098.74	192.83 ± 44.21

Labridae	*Pseudolabrus luculentus*	Luculent wrasse	190	4.52 ± 0.72	90	14.2 ± 0.37	6977.55	166.13 ± 25.57
Labridae	*Suezichthys arquatus*	Painted rainbow wrasse	11	0.26 ± 0.11	6	13.78 ± 1.1	225.99	5.38 ± 2.5
Labridae	*Thalassoma lutescens*	Green moon wrasse	1	0.02 ± 0.02	1	26.69 ± 0	223.97	5.33 ± 5.33
Lethrinidae	*Lethrinus miniatus*	Redthroat Emperor	91	2.17 ± 0.5	47	42.98 ± 1.1	106736.4	2541.34 ± 540.66
Malacanthidae	*Malacanthidae* spp.	Tilefish	1	0.02 ± 0.02	NA	NA	NA	NA
Monacanthidae	*Thamnaconus analis*	Darkvent Leatherjacket	2	0.05 ± 0.03	2	25.67 ± 1.25	548.76	13.07 ± 9.22
Mullidae	*Parupeneus pleurostigma*	Sidespot goatfish	1	0.02 ± 0.02	1	25.11 ± 0	256.84	6.12 ± 6.12
Mullidae	*Parupeneus spilurus*	Black-spotted goatfish	7	0.17 ± 0.1	7	23.96 ± 3.75	1997.61	47.56 ± 33.71
Muraenidae	*Enchelycore ramosa*	Mosaic moray	1	0.02 ± 0.02	NA	NA	NA	NA
Muraenidae	*Gymnothorax annasona*	Lord Howe moray	16	0.38 ± 0.09	1	55.55 ± 0	3970.2	94.53 ± 22.3
Muraenidae	*Gymnothorax eurostus*	Stout Moray	12	0.29 ± 0.09	2	45.13 ± 2.07	2021.54	48.13 ± 14.59
Muraenidae	*Gymnothorax meleagris*	Whitemouth Moray	2	0.05 ± 0.03	1	38.3 ± 0	209.33	4.98 ± 3.48
Muraenidae	*Gymnothorax nubilus*	Grey moray	63	1.5 ± 0.3	7	43.46 ± 3.36	8444.78	201.07 ± 40.11
Muraenidae	*Gymnothorax porphyreus*	Lowfin moray	32	0.76 ± 0.24	1	45.3 ± 0	5165.6	122.99 ± 38.83
Pinguipedidae	*Parapercis colemani*	Coleman's grubfish	2	0.05 ± 0.05	1	14.9 ± 0	56.01	1.33 ± 1.33
Plotosidae	*Plotosus lineatus*	Striped catfish	4	0.1 ± 0.1	NA	NA	NA	NA
Pomacanthidae	*Centropyge tibicen*	Keyhole angelfish	1	0.02 ± 0.02	1	12.58 ± 0	48.28	1.15 ± 1.15
Pomacanthidae	*Chaetodontoplus conspicillatus*	Conspicuous angelfish	20	0.48 ± 0.13	10	26.98 ± 1.36	9120.55	217.16 ± 61.65
Pomacentridae	*Amphiprion latezonatus*	Wide-band Anemonefish	26	0.62 ± 0.18	13	9.96 ± 0.22	566.97	13.5 ± 4.02

Pomacentridae	*Chromis hypsilepis*	One-spot puller	339	8.07 ± 3.95	56	10.88 ± 0.48	6818.14	162.34 ± 83.34
Pomacentridae	*Chromis norfolkensis*	Norfolk Chromis	779	18.55 ± 6.6	103	6.09 ± 0.17	2591.32	61.7 ± 21.16
Pomacentridae	*Chrysiptera notialis*	Southern demoiselle	542	12.9 ± 3.44	104	5.84 ± 0.1	1564.38	37.25 ± 9.9
Pomacentridae	*Parma polylepis*	Banded scalyfin	13	0.31 ± 0.09	9	20.7 ± 0.95	2490.53	59.3 ± 18.41
Pomacentridae	*Plectroglyphidodon fasciolatus*	Pacific gregory	7	0.17 ± 0.06	NA	NA	NA	NA
Pomacentridae	*Plectroglyphidodon johnstonianus*	Johnston damsel	1	0.02 ± 0.02	NA	NA	NA	NA
Pomacentridae	*Stegastes gascoynei*	Coral sea gregory	8	0.19 ± 0.1	6	15.44 ± 0.45	554.05	13.19 ± 6.82
Scombridae	*Sarda australis*	Australian bonito	4	0.1 ± 0.05	2	54.98 ± 8.35	8220.31	195.72 ± 99.42
Scorpaenidae	*Scorpaena cardinalis*	Eastern red scorpionfish	8	0.19 ± 0.08	4	40.27 ± 2.2	10522.4	250.53 ± 101.2
Scorpididae	*Atypichthys latus*	New Zealand Mado	17	0.4 ± 0.17	13	20.05 ± 1.05	3342.78	79.59 ± 27.53
Serranidae	*Acanthistius cinctus*	Yellow-banded wirrah	29	0.69 ± 0.17	17	29.1 ± 1.1	10039.44	239.03 ± 58.91
Serranidae	*Epinephelus rivulatus*	Halfmoon grouper	8	0.19 ± 0.08	5	39.31 ± 1.6	6755.26	160.84 ± 66.57
Serranidae	*Trachypoma macracanthus*	Pacific rockcod	8	0.19 ± 0.07	8	18.76 ± 0.73	735.16	17.5 ± 6.55
Synodontidae	*Trachinocephalus trachinus*	Painted grinner	5	0.12 ± 0.06	3	26.51 ± 0.7	7514.96	178.93 ± 89.67
Tetraodontidae	*Canthigaster callisterna*	Clown toado	5	0.12 ± 0.05	5	14.15 ± 1.57	430.75	10.26 ± 5.25
Tetraodontidae	*Lagocephalus sceleratus*	Silver Toadfish	21	0.5 ± 0.16	11	48.28 ± 4.86	20172.11	480.29 ± 159.41
Tetraodontidae	*Torquigener altipinnis*	Highfin toadfish	59	1.4 ± 0.55	27	17.84 ± 0.24	6126.75	145.88 ± 56.99
Triakidae	*Mustelus* spp.	Gummy shark	1	0.02 ± 0.02	NA	NA	NA	NA